



Search for Higgs bosons produced in association with a high-energy photon via vector-boson fusion and decaying to a pair of b -quarks in the ATLAS detector

The ATLAS Collaboration

A search for Standard Model Higgs bosons produced in association with a high-energy photon and decaying to $b\bar{b}$ is performed using 133 fb^{-1} of $\sqrt{s} = 13 \text{ TeV}$ pp collision data collected with the ATLAS detector at the Large Hadron Collider at CERN. The photon requirement reduces the multijet background, and the $H \rightarrow b\bar{b}$ decay is the dominant decay mode. Event selection requirements target events produced by vector-boson fusion, the dominant production mode in this channel. Several improvements enhance the search sensitivity compared to previous measurements. These improvements include better background modelling and characterization, the use of a neural-network classifier, and an updated signal extraction strategy adopting a direct binned-likelihood fit to the classifier output. With these improvements, the Higgs boson signal strength is measured to be 0.2 ± 0.7 relative to the Standard Model prediction. This corresponds to an observed significance of 0.3 standard deviations, compared to an expectation of 1.5 standard deviations assuming the Standard Model.

Contents

1	Introduction	2
2	ATLAS detector	3
3	Monte Carlo event simulation samples	4
4	Object and event selection	5
5	Multivariate analysis	8
6	Signal and background composition and modelling	8
7	Systematic uncertainties	10
8	Results	14
9	Conclusion	17

1 Introduction

The scalar Higgs boson, discovered in 2012 [1, 2], has been studied extensively in all the expected main production modes and in many of its decay channels. The Higgs boson decays most frequently to a pair of b -quarks, making this a powerful decay channel to study. However, this decay is challenging because of a significant non-resonant QCD multijet background, which complicates the search. By requiring a final state with an associated high-energy photon, a destructive interference effect, arising from diagrams with initial-state and final-state radiation of the photon, reduces this non-resonant background, making this an interesting final-state signature to target [3]. An example Feynman diagram for this dominant non-resonant background is shown in Figure 1(a). Conveniently, the photon also provides a clean signature on which to trigger. Due to the increased number of electroweak vertices in vector-boson fusion (VBF) Higgs boson production, this production mode surpasses gluon–gluon fusion (ggH) and becomes the dominant production mechanism when an associated photon is required. The leading-order Feynman diagram for this mode is shown in Figure 1(b). By requiring a high dijet invariant mass, the signal phase space becomes purer in VBF Higgs production, with vector-boson associated Higgs production ($VH, V = W, Z$) contributing less than 5% of the signal. Additionally, a destructive interference effect, similar to that reducing the non-resonant QCD multijet background, suppresses ZZ -fusion and makes this a unique way to study WW -fusion Higgs production and the HWW interaction more closely.

Searches for VBF Higgs production with decay into b -quarks without the associated photon requirement have been performed by both ATLAS and CMS. In the all-hadronic channel, ATLAS measured a signal strength, or the ratio between the observed signal yield and that predicted by the Standard Model, of $0.95^{+0.38}_{-0.36}$ [4]. In a boosted (high transverse momentum p_T) VBF $H(\rightarrow b\bar{b})$ search, CMS measured a signal strength of $4.9^{+1.9}_{-1.6}$ [5]. This letter presents an analysis of 133 fb^{-1} of $\sqrt{s} = 13 \text{ TeV}$ proton–proton (pp) collision data collected with the ATLAS detector in search of the VBF $H(b\bar{b}) + \gamma$ signature. A previous search for this signature using the same dataset observed a signal strength of $\mu_H = 1.3 \pm 1.0$, with an expected significance of 1.0 standard deviations (1.0σ) [6]. Since the previous effort, the multivariate

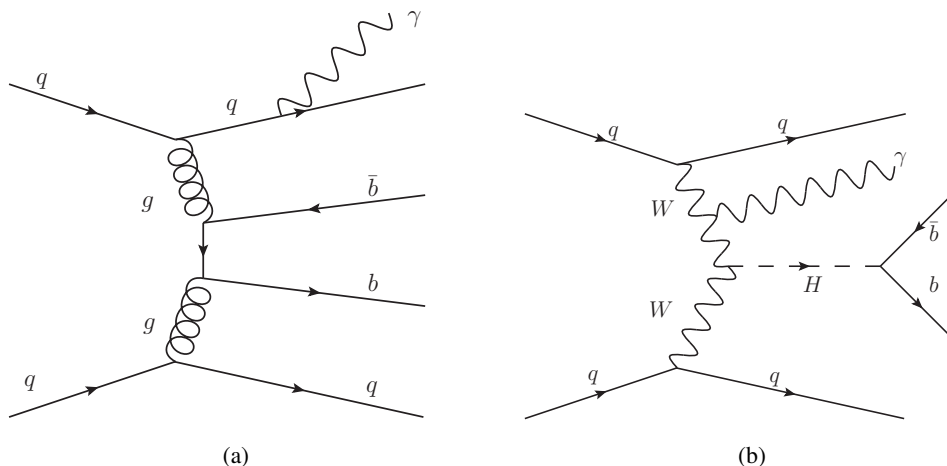


Figure 1: Representative Feynman diagrams for (a) non-resonant multijet background and (b) $H\gamma jj$ signal. The non-resonant multijet background can also have a qg initial state, and the photon can be radiated from an initial-state or final-state quark.

analysis technique has been markedly improved, replacing the previously used boosted decision tree (BDT) classifier with a densely connected neural network (NN) and including the discriminating power of kinematic input variables related to the di- b -jet invariant mass [7]. The data-fitting approach is also quite different from that adopted previously; it now extracts the signal strength directly from the classifier's output score distribution and uses the di- b -jet invariant mass (m_{bb}) to define regions of purity, rather than fitting the m_{bb} distribution. These advances, combined with much larger simulated event samples for the main backgrounds, reduce the signal strength uncertainty and provide improved signal sensitivity.

Details of the analysis procedure are provided in the following sections. Attributes of the experimental detector are given in Section 2. Particulars of the simulated data are presented in Section 3. Characteristics of data collection and event reconstruction and selection are delineated in Section 4. The techniques for separating this rare signal from common backgrounds are described in Section 5, followed in Section 6 with the specifics of ensuring that such backgrounds suitably model the data. Systematic uncertainties related to theory modelling and experimental detector effects are catalogued in Section 7, and the results are presented in Section 8.

2 ATLAS detector

The ATLAS experiment [8] at the Large Hadron Collider (LHC) is a multipurpose particle detector with a forward-backward symmetric cylindrical geometry and nearly 4π coverage in solid angle.¹ It consists of an inner tracking detector surrounded by a thin superconducting solenoid providing a 2 T axial magnetic

¹ ATLAS uses a right-handed coordinate system with its origin at the nominal interaction point (IP) in the centre of the detector and the z -axis along the beam pipe. The x -axis points from the IP to the centre of the LHC ring, and the y -axis points upwards. Polar coordinates (r, ϕ) are used in the transverse plane, ϕ being the azimuthal angle around the z -axis. Transverse momentum (p_T) and energy (E_T) are the components of momentum and energy in this transverse plane, perpendicular to the beamline. The pseudorapidity is defined in terms of the polar angle θ as $\eta = -\ln \tan(\theta/2)$ and is equal to the rapidity $y = \frac{1}{2} \ln((E + p_z)/(E - p_z))$ in the relativistic limit. Angular distance is measured in units of $\Delta R \equiv \sqrt{(\Delta y)^2 + (\Delta\phi)^2}$.

field, electromagnetic and hadronic calorimeters, and a muon spectrometer. The inner tracking detector covers the pseudorapidity range $|\eta| < 2.5$. It consists of silicon pixel, silicon microstrip, and transition radiation tracking detectors. Lead/liquid-argon (LAr) sampling calorimeters provide electromagnetic (EM) energy measurements with high granularity within the region $|\eta| < 3.2$. A steel/scintillator-tile hadronic calorimeter covers the central pseudorapidity range ($|\eta| < 1.7$). The endcap and forward areas are instrumented with copper/LAr and tungsten/LAr calorimeters for EM and hadronic energy measurements in the region $3.2 \leq |\eta| \leq 4.9$. The muon spectrometer surrounds the calorimeters and is based on three large superconducting air-core toroidal magnets with eight coils each. The field integral of the toroids ranges between 2.0 and 6.0 Tm across most of the spectrometer. The muon spectrometer includes a system of precision tracking chambers up to $|\eta| = 2.7$ and fast detectors for triggering up to $|\eta| = 2.4$. The luminosity is measured mainly by the LUCID-2 detector, which is located close to the beampipe. A two-level trigger system is used to select events [9]. The first-level trigger (L1) is implemented in hardware and uses a subset of the detector information to accept events at a rate below 100 kHz. This is followed by a software-based trigger (HLT) that reduces the accepted event rate to around 1.25 kHz on average depending on the data-taking conditions. A software suite [10] is used in data simulation, in the reconstruction and analysis of real and simulated data, in detector operations, and in the trigger and data acquisition systems of the experiment.

3 Monte Carlo event simulation samples

Fully simulated $H(\rightarrow b\bar{b}) + \gamma$ Monte Carlo (MC) signal events were generated at next-to-leading order (NLO) in QCD with MADGRAPH5_AMC@NLO [11] and showered using HERWIG 7 [12, 13], with the PDF4LHC15 parton distribution function (PDF) set [14]. This signal sample consists of Higgs bosons produced through VBF or VH processes. The set of tuned parameters is assigned the HERWIG 7 default values of H7-PS-MMHT2014LO and H7-UE-MMHT. Contributions from Higgs processes that are rarer in the selected phase space were considered separately but are treated as background. To describe the $H + \gamma$ component of other Higgs production processes, photon-filtered samples are derived from inclusive productions samples. The ggH sample used POWHEG [15–17] interfaced with PYTHIA 8 [18]. Higgs production in association with a $t\bar{t}$ pair ($t\bar{t}H$) is described with MC simulated events also generated using POWHEG interfaced with PYTHIA 8 and the NNPDF3.0 PDF set [19].

For the main non-resonant backgrounds, $b\bar{b}\gamma jj$ and $c\bar{c}\gamma jj$, large samples of fully-simulated Monte Carlo background events were generated at leading order (LO) specifically for this analysis, using MADGRAPH5_AMC@NLO for the matrix element calculation and PYTHIA 8 for the showering to final-state particles. Both of these samples used the PDF set PDF4LHC21 [20], and a restriction requiring dijet invariant mass above 500 GeV was applied to improve event selection efficiency in the ‘offline’ phase space discussed in Section 4. This truth-level dijet invariant mass requirement selects about 37% of all non-resonant QCD background events, which are then passed to the detailed detector simulation, without biasing the results. No events with truth-level invariant mass below 500 GeV have reconstructed-level invariant mass passing the offline requirement (>800 GeV) described in the next section. The final non-resonant background considered, $t\bar{t}$ production, is modelled by samples with all-hadronic or either partially or fully leptonic final states that were generated at NLO using POWHEG and showered using PYTHIA 8. These samples were normalized to the next-to-next-to-leading order (NNLO) cross-section predictions [21]. Electroweak $Z\gamma jj$ events were modelled specifically for this analysis at NLO using the same parameter values and PDF set as the signal sample. QCD $Z\gamma jj$ events were generated at LO using MADGRAPH5_AMC@NLO for the hard-scattering and PYTHIA 8 for showering.

Certain simulation configurations are common to all samples. The decays of bottom and charm hadrons were performed by EVTGEN [22]. Fully simulated minimum-bias events were generated using the PYTHIA 8 generator [23] with the NNPDF2.3LO PDF set and the A3 set of tuned parameters [24], and then overlaid on each hard-scatter interaction, in accord with the luminosity profile of the recorded data, to model pileup contributions from the same bunch crossing and neighbouring bunch crossings. All simulated samples include a full simulation of the ATLAS detector and its response [25] based on GEANT4 [26]. Generator choices, the orders of their calculations, and PDF sets used for the considered MC samples are summarized in Table 1.

Table 1: Generators, orders of calculation, and PDF sets used for the MC signal and background samples. The short name of AMC@NLO is used for MADGRAPH5_AMC@NLO.

Sample	Generator	Calculation order	PDF set
$H(\rightarrow b\bar{b}) + \gamma$	AMC@NLO+HERWIG 7	NLO	PDF4LHC15
$ggH + \gamma$	POWHEG NNLOPS+PYTHIA 8	NNLO	PDF4LHC15
$t\bar{t}H$ (all-hadronic)	POWHEG +PYTHIA 8	NNLO	NNPDF3.0
$t\bar{t}H$ (semileptonic)	POWHEG +PYTHIA 8	NNLO	NNPDF3.0
$Z(\rightarrow b\bar{b})\gamma jj$ (EWK)	AMC@NLO+HERWIG 7	NLO	PDF4LHC15
$Z(\rightarrow b\bar{b})\gamma jj$ (QCD)	MADGRAPH 5+PYTHIA 8	LO	PDF4LHC15
$b\bar{b}\gamma jj$ (non-resonant)	MADGRAPH 5+PYTHIA 8	LO	PDF4LHC21
$c\bar{c}\gamma jj$ (non-resonant)	MADGRAPH 5+PYTHIA 8	LO	PDF4LHC21
$t\bar{t}$ (non-all-hadronic)	POWHEG +PYTHIA 8	NLO	NNPDF3.0
$t\bar{t}$ (all-hadronic)	POWHEG +PYTHIA 8	NLO	NNPDF3.0

4 Object and event selection

The target signature of this analysis consists of two jets passing the requirements of a flavour-tagging algorithm (‘b-tagged jets’) from the b -quarks from the Higgs boson decay, of two additional jets (‘VBF-candidate jets’) with large invariant mass originating from the quarks that produced the hard scattering after the emission of the W or Z bosons that fused into a Higgs boson, and of a high-energy photon candidate. Isolated leptons are vetoed to maintain orthogonality with other ATLAS Higgs boson analyses. The selection requirements for these objects, which balance high signal acceptance with high background rejection, are summarized in Table 2.

This analysis uses the full Run-2 dataset recorded from 13 TeV pp collisions by the ATLAS detector from 2015 to 2018. Several triggers were chosen and combined to target the VBF phase space and maximize the acceptance. One motivation for requiring an associated photon in this Higgs boson search is the clean signature the photon provides for triggering, so each trigger chosen in the HLT requires at least one central photon with $p_T > 25$ GeV [27]. These triggers also require at least four jets with $p_T > 35$ GeV. Since the VBF topology tends to produce final-state jets with large angular separation and high invariant mass, the triggers required the largest dijet mass to be at least 700 GeV. Starting from late 2016, these triggers also required at least one jet to be b -tagged at the 77% efficiency working point of the MV2c20 or MV2c10 algorithm [28]. Because of changes in trigger availability and data-quality requirements [29], particularly

in the early Run-2 period, this analysis uses a total integrated luminosity of 133 fb^{-1} , slightly less than the 140 fb^{-1} used in other ATLAS full Run-2 analyses.

Interaction vertices from pp collisions are reconstructed from at least two tracks with $p_T > 500 \text{ MeV}$ that are consistent with originating from the beam collision region. If more than one interaction vertex is found in the event, the vertex with the largest sum of track squared p_T is selected as the primary vertex [30]. Due to trigger requirements, each of the four jets selected offline are required to have $p_T > 40 \text{ GeV}$. Jets are reconstructed using the anti- k_t algorithm [31, 32] with a radius parameter of $R = 0.4$, using as inputs ‘particle flow’ objects determined by matching the energy deposits in the calorimeter with tracks in the inner detector. This choice of particle flow objects leads to better resolution and pileup rejection [33] compared to Ref. [6], for which the jet clustering inputs were topological clusters of neighbouring cells in the calorimeters with significant energy deposits. To enhance pileup rejection, jets in the central region must be tightly matched to the event’s primary vertex according to a likelihood-based discriminant called the jet-vertex tagger (JVT), while the similar forward jet-vertex tagger accepts a looser matching for jets in the forward region [34, 35].

This analysis replaces the MV2c10 offline b -tagging algorithm, used in the previous analysis [6], with the more advanced DL1r algorithm, which employs a deep neural network for jet flavour classification [36]. The pseudorapidity of b -tagged jets must fall within the acceptance of the inner detector ($|\eta| < 2.5$), on which flavour-tagging heavily relies. Jets are b -tagged if they pass a fixed-cut working point of the DL1r tagging discriminant, which was calibrated using $t\bar{t}$ events to give 77% efficiency for true b -jets with $p_T \geq 20 \text{ GeV}$. The 77% efficiency working point provides rejection factors of 6 and 134 for charm and light-flavour jets, respectively. Per-jet scale factors are applied in MC events to account for efficiency differences between data and simulation [37–39]. In the simulation, b -tagging is fully emulated (‘direct tagging’) for all jets for signal events and for events from background processes other than $b\bar{b}\gamma jj$ and $c\bar{c}\gamma jj$. Simulated events that do not have at least two b -tagged jets are rejected outright. In contrast, the two main backgrounds, $b\bar{b}\gamma jj$ and $c\bar{c}\gamma jj$, undergo ‘truth-tagging’ to maximize the number of simulated events used in the subsequent steps of the analysis. Each event is assigned a weight based on the probability of each jet in the event to pass or fail the b -tagging requirement based on their kinematic properties and flavour of the originating quark. These tagging approaches yield kinematic distributions that differ negligibly in shape, but noticeably in normalization due to the online b -tagging trigger requirement which forces a direct-tagging scheme for at least one of the b -jet candidates [40]. This normalization effect is unimportant because the normalization of these two backgrounds combined is determined by a fit to data, as described in Section 6. To compensate for b -jet energy losses due to semileptonic decays and small out-of-cone energy deposits, jet energy corrections are applied, including corrections for muons or undetected neutrinos from such decays [41]. The two b -tagged jets with highest transverse momentum are selected as Higgs boson decay-product candidates. The remaining jets with p_T greater than 40 GeV are combined pairwise, and the VBF-candidate jets are selected as the pair with the highest invariant mass, requiring that this mass exceeds 800 GeV, where the trigger efficiency reaches a plateau.

The high-energy photon in the signal signature is the photon candidate with highest transverse momentum, with minimum $p_T \geq 30 \text{ GeV}$ and pseudorapidity in the range $|\eta| < 1.37$ or $1.52 < |\eta| < 2.37$. Photons are reconstructed from topological clusters of neighbouring cells in the electromagnetic calorimeter, not matched or matched to tracks in the inner detector depending on whether the photon underwent a conversion to e^+e^- prior to reaching the calorimeter. A tight photon identification selection, based on shower-shape criteria is applied to avoid selecting misidentified electrons or jets reconstructed as photons [42]. Photon isolation requirements set an upper bound on the energy deposited in the calorimeter in a cone surrounding the photon, further helping to reject jets faking prompt photons.

Electron candidates must satisfy $p_T > 25$ GeV, $|\eta| < 2.47$, and tight identification criteria [42]. Muon candidates must satisfy $p_T > 25$ GeV and loose identification criteria [43]. For electrons, track-based isolation requirements depend on the electron's p_T , using tracks within a variable cone size of up to $\Delta R = 2$. The calorimeter-based isolation requires that the sum of cluster transverse energies within a cone of $\Delta R = 2$ is less than 3.5 GeV. For muons, the isolation requirement is that tracks within a cone of size $\Delta R = 0.2$ around the muon candidate track must sum to less than 1.25 GeV in p_T . Any events containing isolated electrons or muons with $p_T > 25$ GeV are vetoed. Electron (muon) candidates are matched to the primary vertex by requiring that the significance of their transverse impact parameter d_0 satisfies $|d_0/\sigma(d_0)| < 5.0$ (3.0), where $\sigma(d_0)$ is the measured uncertainty in d_0 , and by requiring that their longitudinal impact parameter $z_0 \sin(\theta)$ satisfies $|z_0 \sin(\theta)| < 0.5$ mm.

To reduce instances of considering the same physics object as two different reconstructed objects, an overlap removal is performed after the kinematic criteria for object selection are met. First, any jet within $\Delta R = 0.2$ of an electron is removed, and a jet with fewer than three associated tracks is removed if it is within $\Delta R = 0.2$ of a muon. Any remaining electrons or muons found within $\Delta R = 0.4$ of a jet are then removed. Then, any photon identified within $\Delta R = 0.4$ of an electron or muon is removed. Finally, any jet that is within a region of $\Delta R = 0.4$ around a photon with $p_T > 30$ GeV is removed, as it is likely to have been reconstructed from the same energy deposits as the photon candidate.

After the event selection criteria have been applied, candidate events are divided into two regions, which are used together in the classifier training and in the signal extraction fit. The signal region (SR) contains most of the signal sensitivity, comprising events with m_{bb} in the range $100 \text{ GeV} \leq m_{bb} \leq 150 \text{ GeV}$ around the Higgs boson mass. The control region (CR) includes events in the m_{bb} sidebands outside this window, specifically $m_{bb} < 100 \text{ GeV}$ and $150 \text{ GeV} < m_{bb} \leq 220 \text{ GeV}$. It is primarily used to extract background normalizations and to constrain nuisance parameters representing correlated systematic uncertainties.

Table 2: Trigger and offline event selection criteria and region definitions for the $H(\rightarrow b\bar{b})jj + \gamma$ signature. The p_T and $|\eta|$ offline jet requirements are used to match trigger selections and b -tagging requirements. Criteria in m_{bb} define the control and signal regions.

Trigger	L1	≥ 1 photon with $p_T > 22$ GeV
	HLT	≥ 1 photon with $p_T > 25$ GeV ≥ 4 jets with $p_T > 35$ GeV and $ \eta < 4.9$ (or ≥ 3 jets with $ \eta < 4.9$ and ≥ 1 b -tagged jet with $ \eta < 2.5$) $m_{jj} > 700$ GeV
Offline		≥ 1 photon with $p_T > 30$ GeV and $ \eta < 1.37$ or $1.52 < \eta < 2.37$ ≥ 2 b -tagged jets with $p_T > 40$ GeV and $ \eta < 2.5$ ≥ 2 additional jets with $p_T > 40$ GeV and $ \eta < 4.5$ $m_{jj} > 800$ GeV No electrons or muons with $p_T > 25$ GeV $m_{bb} \leq 220$ GeV
Region selection	Signal region	$100 \text{ GeV} \leq m_{bb} \leq 150 \text{ GeV}$
	Control region	$m_{bb} < 100 \text{ GeV}$ and $150 \text{ GeV} < m_{bb} \leq 220 \text{ GeV}$

5 Multivariate analysis

An improved multivariate analysis technique is key to this analysis. An NN replaced the BDT used in the previous analysis because the NN showed better signal and background discrimination with identical inputs. KERAS [44], a high-level interface of TENSORFLOW [45], was used to train an NN to provide a classification score, distinguishing signal-like (high score) events from those resembling the non-resonant QCD $b\bar{b}\gamma jj$ or $c\bar{c}\gamma jj$ events constituting the main backgrounds (low score). A two-fold method was used to train and evaluate the performance of the NN: two separate models with identical hyperparameters were trained on separate halves of the MC training samples, which contain both the control- and signal- region phase spaces. Evaluating the MC events using the model that did not include those events during training allows the use of the full size of the MC samples for signal extraction. Data and MC background samples that were not used in training are also split in half, and the two halves are evaluated by each of the two models and then recombined.

In order to optimize the choice of input variables and hyperparameters, a comparison metric was formed to assess the signal-background separation significance after successive trainings epochs. The significance is estimated by binning the NN output score distribution into 20 equal-width bins, dividing the weighted number of signal events by the square root of the weighted number of background events (S/\sqrt{B}) in each bin, and summing these S/\sqrt{B} values in quadrature. Many kinematic variables were considered as inputs; combinations of these variables were used to train individual models, which were evaluated using the defined metric to find the optimal set. After optimization, the 14 input variables listed in Table 3 were selected, and no addition or substitution made to this grouping was found to produce better separation between signal and background. In addition to the improvements gained from the use of an NN, this analysis profits from the use of the discriminating power of m_{bb} and correlated variables, which could not be exploited in the previous analysis because it would sculpt the background parametrization. The use of variables related to an event's jet multiplicity is also a new development, motivated by the signal's tendency, with mostly electroweak vertices, to have fewer jets than the QCD background. The same optimization method was employed to select specific hyperparameter settings: each final NN model has 11 hidden layers with 256 neurons per layer in the bulk. The ratio of the sums of weights of the background and signal training samples was also optimized, after which the signal acceptance contributed more than twice as much as the background rejection to the loss function. To prevent overtraining, the training is stopped when the calculated loss function does not decrease significantly for five consecutive training epochs, which typically occurs within 25 epochs for the final selection of hyperparameters.

6 Signal and background composition and modelling

The previous analysis of this signature with the full Run-2 data relied on a fit to the invariant mass spectrum of the two b -tagged jets (m_{bb}), using an analytic shape for the background, with parameters determined from the fit to the data. That approach introduced large systematic uncertainties from the potential bias arising from the choice of the model for the background. This analysis adopts a binned likelihood fitting strategy to the NN score, based on signal and background templates derived from MC simulations, reducing modeling-related systematic uncertainties and benefitting from the use of a more discriminating variable as the fit observable.

Simulations and calculations of the SM cross-sections predict that non-resonant backgrounds are expected to contribute approximately 99% of the total background. Prior to any constraints from a fit to data, QCD

Table 3: Kinematic variables used as inputs to the neural-network classifier. This list is ordered in decreasing correlation between the input variable and the NN score, i.e. in decreasing order of importance in the NN training.

Input variable	Description
n_{jets}	The total number of jets with $p_{\text{T}} \geq 40$ GeV in the event
$p_{\text{T}}^{\text{bal}}$ [6]	Transverse momentum balance for selected final-state objects
$\Delta\phi(bb, jj)$	Azimuthal angle between the momenta of the di- b -jet system and the two VBF-candidate jets
m_{bb}	Invariant mass of the two leading b -tagged jets
p_{T}^{bb}	Transverse momentum of the two leading b -tagged jets
m_{jj}	Invariant mass of the two VBF-candidate jets
$\cos\theta_C$	Cosine of the angle between the two VBF-candidate jets and the two b -tagged jets planes in the centre-of-mass frame of the $bbjj$ system
$\min(\Delta R(b, \gamma))$	The minimum angular distance between one of the b -tagged jets and the photon
$\Delta\eta(j, j)$	Pseudorapidity difference between two VBF-candidate jets
$\Delta R(b_1, j_1)$	Angular distance between the leading b -tagged jet and the leading VBF-candidate jet
$p_{\text{T}}^{j_1}$	Transverse momentum of the leading VBF-candidate jet
$\text{cen}(\gamma jj)$ [6]	Centrality of the photon relative to the VBF-candidate jets
$\Delta\eta(b, b)$	Pseudorapidity difference between the two leading b -tagged jets
η_{j_5}	Pseudorapidity of a 5th jet (2 b -tagged jets, 2 VBF-candidate jets, plus this extra 5th jet); if no 5th jet is present, a value is assigned using a probability density matching the distribution of 5-jet events from the respective sample population

multijet production with b -quarks in association with a photon ($b\bar{b}\gamma jj$) dominates with a 70% contribution, multijet production with mistagged c -quarks in association with a photon ($c\bar{c}\gamma jj$) contributes an estimated 18%, and non-resonant production of top quarks ($t\bar{t}$) is estimated to contribute 11% of the total expected background. Non-resonant QCD production with light-flavour quarks in association with a photon ($l\bar{l}\gamma jj$) is conservatively estimated to contribute $< 0.5\%$ of the total background yield based on the mistagging rate for light-flavour jets, so no template for this background source is included.

Although resonant backgrounds are estimated to contribute only 1% of the total background, templates are still produced and included in the fit because the kinematics of resonant backgrounds are more similar to signal than to the non-resonant backgrounds. The template for the background from Z boson production in association with a photon and jets, $Z(\rightarrow b\bar{b})\gamma jj$, is built from the sum of two contributions, electroweak and QCD production, as described in Section 3. The contribution from $W\gamma$ production is estimated to be only 1% of that from $Z\gamma$ after selection, so no template is included in the fit for $W\gamma jj$. Other Higgs production modes contribute negligibly to the selected phase space, due to the required associated photon and the VBF-specific event selections. Nevertheless, templates are created for ggH and $t\bar{t}H$ production, which is treated as background to the predominantly VBF Higgs signal.

While this analysis focuses on the VBF $H\gamma$ production mode of the $bb\gamma jj$ signal, $VH\gamma$ contributes an estimated 8.8% of the signal sample at MC generator level, but it is expected to contribute less than 1% after final event selection phase-space requirements. Of the signal VBF events at generator level, about 92.3% are estimated to be from Higgs boson production via WW -fusion, due to production via ZZ -fusion being suppressed by the interference effect mentioned in Section 1.

The templates for the $b\bar{b}\gamma jj$ and $c\bar{c}\gamma jj$ backgrounds use ‘truth-tagging’ to benefit from as many of the MC

events as possible, and tests were performed to ensure that the NN output distribution shapes are compatible with direct-tagged sample templates [40]. These two backgrounds share a floating normalization factor, allowing their combined yield to be fitted directly to data. The remaining background and signal templates use direct-tagged samples. While truth-tagged MC signal events are used in the NN training to have ample training samples, the signal fit template is derived by evaluating the NN on only direct-tagged events.

As mentioned in Section 1, the fitting strategy extracts the signal directly from the NN output score distribution, and uses a control region and signal region defined by ranges in m_{bb} . This fit relies on template distributions derived from MC, so it is important to ensure that the MC background simulation agrees well with data in the control region where there is little signal contamination. In this control region, discrepancies between data and MC simulation are observed for several kinematic variables, particularly n_{jets} , $\min(\Delta R(b, \gamma))$, $\Delta\eta(j, j)$, and m_{bb} . This was also observed in Ref. [6], and is due to both the difficulty of modelling non-resonant multijet backgrounds and the low order at which the dominant MC samples were generated.

To achieve better agreement between data and MC events in the NN output distribution, reweighting scale factors for the two main background, $b\bar{b}\gamma jj$ and $c\bar{c}\gamma jj$, are extracted from distributions of the 14 NN input kinematic variables listed in Table 3. These backgrounds are reweighted together with identical kinematic scale-factor functions as follows. After the MC-estimated $t\bar{t}$ contribution is subtracted, the data are compared with the predicted $b\bar{b}\gamma jj + c\bar{c}\gamma jj$ background, via the ratio of the normalized binned kinematic input-variable distributions in the m_{bb} -sideband control region. To this ratio, a sixth-order polynomial is fitted successively and iteratively for each input variable, in the reverse order of their correlation with NN score. The function is then applied to the MC $b\bar{b}\gamma jj$ and $c\bar{c}\gamma jj$ samples, in both the control region and signal regions, in order to scale these dominant backgrounds to better represent the data. These kinematic reweighting scale factors account for any mismodelling of these non-resonant QCD backgrounds, as well as for any contamination from backgrounds not otherwise considered, such as jets misidentified as photons.

The NN training is repeated after kinematic reweighting to obtain the final model, such that the modified event weights can affect the loss function and training results accordingly. Despite the large number of compounding scale factors, the overall impact on the NN output is relatively small because their effects partially cancel. Additionally, the reweighted result is largely immune to procedural changes, as reflected in the shape uncertainty due to this kinematic reweighting (see Section 7). Very good closure between MC and data distribution shapes after kinematic reweighting can be seen in the control region and the background-rich areas of the signal region, i.e. in the m_{bb} SR window $100 \leq m_{bb} \leq 150$ GeV but with an NN score less than 0.6. Figure 2 shows the NN output distributions for the MC backgrounds before and after kinematic reweighting in comparison with data in the control region and signal region. In the CR and in the background-rich bins of the SR, the data and reweighted MC distributions agree within statistical uncertainties.

7 Systematic uncertainties

Theory and experimental uncertainties are described with a total of 78 nuisance parameters that can modify the normalization and shape of the signal and background templates. The effects of these nuisance parameters on the signal strength uncertainty ($\sigma(\mu_H)$) are categorized and summarized in Table 4. The grouped effect of each uncertainty category is calculated by performing a fit with the category's corresponding nuisance parameters fixed to their best-fit values, and taking the difference in quadrature between $\sigma(\mu_H)$ from the nominal fit and from this fit as the impact of that group of systematic uncertainties.

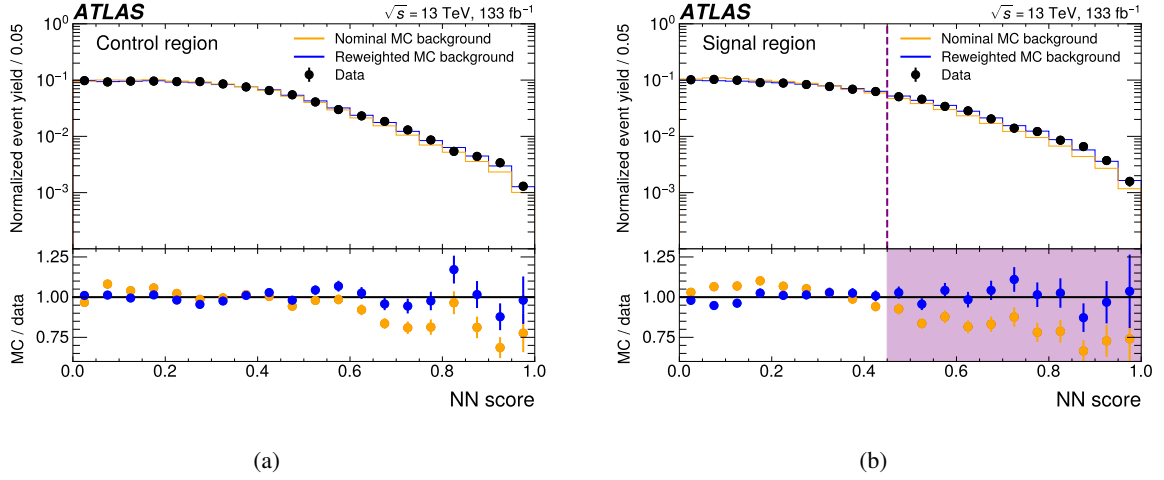


Figure 2: NN output distributions for data compared with those for all MC backgrounds with and without kinematic reweighting. Reweighting scale factors are extracted from comparisons between kinematic distributions for MC backgrounds and data in the (a) control region m_{bb} sidebands. The low score bins of the (b) signal region, which have negligible signal, are used for validation. The purple dashed line marks the divide between the low-score SR bins, used for validation of the reweighting scale factors, and high-score bins containing most of the signal. The total yields of MC and data events are individually normalized to 1, making this a direct comparison of NN output distribution shapes.

Template smoothing is employed in these final-fit variations to reduce the inflation of uncertainties due to correlated statistical fluctuations.

The dominant source of signal strength uncertainty is the statistical uncertainty, which contributes $\sigma(\mu_H) = 0.57$. This is due to the small $H + \gamma$ production cross section at $\sqrt{s} = 13$ TeV. Nevertheless, much attention was paid to reducing the experimental and modelling uncertainties as much as possible relative to the previous analysis. To reduce the statistical uncertainties of the background templates, new and enlarged $b\bar{b}\gamma jj$ and $c\bar{c}\gamma jj$ samples were simulated; these reduced the MC statistical uncertainty contributions to a total of $\sigma(\mu_H) = 0.25$.

Theory uncertainties arising from the lack of higher-order corrections, the PDF and α_s , and the parton shower generator are considered for the signal and major backgrounds. To estimate the contributions from missing higher-order corrections in the calculations, an envelope of the effects of varying the chosen renormalization and factorization scale values is used. The dominant normalization uncertainties of the $b\bar{b}\gamma jj$ and $c\bar{c}\gamma jj$ backgrounds come from this variation of the renormalization scale μ_R and the factorization scale μ_F . MC events were reweighted in accord with changes in these QCD scales, leading to a change of roughly +60% and -40% in the yield for each sample, independent of NN score. The effects of a seven-point variation, $(\{\mu_R, \mu_F\} \times \{0.5, 0.5\}, \{1.0, 0.5\}, \{0.5, 1.0\}, \{1.0, 1.0\}, \{1.0, 2.0\}, \{2.0, 1.0\}, \{2.0, 2.0\})$, is taken as the systematic uncertainty, including both the cross-section and acceptance uncertainties. Shape effects from these scale variations are not large, but are included and treated as being uncorrelated with the normalization effects to avoid a degeneracy between these nuisance parameters and the floating normalization factor. The scale-uncertainty nuisance parameters for $b\bar{b}\gamma jj$ and $c\bar{c}\gamma jj$ are assumed to be uncorrelated as well, despite their production processes being similar, and in doing so, the ratio of the yields of the two samples is given a large range of freedom.

The uncertainties due to missing higher orders for the signal are evaluated in the same way as for the

Table 4: The observed impacts of the statistical, theory, and experimental uncertainties on the signal strength uncertainty, as extracted from the final fit to observed data. Data statistical uncertainty is the single largest contribution to the total uncertainty.

Source of uncertainty	$+\sigma(\mu_H)$	$-\sigma(\mu_H)$
Statistical		
Data sample size	+0.57	-0.56
MC background templates	+0.25	-0.22
Theory and modelling		
Kinematic reweighting	+0.07	-0.06
MC modelling	+0.19	-0.15
Background normalization	+0.13	-0.08
Experimental		
Luminosity	+0.004	-0.006
Jet + photon selection	+0.15	-0.11
b -tagging	+0.03	-0.03
Total	+0.69	-0.64
Total MC statistical	+0.25	-0.22
Total theory	+0.24	-0.18
Total experimental	+0.16	-0.12

background, but they are found to be much smaller, about 1%, and correlation between normalization and shape components is allowed in the fit. For the $t\bar{t}$ background, the uncertainty in the cross-section estimated at NNLO in QCD [46] is used to account for QCD scale-variation effects, and thus an overall relative uncertainty of $^{+2.5\%}_{-3.6\%}$ is assigned to the $t\bar{t}$ background. For the small $Z\gamma jj$ background, a conservative estimate of $\pm 16\%$ is adopted for the overall magnitude of scale-variation effects, matching the uncertainty estimated in Ref. [47].

Systematic uncertainties due to the choice of PDF and α_s are estimated by reweighting probability densities at the event level. For signal, 42 members of the set PDF4LHC15 are considered, including 40 PDF eigenvariations along with α_s variations upward and downward by 1 standard deviation. The uncertainty is calculated as the sum in quadrature of the effects of these variations [14], which leads to an uncertainty of 2.2% for signal. For $b\bar{b}\gamma jj$ and $c\bar{c}\gamma jj$, 100 PDF variations of the set PDF4LHC21 are considered, and the uncertainty is computed as the standard deviation of the yields from each variation. This PDF uncertainty is combined in quadrature with the change in yield from the average of the upward and downward α_s variations. The resulting PDF and α_s choice uncertainty is 3.2% for $b\bar{b}\gamma jj$ and 3.3% for $c\bar{c}\gamma jj$. The equivalent uncertainty for $t\bar{t}$ production is 2.5%, again taken from the uncertainty in the best prediction of the NNLO cross-section [48]. PDF and α_s uncertainties are not considered directly for the other backgrounds, as such small variations on the rarer backgrounds have negligible impact on the signal measurement. However, for the minor Higgs boson production modes that are treated as backgrounds in this analysis, an overall normalization uncertainty of 20% is introduced to conservatively cover any modelling uncertainties.

The largest shape variation from a single systematic uncertainty source comes from the choice of parton shower generator, giving bin-by-bin variations as large as 5%. For the dominant $b\bar{b}\gamma jj$ and $c\bar{c}\gamma jj$

backgrounds, alternative samples were produced using MADGRAPH5_AMC@NLO and HERWIG, instead of the MADGRAPH5_AMC@NLO and PYTHIA combination used in obtaining the nominal templates. These samples were produced at MC truth-level, so a method was designed to extract the truth-level effects of differences between PYTHIA and HERWIG showering and transfer those effects to modifications of the fully simulated NN output distributions. Scale factors are extracted from the ratios of truth-level PYTHIA and HERWIG kinematic distributions for each of the 14 NN input variables (similar to the process for kinematic reweighting discussed in Section 6). These scale factors are then applied to the fully simulated PYTHIA NN output to obtain a facsimile of a fully simulated HERWIG NN output. The effects of these representative parton shower variations are included as systematic uncertainties with two-sided symmetrization. Separate nuisance parameters were introduced for the signal region and control region for these dominant backgrounds, because the NN output distribution shape is affected differently in the two regions.

For signal, the alternative shower samples were generated with HERWIG 7 like the nominal samples but with variations of the hard scale factor by factors of two, which affects the maximum allowed transverse momentum for shower emissions [13]. The method used for transfer from truth-level to proxy fully simulated distributions is the same as described for the two main non-resonant backgrounds, and it results in bin-by-bin variations as large as 20% in signal-sensitive regions. For $t\bar{t}$ production, hard-scatter (matrix element) and parton shower uncertainties are estimated by comparing the nominal samples directly with fully simulated samples generated with MADGRAPH5_AMC@NLO 5 replacing POWHEG and HERWIG 7 replacing PYTHIA 8. The parton shower variation changes the $t\bar{t}$ sample normalization by almost 10%. The effects of the matrix element variation are small in the control region, changing the $t\bar{t}$ normalization by 0.6%, but larger in the signal region, with a normalization change of 5.3%.

The kinematic reweighting of the dominant $b\bar{b}\gamma jj$ and $c\bar{c}\gamma jj$ backgrounds also has associated systematic uncertainties. The reweighting is performed by extracting scale factors from the ratio of the sum of these two simulated backgrounds to the $t\bar{t}$ -subtracted data. Thus, the systematic uncertainty is derived by considering how the result of this reweighting changes if the $t\bar{t}$ contribution is overestimated or underestimated within its theoretical uncertainties. Since the scale factors are extracted concurrently for $b\bar{b}\gamma jj$ and $c\bar{c}\gamma jj$ directly in the control region and extrapolated to the signal region, uncertainty is considered only in the signal region and is correlated between the two backgrounds. Due to the robustness of the kinematic reweighting procedure, these $t\bar{t}$ contribution variations have little impact on the NN output distribution's shape. In the unique case of m_{bb} , for which the phase space covered in the signal region is not represented in the control region, the entire reweighting is taken as an uncertainty: a systematic variation without the scale factors derived for m_{bb} is included in the signal region, and the associated nuisance parameter ranks among the highest in terms of impact to the signal strength uncertainty. The combination of these two kinematic reweighting uncertainty nuisance parameters gives a 6 – 7% impact on the signal strength uncertainty.

Experimental systematic uncertainties arise from uncertainties in the integrated luminosity, jet energies and resolutions, electromagnetic object identification and isolation, and b -jet tagging efficiency. These systematic uncertainties are correlated between samples and fit regions via shared nuisance parameters. Due to the uncertainty in the measurement of the integrated luminosity collected by ATLAS [49], an overall normalization uncertainty of 0.83% is applied to every template sample, but this has negligible impact on the final signal strength uncertainty. Systematic uncertainties arising from jet energy scale (JES) and resolution (JER) uncertainties [50] dominate the experimental category with a 13% contribution to the signal strength uncertainty. Experimental uncertainties arising from the identification and isolation of photons and electrons, as well as their energy and its resolution [42], are also considered but have negligible impact. Uncertainties in b -jet tagging efficiency include effects for both online and offline

selections [37–39]. The overall background uncertainty arising from b -tagging requirements is about 2–3% and fairly independent of NN score for all samples, but variations in both shape and normalization are considered for the signal and dominant background samples. In all, b -jet tagging uncertainties contribute 3% to the signal strength uncertainty.

8 Results

To extract the signal strength, a binned maximum-likelihood fit is performed directly on the neural-network classifier’s output distribution using TRExFitter, which is built from HISTFACTORY [51] and ROOFIT [52]. The signal strength and the floating normalization factor for the sum of the two main non-resonant backgrounds, $b\bar{b}\gamma jj$ and $c\bar{c}\gamma jj$, are extracted [53] by a simultaneous fit of the control and signal regions, which are defined by the invariant mass of the two leading b -tagged jets as described in Section 6.

Both the control region and signal region have 20 NN score bins with widths optimized independently for each region to maximize the signal sensitivity while keeping the total statistical uncertainties low. The optimization results in very fine binning in the high score range of the signal region, where the signal purity is highest, as well as fine binning in the low score range of the control region, where the number of background events is large. The highest-score bins of the signal region have by far the highest signal purity and sensitivity in the fit. The post-fit NN score distributions in the control region and signal region are shown in Figure 3. The pre-fit and post-fit yields for the MC-simulated backgrounds and signal are listed in Table 5 together with the number of data events.

The Higgs boson signal strength is defined relative to the Standard Model prediction. An inclusive signal strength of $\mu_H = 0.2 \pm 0.7$ is observed, compared to an expected value of 1.0 ± 0.7 . This corresponds to an observed significance of 0.3 standard deviations, compared to an expected significance of 1.5 standard deviations. A likelihood ratio comparison between the observed fit and a saturated model, which has complete freedom for a perfect fit to data, gives a goodness-of-fit p -value of 30%. The final fit’s normalization of the dominant backgrounds is about 85% of the leading-order MC estimate. The measured signal strength is compatible with the previous result, with a p -value of 37%. This probability is calculated without considering correlations because the overlap of data events in the signal-sensitive regions of the two analyses is less than 5%.

To further confirm that the background modelling using the MC-derived templates is acceptable, kinematic distributions are compared with data in the signal region, in slices of NN score, with the propagation of post-fit pulls from the fit to NN score. Figure 4 shows the di- b -jet invariant mass spectrum in four NN score slices of the signal region. The post-fit MC and data spectra agree within their uncertainties, and no divergence in agreement appears at high score.

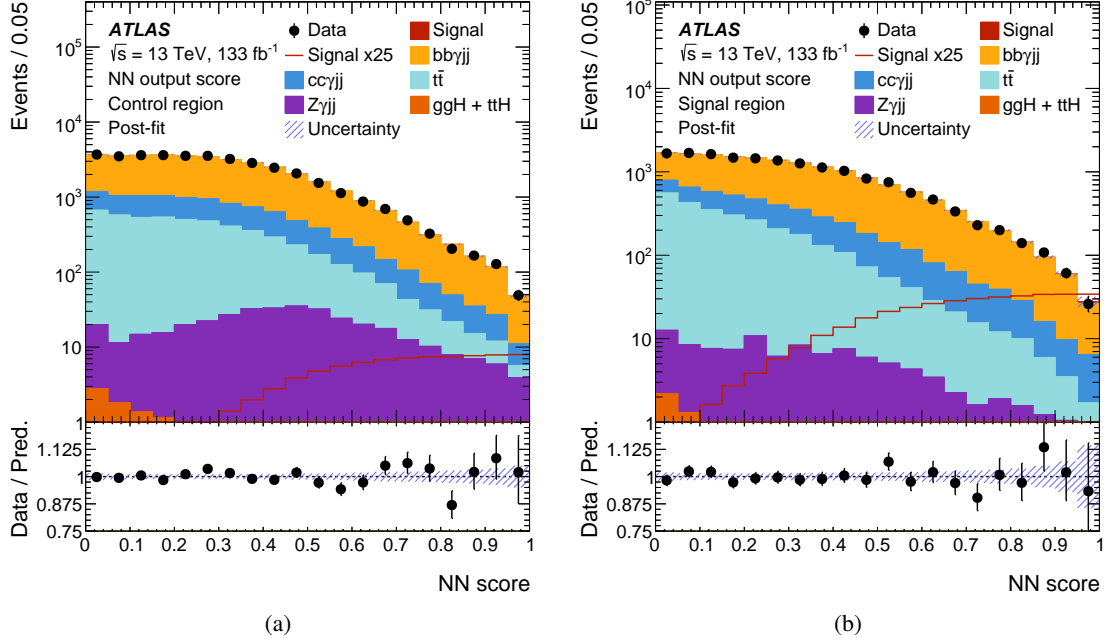


Figure 3: Post-fit plots for the observed dataset, showing (a) the control region and (b) the signal region. Background and signal templates are shown with all normalization factors and post-fit nuisance parameter pulls incorporated. Data bin yields are represented with black markers, with error bars representing statistical uncertainties. The red line represents the post-fit signal scaled by a factor of 25, while the stacked red signal histogram, which is only visible at high NN score in the signal region, is normalized to the fitted signal strength of $\mu = 0.2$. The ratio plots in the lower panels display the bin-by-bin ratio of the data to the post-fit total of signal and background yields. Post-fit uncertainties are depicted with a blue hashed band in both the yield and ratio plots. The NN score is renormalized in the post-fit distributions to give regular bin widths, so the binning does not reflect the raw score optimized binning, which is finer in high score signal region bins and low score control region bins.

Table 5: Pre-fit and post-fit signal and background yields and data yields in the control region, and in the signal region in the sum of the 17 lowest-NN-score bins and individually in the three highest-NN-score bins. The total background yield and its uncertainty are given post-fit.

Yields	CR		SR Bins 0-16		SR Bin 17		SR Bin 18		SR Bin 19	
	Pre	Post	Pre	Post	Pre	Post	Pre	Post	Pre	Post
$b\bar{b}\gamma jj$	30600	27400	12400	11100	86	78	55	49	23	20
$c\bar{c}\gamma jj$	7400	5100	3200	2200	15	10	9	6	7	5
$t\bar{t}$	4600	4800	2600	2700	4	5	2	2	1	1
$Z\gamma jj$	400	400	100	100	1	1	1	1	0.4	0.4
$ggH + t\bar{t}H$	10	10	8	8	<0.1	<0.1	<0.1	<0.1	<0.1	<0.1
Total background	37700 ± 130		16100 ± 76		94 ± 5		59 ± 4		27 ± 4	
Signal	14	3	41	9	6	1	6	1	6	1
Data	37701		16070		108		61		26	

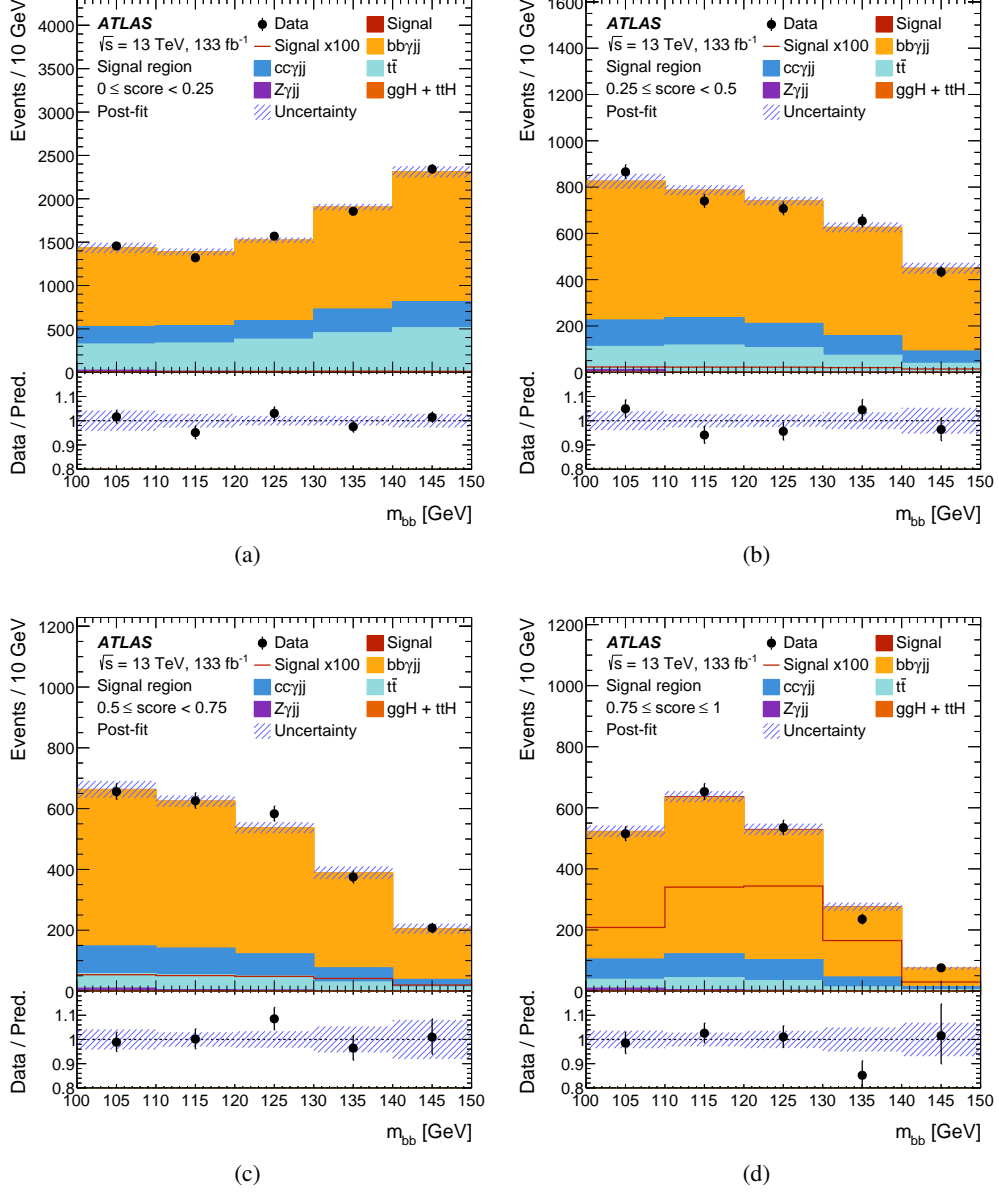


Figure 4: Post-fit signal region m_{bb} distributions in slices of NN score. Stacked histograms represent post-fit MC background and signal, and the black markers with error bars represent data. The red lines represent post-fit signal distributions scaled by a factor of 100. The stacked red histogram, which can only be visualized in some bins of the highest NN score slice, is normalized to the post-fit signal strength, $\mu = 0.2$. The lower panels show the ratio of data to post-fit MC signal plus background. Post-fit uncertainties are depicted by blue hashed lines.

9 Conclusion

A search was conducted for associated production of a Higgs boson and a high-energy photon. The full Run-2 dataset from 13 TeV proton–proton collisions collected by the ATLAS detector at the LHC is examined, corresponding to an integrated luminosity of 133 fb^{-1} . The search focuses on the $H(\rightarrow b\bar{b}) + \gamma$ final state, the dominant Higgs boson decay mode, and the photon requirement greatly reduces the multijet background. The photon requirement also makes vector-boson fusion the dominant Higgs boson production mode, with events characterized by the additional presence of two well-separated VBF-candidate jets having a high invariant mass. This analysis improves on a previous one in this channel by using updated and extended Monte Carlo background samples, finely optimized multivariate analysis techniques for signal–background separation, and a novel data-fitting approach to measure the signal strength. With these improvements, a signal significance of 1.5σ is expected, nearly 50% higher than the expected significance in the previous full Run-2 analysis. A Higgs boson signal strength of 0.2 ± 0.7 is measured, with an observed significance of 0.3σ .

Acknowledgements

We thank CERN for the very successful operation of the LHC and its injectors, as well as the support staff at CERN and at our institutions worldwide without whom ATLAS could not be operated efficiently.

The crucial computing support from all WLCG partners is acknowledged gratefully, in particular from CERN, the ATLAS Tier-1 facilities at TRIUMF/SFU (Canada), NDGF (Denmark, Norway, Sweden), CC-IN2P3 (France), KIT/GridKA (Germany), INFN-CNAF (Italy), NL-T1 (Netherlands), PIC (Spain), RAL (UK) and BNL (USA), the Tier-2 facilities worldwide and large non-WLCG resource providers. Major contributors of computing resources are listed in Ref. [54].

We gratefully acknowledge the support of ANPCyT, Argentina; YerPhI, Armenia; ARC, Australia; BMWFW and FWF, Austria; ANAS, Azerbaijan; CNPq and FAPESP, Brazil; NSERC, NRC and CFI, Canada; CERN; ANID, Chile; CAS, MOST and NSFC, China; Minciencias, Colombia; MEYS CR, Czech Republic; DNRf and DNSRC, Denmark; IN2P3-CNRS and CEA-DRF/IRFU, France; SRNSFG, Georgia; BMFTR, HGF and MPG, Germany; GSRI, Greece; RGC and Hong Kong SAR, China; ICHEP and Academy of Sciences and Humanities, Israel; INFN, Italy; MEXT and JSPS, Japan; CNRST, Morocco; NWO, Netherlands; RCN, Norway; MNiSW, Poland; FCT, Portugal; MNE/IFA, Romania; MSTDI, Serbia; MSSR, Slovakia; ARIS and MVZI, Slovenia; DSI/NRF, South Africa; MICIU/AEI, Spain; SRC and Wallenberg Foundation, Sweden; SERI, SNSF and Cantons of Bern and Geneva, Switzerland; NSTC, Taipei; TENMAK, Türkiye; STFC/UKRI, United Kingdom; DOE and NSF, United States of America.

Individual groups and members have received support from BCKDF, CANARIE, CRC and DRAC, Canada; CERN-CZ, FORTE and PRIMUS, Czech Republic; COST, ERC, ERDF, Horizon 2020, ICSC-NextGenerationEU and Marie Skłodowska-Curie Actions, European Union; Investissements d’Avenir Labex, Investissements d’Avenir Idex and ANR, France; DFG and AvH Foundation, Germany; Herakleitos, Thales and Aristeia programmes co-financed by EU-ESF and the Greek NSRF, Greece; BSF-NSF and MINERVA, Israel; NCN and NAWA, Poland; La Caixa Banking Foundation, CERCA Programme Generalitat de Catalunya and PROMETEO and GenT Programmes Generalitat Valenciana, Spain; Göran Gustafssons Stiftelse, Sweden; The Royal Society and Leverhulme Trust, United Kingdom.

In addition, individual members wish to acknowledge support from Armenia: Yerevan Physics Institute (FAPERJ); CERN: European Organization for Nuclear Research (CERN DOCT); Chile: Agencia Nacional de Investigación y Desarrollo (FONDECYT 1230812, FONDECYT 1240864, Fondecyt 3240661); China: Chinese Ministry of Science and Technology (MOST-2023YFA1605700, MOST-2023YFA1609300), National Natural Science Foundation of China (NSFC - 12175119, NSFC 12275265, NSFC-12075060); Czech Republic: Czech Science Foundation (GACR - 24-11373S), Ministry of Education Youth and Sports (ERC-CZ-LL2327, FORTE CZ.02.01.01/00/22_008/0004632), PRIMUS Research Programme (PRIMUS/21/SCI/017); EU: H2020 European Research Council (ERC - 101002463); European Union: European Research Council (BARD No. 101116429, ERC - 948254, ERC 101089007), Horizon 2020 Framework Programme (MUCCA - CHIST-ERA-19-XAI-00), European Union, Future Artificial Intelligence Research (FAIR-NextGenerationEU PE00000013), Italian Center for High Performance Computing, Big Data and Quantum Computing (ICSC, NextGenerationEU); France: Agence Nationale de la Recherche (ANR-20-CE31-0013, ANR-21-CE31-0013, ANR-21-CE31-0022, ANR-22-EDIR-0002); Germany: Baden-Württemberg Stiftung (BW Stiftung-Postdoc Eliteprogramme), Deutsche Forschungsgemeinschaft (DFG - 469666862, DFG - CR 312/5-2); Italy: Istituto Nazionale di Fisica Nucleare (ICSC, NextGenerationEU), Ministero dell'Università e della Ricerca (NextGenEU I53D23001490006 M4C2.1.1, NextGenEU I53D23000820006 M4C2.1.1, NextGenEU I53D23001490006 M4C2.1.1); Japan: Japan Society for the Promotion of Science (JSPS KAKENHI JP22H01227, JSPS KAKENHI JP22H04944, JSPS KAKENHI JP22KK0227, JSPS KAKENHI JP23KK0245); Norway: Research Council of Norway (RCN-314472); Poland: Ministry of Science and Higher Education (IDUB AGH, POB8, D4 no 9722), Polish National Agency for Academic Exchange (PPN/PPO/2020/1/00002/U/00001), Polish National Science Centre (NCN 2021/42/E/ST2/00350, NCN OPUS 2023/51/B/ST2/02507, NCN OPUS nr 2022/47/B/ST2/03059, NCN UMO-2019/34/E/ST2/00393, UMO-2020/37/B/ST2/01043, UMO-2021/40/C/ST2/00187, UMO-2022/47/O/ST2/00148, UMO-2023/49/B/ST2/04085, UMO-2023/51/B/ST2/00920); Portugal: Foundation for Science and Technology (FCT); Spain: Generalitat Valenciana (Artemisa, FEDER, ID-IFEDER/2018/048), Ministry of Science and Innovation (MCIN & NextGenEU PCI2022-135018-2, MICIN & FEDER PID2021-125273NB, RYC2019-028510-I, RYC2020-030254-I, RYC2021-031273-I, RYC2022-038164-I); Sweden: Carl Trygger Foundation (Carl Trygger Foundation CTS 22:2312), Swedish Research Council (Swedish Research Council 2023-04654, VR 2018-00482, VR 2021-03651, VR 2022-03845, VR 2022-04683, VR 2023-03403), Knut and Alice Wallenberg Foundation (KAW 2018.0458, KAW 2019.0447, KAW 2022.0358); Switzerland: Swiss National Science Foundation (SNSF - PCEFP2_194658); United Kingdom: Leverhulme Trust (Leverhulme Trust RPG-2020-004), Royal Society (NIF-R1-231091); United States of America: U.S. Department of Energy (ECA DE-AC02-76SF00515), Neubauer Family Foundation.

References

- [1] ATLAS Collaboration, *Observation of a new particle in the search for the Standard Model Higgs boson with the ATLAS detector at the LHC*, *Phys. Lett. B* **716** (2012) 1, arXiv: [1207.7214 \[hep-ex\]](https://arxiv.org/abs/1207.7214).
- [2] CMS Collaboration, *Observation of a new boson at a mass of 125 GeV with the CMS experiment at the LHC*, *Phys. Lett. B* **716** (2012) 30, arXiv: [1207.7235 \[hep-ex\]](https://arxiv.org/abs/1207.7235).

- [3] E. Gabrielli, B. Mele, F. Piccinini, and R. Pittau, *Asking for an extra photon in Higgs production at the LHC and beyond*, *JHEP* **07** (2016) 003, arXiv: [1601.03635 \[hep-ph\]](#).
- [4] ATLAS Collaboration, *Measurements of Higgs bosons decaying to bottom quarks from vector boson fusion production with the ATLAS experiment at $\sqrt{s} = 13$ TeV*, *Eur. Phys. J. C* **81** (2021) 537, arXiv: [2011.08280 \[hep-ex\]](#).
- [5] CMS Collaboration, *Measurement of boosted Higgs bosons produced via vector boson fusion or gluon fusion in the $H \rightarrow b\bar{b}$ decay mode using LHC proton–proton collision data at $\sqrt{s} = 13$ TeV*, *JHEP* **12** (2024) 035, arXiv: [2407.08012 \[hep-ex\]](#).
- [6] ATLAS Collaboration, *Search for Higgs boson production in association with a high-energy photon via vector-boson fusion with decay into bottom quark pairs at $\sqrt{s} = 13$ TeV with the ATLAS detector*, *JHEP* **03** (2021) 268, arXiv: [2010.13651 \[hep-ex\]](#).
- [7] B. Denby, *Neural networks and cellular automata in experimental high energy physics*, *Comput. Phys. Commun.* **49** (1988) 429.
- [8] ATLAS Collaboration, *The ATLAS Experiment at the CERN Large Hadron Collider*, *JINST* **3** (2008) S08003.
- [9] ATLAS Collaboration, *Performance of the ATLAS trigger system in 2015*, *Eur. Phys. J. C* **77** (2017) 317, arXiv: [1611.09661 \[hep-ex\]](#).
- [10] ATLAS Collaboration, *Software and computing for Run 3 of the ATLAS experiment at the LHC*, *Eur. Phys. J. C* **85** (2025) 234, arXiv: [2404.06335 \[hep-ex\]](#).
- [11] J. Alwall et al., *The automated computation of tree-level and next-to-leading order differential cross sections, and their matching to parton shower simulations*, *JHEP* **07** (2014) 079, arXiv: [1405.0301 \[hep-ph\]](#).
- [12] M. Bähr et al., *Herwig++ physics and manual*, *Eur. Phys. J. C* **58** (2008) 639, arXiv: [0803.0883 \[hep-ph\]](#).
- [13] J. Bellm et al., *Herwig 7.0/Herwig++ 3.0 release note*, *Eur. Phys. J. C* **76** (2016) 196, arXiv: [1512.01178 \[hep-ph\]](#).
- [14] J. Butterworth et al., *PDF4LHC recommendations for LHC Run II*, *J. Phys. G* **43** (2016) 023001, arXiv: [1510.03865 \[hep-ph\]](#).
- [15] P. Nason, *A new method for combining NLO QCD with shower Monte Carlo algorithms*, *JHEP* **11** (2004) 040, arXiv: [hep-ph/0409146](#).
- [16] S. Frixione, P. Nason, and C. Oleari, *Matching NLO QCD computations with parton shower simulations: the POWHEG method*, *JHEP* **11** (2007) 070, arXiv: [0709.2092 \[hep-ph\]](#).
- [17] S. Alioli, P. Nason, C. Oleari, and E. Re, *A general framework for implementing NLO calculations in shower Monte Carlo programs: the POWHEG BOX*, *JHEP* **06** (2010) 043, arXiv: [1002.2581 \[hep-ph\]](#).
- [18] T. Sjöstrand et al., *An introduction to PYTHIA 8.2*, *Comput. Phys. Commun.* **191** (2015) 159, arXiv: [1410.3012 \[hep-ph\]](#).
- [19] NNPDF Collaboration, R. D. Ball, et al., *Parton distributions for the LHC run II*, *JHEP* **04** (2015) 040, arXiv: [1410.8849 \[hep-ph\]](#).

- [20] R. D. Ball et al., *The PDF4LHC21 combination of global PDF fits for the LHC Run III*, *J. Phys. G* **49** (2022) 080501, arXiv: 2203.05506 [hep-ph].
- [21] M. Czakon and A. Mitov, *Top++: A program for the calculation of the top-pair cross-section at hadron colliders*, *Comput. Phys. Commun.* **185** (2014) 2930, arXiv: 1112.5675 [hep-ph].
- [22] D. J. Lange, *The EvtGen particle decay simulation package*, *Nucl. Instrum. Meth. A* **462** (2001) 152.
- [23] T. Sjöstrand, S. Mrenna, and P. Skands, *A brief introduction to PYTHIA 8.1*, *Comput. Phys. Commun.* **178** (2008) 852, arXiv: 0710.3820 [hep-ph].
- [24] ATLAS Collaboration, *The Pythia 8 A3 tune description of ATLAS minimum bias and inelastic measurements incorporating the Donnachie–Landshoff diffractive model*, ATL-PHYS-PUB-2016-017, 2016, URL: <https://cds.cern.ch/record/2206965>.
- [25] ATLAS Collaboration, *The ATLAS Simulation Infrastructure*, *Eur. Phys. J. C* **70** (2010) 823, arXiv: 1005.4568 [physics.ins-det].
- [26] S. Agostinelli et al., *GEANT4 – a simulation toolkit*, *Nucl. Instrum. Meth. A* **506** (2003) 250.
- [27] ATLAS Collaboration, *Performance of electron and photon triggers in ATLAS during LHC Run 2*, *Eur. Phys. J. C* **80** (2020) 47, arXiv: 1909.00761 [hep-ex].
- [28] ATLAS Collaboration, *Configuration and performance of the ATLAS b-jet triggers in Run 2*, *Eur. Phys. J. C* **81** (2021) 1087, arXiv: 2106.03584 [hep-ex].
- [29] ATLAS Collaboration, *ATLAS data quality operations and performance for 2015–2018 data-taking*, *JINST* **15** (2020) P04003, arXiv: 1911.04632 [physics.ins-det].
- [30] ATLAS Collaboration, *Vertex Reconstruction Performance of the ATLAS Detector at $\sqrt{s} = 13$ TeV*, ATL-PHYS-PUB-2015-026, 2015, URL: <https://cds.cern.ch/record/2037717>.
- [31] M. Cacciari, G. P. Salam, and G. Soyez, *The anti- k_t jet clustering algorithm*, *JHEP* **04** (2008) 063, arXiv: 0802.1189 [hep-ph].
- [32] M. Cacciari, G. P. Salam, and G. Soyez, *FastJet user manual*, *Eur. Phys. J. C* **72** (2012) 1896, arXiv: 1111.6097 [hep-ph].
- [33] ATLAS Collaboration, *Jet reconstruction and performance using particle flow with the ATLAS Detector*, *Eur. Phys. J. C* **77** (2017) 466, arXiv: 1703.10485 [hep-ex].
- [34] ATLAS Collaboration, *Performance of pile-up mitigation techniques for jets in pp collisions at $\sqrt{s} = 8$ TeV using the ATLAS detector*, *Eur. Phys. J. C* **76** (2016) 581, arXiv: 1510.03823 [hep-ex].
- [35] ATLAS Collaboration, *Forward jet vertex tagging using the particle flow algorithm*, ATL-PHYS-PUB-2019-026, 2019, URL: <https://cds.cern.ch/record/2683100>.
- [36] ATLAS Collaboration, *ATLAS flavour-tagging algorithms for the LHC Run 2 pp collision dataset*, *Eur. Phys. J. C* **83** (2023) 681, arXiv: 2211.16345 [physics.data-an].
- [37] ATLAS Collaboration, *ATLAS b-jet identification performance and efficiency measurement with $t\bar{t}$ events in pp collisions at $\sqrt{s} = 13$ TeV*, *Eur. Phys. J. C* **79** (2019) 970, arXiv: 1907.05120 [hep-ex].

- [38] ATLAS Collaboration, *Measurement of the c -jet mistagging efficiency in $t\bar{t}$ events using pp collision data at $\sqrt{s} = 13$ TeV collected with the ATLAS detector*, *Eur. Phys. J. C* **82** (2022) 95, arXiv: 2109.10627 [hep-ex].
- [39] ATLAS Collaboration, *Calibration of the light-flavour jet mistagging efficiency of the b -tagging algorithms with Z +jets events using 139 fb^{-1} of ATLAS proton–proton collision data at $\sqrt{s} = 13$ TeV*, *Eur. Phys. J. C* **83** (2023) 728, arXiv: 2301.06319 [hep-ex].
- [40] ATLAS Collaboration, *Flavor Tagging Efficiency Parametrisations with Graph Neural Networks*, ATL-PHYS-PUB-2022-041, 2022, URL: <https://cds.cern.ch/record/2825433>.
- [41] ATLAS Collaboration, *New techniques for jet calibration with the ATLAS detector*, *Eur. Phys. J. C* **83** (2023) 761, arXiv: 2303.17312 [hep-ex].
- [42] ATLAS Collaboration, *Electron and photon performance measurements with the ATLAS detector using the 2015–2017 LHC proton–proton collision data*, *JINST* **14** (2019) P12006, arXiv: 1908.00005 [hep-ex].
- [43] ATLAS Collaboration, *Muon reconstruction performance of the ATLAS detector in proton–proton collision data at $\sqrt{s} = 13$ TeV*, *Eur. Phys. J. C* **76** (2016) 292, arXiv: 1603.05598 [hep-ex].
- [44] F. Chollet et al., *Keras*, 2015, URL: <https://keras.io>.
- [45] Martín Abadi et al., *TensorFlow: Large-Scale Machine Learning on Heterogeneous Systems*, Software available from tensorflow.org, 2015, URL: <https://www.tensorflow.org/>.
- [46] A. D. Martin, W. J. Stirling, R. S. Thorne, and G. Watt, *Uncertainties on α_S in global PDF analyses and implications for predicted hadronic cross sections*, *Eur. Phys. J. C* **64** (2009) 653, arXiv: 0905.3531 [hep-ph].
- [47] ATLAS Collaboration, *Observation of electroweak production of two jets in association with an isolated photon and missing transverse momentum, and search for a Higgs boson decaying into invisible particles at 13 TeV with the ATLAS detector*, *Eur. Phys. J. C* **82** (2022) 105, arXiv: 2109.00925 [hep-ex].
- [48] M. Botje et al., *The PDF4LHC Working Group Interim Recommendations*, 2011, arXiv: 1101.0538 [hep-ph], URL: <https://arxiv.org/abs/1101.0538>.
- [49] ATLAS Collaboration, *Luminosity determination in pp collisions at $\sqrt{s} = 13$ TeV using the ATLAS detector at the LHC*, *Eur. Phys. J. C* **83** (2023) 982, arXiv: 2212.09379 [hep-ex].
- [50] ATLAS Collaboration, *Jet energy scale and resolution measured in proton–proton collisions at $\sqrt{s} = 13$ TeV with the ATLAS detector*, *Eur. Phys. J. C* **81** (2021) 689, arXiv: 2007.02645 [hep-ex].
- [51] K. Cranmer, G. Lewis, L. Moneta, A. Shibata, and W. Verkerke, *HistFactory: A tool for creating statistical models for use with RooFit and RooStats*, (2012), URL: <https://cds.cern.ch/record/1456844>.
- [52] W. Verkerke and D. Kirkby, *The RooFit toolkit for data modeling*, 2003, arXiv: physics/0306116 [physics.data-an].
- [53] W. A. Rolke, A. M. López, and J. Conrad, *Limits and confidence intervals in the presence of nuisance parameters*, *Nucl. Instrum. Meth. A* **551** (2005) 493, ed. by L. Lyons and M. Karagoz, arXiv: physics/0403059.

- [54] ATLAS Collaboration, *ATLAS Computing Acknowledgements*, ATL-SOFT-PUB-2025-001, 2025,
URL: <https://cds.cern.ch/record/2922210>.

The ATLAS Collaboration

G. Aad ¹⁰⁵, E. Aakvaag ¹⁷, B. Abbott ¹²⁴, S. Abdelhameed ^{120a}, K. Abeling ⁵⁶, N.J. Abicht ⁵⁰, S.H. Abidi ³⁰, M. Aboeela ⁴⁶, A. Aboulhorma ^{36e}, H. Abramowicz ¹⁵⁸, Y. Abulaiti ¹²¹, B.S. Acharya ^{70a,70b,o}, A. Ackermann ^{64a}, C. Adam Bourdarios ⁴, L. Adamczyk ^{88a}, S.V. Addepalli ¹⁵⁰, M.J. Addison ¹⁰⁴, J. Adelman ¹¹⁹, A. Adiguzel ^{22c}, T. Adye ¹³⁸, A.A. Affolder ¹⁴⁰, Y. Afik ⁴¹, M.N. Agaras ¹³, A. Aggarwal ¹⁰³, C. Agheorghiesei ^{28c}, F. Ahmadov ^{40,ae}, S. Ahuja ⁹⁸, X. Ai ^{144b}, G. Aielli ^{77a,77b}, A. Aikot ¹⁷⁰, M. Ait Tamlihat ^{36e}, B. Aitbenkikh ^{36a}, M. Akbiyik ¹⁰³, T.P.A. Åkesson ¹⁰¹, A.V. Akimov ¹⁵², D. Akiyama ¹⁷⁵, N.N. Akolkar ²⁵, S. Aktas ^{22a}, G.L. Alberghi ^{24b}, J. Albert ¹⁷², P. Albicocco ⁵⁴, G.L. Albouy ⁶¹, S. Alderweireldt ⁵³, Z.L. Alegria ¹²⁵, M. Aleksa ³⁷, I.N. Aleksandrov ⁴⁰, C. Alexa ^{28b}, T. Alexopoulos ¹⁰, F. Alfonsi ^{24b}, M. Algren ⁵⁷, M. Alhroob ¹⁷⁴, B. Ali ¹³⁶, H.M.J. Ali ^{94,x}, S. Ali ³², S.W. Alibocus ⁹⁵, M. Aliev ^{34c}, G. Alimonti ^{72a}, W. Alkahi ⁵⁶, C. Allaire ⁶⁷, B.M.M. Allbrooke ¹⁵³, J.S. Allen ¹⁰⁴, J.F. Allen ⁵³, P.P. Allport ²¹, A. Aloisio ^{73a,73b}, F. Alonso ⁹³, C. Alpigiani ¹⁴³, Z.M.K. Alsolami ⁹⁴, A. Alvarez Fernandez ¹⁰³, M. Alves Cardoso ⁵⁷, M.G. Alviggi ^{73a,73b}, M. Aly ¹⁰⁴, Y. Amaral Coutinho ^{84b}, A. Ambler ¹⁰⁷, C. Amelung ³⁷, M. Amerl ¹⁰⁴, C.G. Ames ¹¹², D. Amidei ¹⁰⁹, B. Amini ⁵⁵, K. Amirie ¹⁶², A. Amirkhanov ⁴⁰, S.P. Amor Dos Santos ^{134a}, K.R. Amos ¹⁷⁰, D. Amperiadou ¹⁵⁹, S. An ⁸⁵, V. Ananiev ¹²⁹, C. Anastopoulos ¹⁴⁶, T. Andeen ¹¹, J.K. Anders ⁹⁵, A.C. Anderson ⁶⁰, A. Andreazza ^{72a,72b}, S. Angelidakis ⁹, A. Angerami ⁴³, A.V. Anisenkov ⁴⁰, A. Annovi ^{75a}, C. Antel ⁵⁷, E. Antipov ¹⁵², M. Antonelli ⁵⁴, F. Anulli ^{76a}, M. Aoki ⁸⁵, T. Aoki ¹⁶⁰, M.A. Aparo ¹⁵³, L. Aperio Bella ⁴⁹, C. Appelt ¹⁵⁸, A. Apyan ²⁷, S.J. Arbiol Val ⁸⁹, C. Arcangeletti ⁵⁴, A.T.H. Arce ⁵², J-F. Arguin ¹¹¹, S. Argyropoulos ¹⁵⁹, J.-H. Arling ⁴⁹, O. Arnaez ⁴, H. Arnold ¹⁵², G. Artoni ^{76a,76b}, H. Asada ¹¹⁴, K. Asai ¹²², S. Asai ¹⁶⁰, N.A. Asbah ³⁷, R.A. Ashby Pickering ¹⁷⁴, A.M. Aslam ⁹⁸, K. Assamagan ³⁰, R. Astalos ^{29a}, K.S.V. Astrand ¹⁰¹, S. Atashi ¹⁶⁶, R.J. Atkin ^{34a}, H. Atmani ^{36f}, P.A. Atlasiddha ¹³², K. Augsten ¹³⁶, A.D. Auriol ⁴², V.A. Austrup ¹⁰⁴, G. Avolio ³⁷, K. Axiotis ⁵⁷, G. Azuelos ^{111,aj}, D. Babal ^{29b}, H. Bachacou ¹³⁹, K. Bachas ^{159,s}, A. Bachiu ³⁵, E. Bachmann ⁵¹, M.J. Backes ^{64a}, A. Badea ⁴¹, T.M. Baer ¹⁰⁹, P. Bagnaia ^{76a,76b}, M. Bahmani ¹⁹, D. Bahner ⁵⁵, K. Bai ¹²⁷, J.T. Baines ¹³⁸, L. Baines ⁹⁷, O.K. Baker ¹⁷⁹, E. Bakos ¹⁶, D. Bakshi Gupta ⁸, L.E. Balabram Filho ^{84b}, V. Balakrishnan ¹²⁴, R. Balasubramanian ⁴, E.M. Baldin ³⁹, P. Balek ^{88a}, E. Ballabene ^{24b,24a}, F. Balli ¹³⁹, L.M. Baltes ^{64a}, W.K. Balunas ³³, J. Balz ¹⁰³, I. Bamwidhi ^{120b}, E. Banas ⁸⁹, M. Bandieramonte ¹³³, A. Bandyopadhyay ²⁵, S. Bansal ²⁵, L. Barak ¹⁵⁸, M. Barakat ⁴⁹, E.L. Barberio ¹⁰⁸, D. Barberis ^{18b}, M. Barbero ¹⁰⁵, M.Z. Barel ¹¹⁸, T. Barillari ¹¹³, M-S. Barisits ³⁷, T. Barklow ¹⁵⁰, P. Baron ¹²⁶, D.A. Baron Moreno ¹⁰⁴, A. Baroncelli ⁶³, A.J. Barr ¹³⁰, J.D. Barr ⁹⁹, F. Barreiro ¹⁰², J. Barreiro Guimarães da Costa ¹⁴, M.G. Barros Teixeira ^{134a}, S. Barsov ³⁹, F. Bartels ^{64a}, R. Bartoldus ¹⁵⁰, A.E. Barton ⁹⁴, P. Bartos ^{29a}, A. Basan ¹⁰³, M. Baselga ⁵⁰, S. Bashiri ⁸⁹, A. Bassalat ^{67,b}, M.J. Basso ^{163a}, S. Bataju ⁴⁶, R. Bate ¹⁷¹, R.L. Bates ⁶⁰, S. Batlamous ¹⁰², M. Battaglia ¹⁴⁰, D. Battulga ¹⁹, M. Bauce ^{76a,76b}, M. Bauer ⁸⁰, P. Bauer ²⁵, L.T. Bayer ⁴⁹, L.T. Bazzano Hurrell ³¹, J.B. Beacham ¹¹³, T. Beau ¹³¹, J.Y. Beauchamp ⁹³, P.H. Beauchemin ¹⁶⁵, P. Bechtel ²⁵, H.P. Beck ^{20,r}, K. Becker ¹⁷⁴, A.J. Beddall ⁸³, V.A. Bednyakov ⁴⁰, C.P. Bee ¹⁵², L.J. Beemster ¹⁶, M. Begalli ^{84d}, M. Begel ³⁰, J.K. Behr ⁴⁹, J.F. Beirer ³⁷, F. Beisiegel ²⁵, M. Belfkir ^{120b}, G. Bella ¹⁵⁸, L. Bellagamba ^{24b}, A. Bellerive ³⁵, P. Bellos ²¹, K. Beloborodov ³⁹, D. Benchebroun ^{36a}, F. Bendebba ^{36a}, Y. Benhammou ¹⁵⁸, K.C. Benkendorfer ⁶², L. Beresford ⁴⁹, M. Beretta ⁵⁴, E. Bergeas Kuutmann ¹⁶⁸, N. Berger ⁴,

B. Bergmann [id](#)¹³⁶, J. Beringer [id](#)^{18a}, G. Bernardi [id](#)⁵, C. Bernius [id](#)¹⁵⁰, F.U. Bernlochner [id](#)²⁵,
 F. Bernon [id](#)³⁷, A. Berrocal Guardia [id](#)¹³, T. Berry [id](#)⁹⁸, P. Berta [id](#)¹³⁷, A. Berthold [id](#)⁵¹, R. Bertrand [id](#)¹⁰⁵,
 S. Bethke [id](#)¹¹³, A. Betti [id](#)^{76a,76b}, A.J. Bevan [id](#)⁹⁷, L. Bezio [id](#)⁵⁷, N.K. Bhalla [id](#)⁵⁵, S. Bharthuar [id](#)¹¹³,
 S. Bhatta [id](#)¹⁵², D.S. Bhattacharya [id](#)¹⁷³, P. Bhattarai [id](#)¹⁵⁰, Z.M. Bhatti [id](#)¹²¹, K.D. Bhide [id](#)⁵⁵,
 V.S. Bhopatkar [id](#)¹²⁵, R.M. Bianchi [id](#)¹³³, G. Bianco [id](#)^{24b,24a}, O. Biebel [id](#)¹¹², M. Biglietti [id](#)^{78a},
 C.S. Billingsley [id](#)⁴⁶, Y. Bimngdi [id](#)^{36f}, M. Bindi [id](#)⁵⁶, A. Bingham [id](#)¹⁷⁸, A. Bingul [id](#)^{22b}, C. Bini [id](#)^{76a,76b},
 G.A. Bird [id](#)³³, M. Birman [id](#)¹⁷⁶, M. Biroš [id](#)¹³⁷, S. Biryukov [id](#)¹⁵³, T. Bisanz [id](#)⁵⁰, E. Bisceglie [id](#)^{24b,24a},
 J.P. Biswal [id](#)¹³⁸, D. Biswas [id](#)¹⁴⁸, I. Bloch [id](#)⁴⁹, A. Blue [id](#)⁶⁰, U. Blumenschein [id](#)⁹⁷, J. Blumenthal [id](#)¹⁰³,
 V.S. Bobrovnikov [id](#)⁴⁰, M. Boehler [id](#)⁵⁵, B. Boehm [id](#)¹⁷³, D. Bogavac [id](#)³⁷, A.G. Bogdanchikov [id](#)³⁹,
 L.S. Boggia [id](#)¹³¹, V. Boisvert [id](#)⁹⁸, P. Bokan [id](#)³⁷, T. Bold [id](#)^{88a}, M. Bomben [id](#)⁵, M. Bona [id](#)⁹⁷,
 M. Boonekamp [id](#)¹³⁹, A.G. Borbély [id](#)⁶⁰, I.S. Bordulev [id](#)³⁹, G. Borissov [id](#)⁹⁴, D. Bortoletto [id](#)¹³⁰,
 D. Boscherini [id](#)^{24b}, M. Bosman [id](#)¹³, K. Bouaouda [id](#)^{36a}, N. Bouchhar [id](#)¹⁷⁰, L. Boudet [id](#)⁴,
 J. Boudreau [id](#)¹³³, E.V. Bouhova-Thacker [id](#)⁹⁴, D. Boumediene [id](#)⁴², R. Bouquet [id](#)^{58b,58a}, A. Boveia [id](#)¹²³,
 J. Boyd [id](#)³⁷, D. Boye [id](#)³⁰, I.R. Boyko [id](#)⁴⁰, L. Bozianu [id](#)⁵⁷, J. Bracinek [id](#)²¹, N. Brahimi [id](#)⁴,
 G. Brandt [id](#)¹⁷⁸, O. Brandt [id](#)³³, B. Brau [id](#)¹⁰⁶, J.E. Brau [id](#)¹²⁷, R. Brener [id](#)¹⁷⁶, L. Brenner [id](#)¹¹⁸,
 R. Brenner [id](#)¹⁶⁸, S. Bressler [id](#)¹⁷⁶, G. Brianti [id](#)^{79a,79b}, D. Britton [id](#)⁶⁰, D. Britzger [id](#)¹¹³, I. Brock [id](#)²⁵,
 R. Brock [id](#)¹¹⁰, G. Brooijmans [id](#)⁴³, A.J. Brooks [id](#)⁶⁹, E.M. Brooks [id](#)^{163b}, E. Brost [id](#)³⁰,
 L.M. Brown [id](#)^{172,163a}, L.E. Bruce [id](#)⁶², T.L. Bruckler [id](#)¹³⁰, P.A. Bruckman de Renstrom [id](#)⁸⁹,
 B. Brüers [id](#)⁴⁹, A. Bruni [id](#)^{24b}, G. Bruni [id](#)^{24b}, D. Brunner [id](#)^{48a,48b}, M. Bruschi [id](#)^{24b}, N. Bruscinò [id](#)^{76a,76b},
 T. Buanes [id](#)¹⁷, Q. Buat [id](#)¹⁴³, D. Buchin [id](#)¹¹³, A.G. Buckley [id](#)⁶⁰, O. Bulekov [id](#)³⁹, B.A. Bullard [id](#)¹⁵⁰,
 S. Burdin [id](#)⁹⁵, C.D. Burgard [id](#)⁵⁰, A.M. Burger [id](#)³⁷, B. Burghgrave [id](#)⁸, O. Burlayenko [id](#)⁵⁵,
 J. Burleson [id](#)¹⁶⁹, J.T.P. Burr [id](#)³³, J.C. Burzynski [id](#)¹⁴⁹, E.L. Busch [id](#)⁴³, V. Büscher [id](#)¹⁰³, P.J. Bussey [id](#)⁶⁰,
 J.M. Butler [id](#)²⁶, C.M. Buttar [id](#)⁶⁰, J.M. Butterworth [id](#)⁹⁹, W. Buttinger [id](#)¹³⁸, C.J. Buxo Vazquez [id](#)¹¹⁰,
 A.R. Buzykaev [id](#)⁴⁰, S. Cabrera Urbán [id](#)¹⁷⁰, L. Cadamuro [id](#)⁶⁷, D. Caforio [id](#)⁵⁹, H. Cai [id](#)¹³³,
 Y. Cai [id](#)^{24b,115c,24a}, Y. Cai [id](#)^{115a}, V.M.M. Cairo [id](#)³⁷, O. Cakir [id](#)^{3a}, N. Calace [id](#)³⁷, P. Calafiura [id](#)^{18a},
 G. Calderini [id](#)¹³¹, P. Calfayan [id](#)³⁵, G. Callea [id](#)⁶⁰, L.P. Caloba [id](#)^{84b}, D. Calvet [id](#)⁴², S. Calvet [id](#)⁴²,
 R. Camacho Toro [id](#)¹³¹, S. Camarda [id](#)³⁷, D. Camarero Munoz [id](#)²⁷, P. Camarri [id](#)^{77a,77b},
 M.T. Camerlingo [id](#)^{73a,73b}, C. Camincher [id](#)¹⁷², M. Campanelli [id](#)⁹⁹, A. Camplani [id](#)⁴⁴, V. Canale [id](#)^{73a,73b},
 A.C. Canbay [id](#)^{3a}, E. Canonero [id](#)⁹⁸, J. Cantero [id](#)¹⁷⁰, Y. Cao [id](#)¹⁶⁹, F. Capocasa [id](#)²⁷, M. Capua [id](#)^{45b,45a},
 A. Carbone [id](#)^{72a,72b}, R. Cardarelli [id](#)^{77a}, J.C.J. Cardenas [id](#)⁸, M.P. Cardiff [id](#)²⁷, G. Carducci [id](#)^{45b,45a},
 T. Carli [id](#)³⁷, G. Carlino [id](#)^{73a}, J.I. Carlotto [id](#)¹³, B.T. Carlson [id](#)^{133,t}, E.M. Carlson [id](#)¹⁷²,
 J. Carmignani [id](#)⁹⁵, L. Carminati [id](#)^{72a,72b}, A. Carnelli [id](#)⁴, M. Carnesale [id](#)³⁷, S. Caron [id](#)¹¹⁷,
 E. Carquin [id](#)^{141f}, I.B. Carr [id](#)¹⁰⁸, S. Carrá [id](#)^{72a}, G. Carratta [id](#)^{24b,24a}, A.M. Carroll [id](#)¹²⁷,
 M.P. Casado [id](#)^{13,i}, M. Caspar [id](#)⁴⁹, F.L. Castillo [id](#)⁴, L. Castillo Garcia [id](#)¹³, V. Castillo Gimenez [id](#)¹⁷⁰,
 N.F. Castro [id](#)^{134a,134e}, A. Catinaccio [id](#)³⁷, J.R. Catmore [id](#)¹²⁹, T. Cavaliere [id](#)⁴, V. Cavaliere [id](#)³⁰,
 L.J. Caviedes Betancourt [id](#)^{23b}, Y.C. Cekmecelioglu [id](#)⁴⁹, E. Celebi [id](#)⁸³, S. Cella [id](#)³⁷, V. Cepaitis [id](#)⁵⁷,
 K. Cerny [id](#)¹²⁶, A.S. Cerqueira [id](#)^{84a}, A. Cerri [id](#)^{75a,75b,am}, L. Cerrito [id](#)^{77a,77b}, F. Cerutti [id](#)^{18a},
 B. Cervato [id](#)^{72a,72b}, A. Cervelli [id](#)^{24b}, G. Cesarini [id](#)⁵⁴, S.A. Cetin [id](#)⁸³, P.M. Chabrilat [id](#)¹³¹, J. Chan [id](#)^{18a},
 W.Y. Chan [id](#)¹⁶⁰, J.D. Chapman [id](#)³³, E. Chapon [id](#)¹³⁹, B. Chargeishvili [id](#)^{156b}, D.G. Charlton [id](#)²¹,
 C. Chauhan [id](#)¹³⁷, Y. Che [id](#)^{115a}, S. Chekanov [id](#)⁶, S.V. Chekulaev [id](#)^{163a}, G.A. Chelkov [id](#)^{40,a},
 B. Chen [id](#)¹⁵⁸, B. Chen [id](#)¹⁷², H. Chen [id](#)^{115a}, H. Chen [id](#)³⁰, J. Chen [id](#)^{145a}, J. Chen [id](#)¹⁴⁹, M. Chen [id](#)¹³⁰,
 S. Chen [id](#)⁹⁰, S.J. Chen [id](#)^{115a}, X. Chen [id](#)^{145a}, X. Chen [id](#)^{15,ai}, Z. Chen [id](#)⁶³, C.L. Cheng [id](#)¹⁷⁷,
 H.C. Cheng [id](#)^{65a}, S. Cheong [id](#)¹⁵⁰, A. Cheplakov [id](#)⁴⁰, E. Cheremushkina [id](#)⁴⁹, E. Cherepanova [id](#)¹¹⁸,
 R. Cherkaoui El Moursli [id](#)^{36e}, E. Cheu [id](#)⁷, K. Cheung [id](#)⁶⁶, L. Chevalier [id](#)¹³⁹, V. Chiarella [id](#)⁵⁴,
 G. Chiarelli [id](#)^{75a}, N. Chiedde [id](#)¹⁰⁵, G. Chiodini [id](#)^{71a}, A.S. Chisholm [id](#)²¹, A. Chitan [id](#)^{28b},
 M. Chitishvili [id](#)¹⁷⁰, M.V. Chizhov [id](#)^{40,u}, K. Choi [id](#)¹¹, Y. Chou [id](#)¹⁴³, E.Y.S. Chow [id](#)¹¹⁷, K.L. Chu [id](#)¹⁷⁶,
 M.C. Chu [id](#)^{65a}, X. Chu [id](#)^{14,115c}, Z. Chubinidze [id](#)⁵⁴, J. Chudoba [id](#)¹³⁵, J.J. Chwastowski [id](#)⁸⁹,

D. Cieri [id113](#), K.M. Ciesla [id88a](#), V. Cindro [id96](#), A. Ciocio [id18a](#), F. Cirotto [id73a,73b](#), Z.H. Citron [id176](#),
 M. Citterio [id72a](#), D.A. Ciubotaru [id28b](#), A. Clark [id57](#), P.J. Clark [id53](#), N. Clarke Hall [id99](#), C. Clarry [id162](#),
 S.E. Clawson [id49](#), C. Clement [id48a,48b](#), Y. Coadou [id105](#), M. Cobal [id70a,70c](#), A. Coccaro [id58b](#),
 R.F. Coelho Barrue [id134a](#), R. Coelho Lopes De Sa [id106](#), S. Coelli [id72a](#), L.S. Colangeli [id162](#), B. Cole [id43](#),
 P. Collado Soto [id102](#), J. Collot [id61](#), P. Conde Muiño [id134a,134g](#), M.P. Connell [id34c](#), S.H. Connell [id34c](#),
 E.I. Conroy [id130](#), M. Contreras Cossio [id11](#), F. Conventi [id73a,ak](#), H.G. Cooke [id21](#),
 A.M. Cooper-Sarkar [id130](#), L. Corazzina [id76a,76b](#), F.A. Corchia [id24b,24a](#), A. Cordeiro Oudot Choi [id131](#),
 L.D. Corpe [id42](#), M. Corradi [id76a,76b](#), F. Corriveau [id107,ac](#), A. Cortes-Gonzalez [id19](#), M.J. Costa [id170](#),
 F. Costanza [id4](#), D. Costanzo [id146](#), B.M. Cote [id123](#), J. Couthures [id4](#), G. Cowan [id98](#), K. Cranmer [id177](#),
 L. Cremer [id50](#), D. Cremonini [id24b,24a](#), S. Crépe-Renaudin [id61](#), F. Crescioli [id131](#), T. Cresta [id74a,74b](#),
 M. Cristinziani [id148](#), M. Cristoforetti [id79a,79b](#), V. Croft [id118](#), J.E. Crosby [id125](#), G. Crosetti [id45b,45a](#),
 A. Cueto [id102](#), H. Cui [id99](#), Z. Cui [id7](#), W.R. Cunningham [id60](#), F. Curcio [id170](#), J.R. Curran [id53](#),
 P. Czodrowski [id37](#), M.J. Da Cunha Sargedas De Sousa [id58b,58a](#), J.V. Da Fonseca Pinto [id84b](#),
 C. Da Via [id104](#), W. Dabrowski [id88a](#), T. Dado [id37](#), S. Dahbi [id155](#), T. Dai [id109](#), D. Dal Santo [id20](#),
 C. Dallapiccola [id106](#), M. Dam [id44](#), G. D'amen [id30](#), V. D'Amico [id112](#), J. Damp [id103](#), J.R. Dandoy [id35](#),
 D. Dannheim [id37](#), M. Danninger [id149](#), V. Dao [id152](#), G. Darbo [id58b](#), S.J. Das [id30](#), F. Dattola [id49](#),
 S. D'Auria [id72a,72b](#), A. D'Avanzo [id73a,73b](#), T. Davidek [id137](#), J. Davidson [id174](#), I. Dawson [id97](#),
 H.A. Day-hall [id136](#), K. De [id8](#), C. De Almeida Rossi [id162](#), R. De Asmundis [id73a](#), N. De Biase [id49](#),
 S. De Castro [id24b,24a](#), N. De Groot [id117](#), P. de Jong [id118](#), H. De la Torre [id119](#), A. De Maria [id115a](#),
 A. De Salvo [id76a](#), U. De Sanctis [id77a,77b](#), F. De Santis [id71a,71b](#), A. De Santo [id153](#),
 J.B. De Vivie De Regie [id61](#), J. Debevc [id96](#), D.V. Dedovich [id40](#), J. Degens [id95](#), A.M. Deiana [id46](#),
 J. Del Peso [id102](#), L. Delagrangé [id131](#), F. Deliot [id139](#), C.M. Delitzsch [id50](#), M. Della Pietra [id73a,73b](#),
 D. Della Volpe [id57](#), A. Dell'Acqua [id37](#), L. Dell'Asta [id72a,72b](#), M. Delmastro [id4](#), C.C. Delogu [id103](#),
 P.A. Delsart [id61](#), S. Demers [id179](#), M. Demichev [id40](#), S.P. Denisov [id39](#), H. Denizli [id22a,m](#),
 L. D'Eramo [id42](#), D. Derendarz [id89](#), F. Derue [id131](#), P. Dervan [id95,*](#), K. Desch [id25](#), C. Deutsch [id25](#),
 F.A. Di Bello [id58b,58a](#), A. Di Ciaccio [id77a,77b](#), L. Di Ciaccio [id4](#), A. Di Domenico [id76a,76b](#),
 C. Di Donato [id73a,73b](#), A. Di Girolamo [id37](#), G. Di Gregorio [id37](#), A. Di Luca [id79a,79b](#),
 B. Di Micco [id78a,78b](#), R. Di Nardo [id78a,78b](#), K.F. Di Petrillo [id41](#), M. Diamantopoulou [id35](#), F.A. Dias [id118](#),
 T. Dias Do Vale [id149](#), M.A. Diaz [id141a,141b](#), A.R. Didenko [id40](#), M. Didenko [id170](#), E.B. Diehl [id109](#),
 S. Díez Cornell [id49](#), C. Díez Pardos [id148](#), C. Dimitriadi [id151](#), A. Dimitrievska [id21](#), A. Dimri [id152](#),
 J. Dingfelder [id25](#), T. Dingley [id130](#), I-M. Dinu [id28b](#), S.J. Dittmeier [id64b](#), F. Dittus [id37](#), M. Divisek [id137](#),
 B. Dixit [id95](#), F. Djama [id105](#), T. Djobava [id156b](#), C. Doglioni [id104,101](#), A. Dohnalova [id29a](#), Z. Dolezal [id137](#),
 K. Domijan [id88a](#), K.M. Dona [id41](#), M. Donadelli [id84d](#), B. Dong [id110](#), J. Donini [id42](#),
 A. D'Onofrio [id73a,73b](#), M. D'Onofrio [id95](#), J. Dopke [id138](#), A. Doria [id73a](#), N. Dos Santos Fernandes [id134a](#),
 P. Dougan [id104](#), M.T. Dova [id93](#), A.T. Doyle [id60](#), M.A. Draguet [id130](#), M.P. Drescher [id56](#), E. Dreyer [id176](#),
 I. Drivas-koulouris [id10](#), M. Drnevich [id121](#), M. Drozdova [id57](#), D. Du [id63](#), T.A. du Pree [id118](#),
 F. Dubinin [id40](#), M. Dubovsky [id29a](#), E. Duchovni [id176](#), G. Duckeck [id112](#), P.K. Duckett [id99](#), O.A. Ducu [id28b](#),
 D. Duda [id53](#), A. Dudarev [id37](#), E.R. Duden [id27](#), M. D'uffizi [id104](#), L. Duflost [id67](#), M. Dührssen [id37](#),
 I. Duminica [id28g](#), A.E. Dumitriu [id28b](#), M. Dunford [id64a](#), S. Dungs [id50](#), K. Dunne [id48a,48b](#),
 A. Duperrin [id105](#), H. Duran Yildiz [id3a](#), M. Düren [id59](#), A. Durglishvili [id156b](#), D. Duvnjak [id35](#),
 B.L. Dwyer [id119](#), G.I. Dyckes [id18a](#), M. Dyndal [id88a](#), B.S. Dziedzic [id37](#), Z.O. Earnshaw [id153](#),
 G.H. Eberwein [id130](#), B. Eckerova [id29a](#), S. Eggebrecht [id56](#), E. Egidio Purcino De Souza [id84e](#),
 G. Eigen [id17](#), K. Einsweiler [id18a](#), T. Ekelof [id168](#), P.A. Ekman [id101](#), S. El Farkh [id36b](#), Y. El Ghazali [id63](#),
 H. El Jarrari [id37](#), A. El Moussaouy [id36a](#), V. Ellajosyula [id168](#), M. Ellert [id168](#), F. Ellinghaus [id178](#),
 N. Ellis [id37](#), J. Elmsheuser [id30](#), M. Elsayy [id120a](#), M. Elsing [id37](#), D. Emelianov [id138](#), Y. Enari [id85](#),
 I. Ene [id18a](#), S. Epari [id111](#), D. Ernani Martins Neto [id89](#), M. Errenst [id178](#), M. Escalier [id67](#),
 C. Escobar [id170](#), E. Etzion [id158](#), G. Evans [id134a,134b](#), H. Evans [id69](#), L.S. Evans [id98](#), A. Ezhilov [id39](#),

S. Ezzarqtouni [id](#)^{36a}, F. Fabbri [id](#)^{24b,24a}, L. Fabbri [id](#)^{24b,24a}, G. Facini [id](#)⁹⁹, V. Fadeyev [id](#)¹⁴⁰,
 R.M. Fakhrutdinov [id](#)³⁹, D. Fakoudis [id](#)¹⁰³, S. Falciano [id](#)^{76a}, L.F. Falda Ulhoa Coelho [id](#)^{134a},
 F. Fallavollita [id](#)¹¹³, G. Falsetti [id](#)^{45b,45a}, J. Faltova [id](#)¹³⁷, C. Fan [id](#)¹⁶⁹, K.Y. Fan [id](#)^{65b}, Y. Fan [id](#)¹⁴,
 Y. Fang [id](#)^{14,115c}, M. Fanti [id](#)^{72a,72b}, M. Faraj [id](#)^{70a,70b}, Z. Farazpay [id](#)¹⁰⁰, A. Farbin [id](#)⁸, A. Farilla [id](#)^{78a},
 T. Farooque [id](#)¹¹⁰, J.N. Farr [id](#)¹⁷⁹, S.M. Farrington [id](#)^{138,53}, F. Fassi [id](#)^{36c}, D. Fassouliotis [id](#)⁹,
 L. Fayard [id](#)⁶⁷, P. Federic [id](#)¹³⁷, P. Federicova [id](#)¹³⁵, O.L. Fedin [id](#)^{39,a}, M. Feickert [id](#)¹⁷⁷, L. Feligioni [id](#)¹⁰⁵,
 D.E. Fellers [id](#)^{18a}, C. Feng [id](#)^{144a}, Z. Feng [id](#)¹¹⁸, M.J. Fenton [id](#)¹⁶⁶, L. Ferencz [id](#)⁴⁹,
 B. Fernandez Barbadillo [id](#)⁹⁴, P. Fernandez Martinez [id](#)⁶⁸, M.J.V. Fernoux [id](#)¹⁰⁵, J. Ferrando [id](#)⁹⁴,
 A. Ferrari [id](#)¹⁶⁸, P. Ferrari [id](#)^{118,117}, R. Ferrari [id](#)^{74a}, D. Ferrere [id](#)⁵⁷, C. Ferretti [id](#)¹⁰⁹, M.P. Fewell [id](#)¹,
 D. Fiacco [id](#)^{76a,76b}, F. Fiedler [id](#)¹⁰³, P. Fiedler [id](#)¹³⁶, S. Filimonov [id](#)⁴⁰, A. Filipičič [id](#)⁹⁶, E.K. Filmer [id](#)^{163a},
 F. Filthaut [id](#)¹¹⁷, M.C.N. Fiolhais [id](#)^{134a,134c,c}, L. Fiorini [id](#)¹⁷⁰, W.C. Fisher [id](#)¹¹⁰, T. Fitschen [id](#)¹⁰⁴,
 P.M. Fitzhugh [id](#)¹³⁹, I. Fleck [id](#)¹⁴⁸, P. Fleischmann [id](#)¹⁰⁹, T. Flick [id](#)¹⁷⁸, M. Flores [id](#)^{34d,ag},
 L.R. Flores Castillo [id](#)^{65a}, L. Flores Sanz De Acedo [id](#)³⁷, F.M. Follega [id](#)^{79a,79b}, N. Fomin [id](#)³³,
 J.H. Foo [id](#)¹⁶², A. Formica [id](#)¹³⁹, A.C. Forti [id](#)¹⁰⁴, E. Fortin [id](#)³⁷, A.W. Fortman [id](#)^{18a}, L. Fountas [id](#)^{9,j},
 D. Fournier [id](#)⁶⁷, H. Fox [id](#)⁹⁴, P. Francavilla [id](#)^{75a,75b}, S. Francescato [id](#)⁶², S. Franchellucci [id](#)⁵⁷,
 M. Franchini [id](#)^{24b,24a}, S. Franchino [id](#)^{64a}, D. Francis [id](#)³⁷, L. Franco [id](#)¹¹⁷, V. Franco Lima [id](#)³⁷,
 L. Franconi [id](#)⁴⁹, M. Franklin [id](#)⁶², G. Frattari [id](#)²⁷, Y.Y. Frid [id](#)¹⁵⁸, J. Friend [id](#)⁶⁰, N. Fritzsche [id](#)³⁷,
 A. Froch [id](#)⁵⁷, D. Froidevaux [id](#)³⁷, J.A. Frost [id](#)¹³⁰, Y. Fu [id](#)¹¹⁰, S. Fuenzalida Garrido [id](#)^{141f},
 M. Fujimoto [id](#)¹⁰⁵, K.Y. Fung [id](#)^{65a}, E. Furtado De Simas Filho [id](#)^{84e}, M. Furukawa [id](#)¹⁶⁰, J. Fuster [id](#)¹⁷⁰,
 A. Gaa [id](#)⁵⁶, A. Gabrielli [id](#)^{24b,24a}, A. Gabrielli [id](#)¹⁶², P. Gadow [id](#)³⁷, G. Gagliardi [id](#)^{58b,58a},
 L.G. Gagnon [id](#)^{18a}, S. Gaid [id](#)^{86b}, S. Galantzan [id](#)¹⁵⁸, J. Gallagher [id](#)¹, E.J. Gallas [id](#)¹³⁰, A.L. Gallen [id](#)¹⁶⁸,
 B.J. Gallop [id](#)¹³⁸, K.K. Gan [id](#)¹²³, S. Ganguly [id](#)¹⁶⁰, Y. Gao [id](#)⁵³, A. Garabaglu [id](#)¹⁴³,
 F.M. Garay Walls [id](#)^{141a,141b}, B. Garcia [id](#)³⁰, C. García [id](#)¹⁷⁰, A. Garcia Alonso [id](#)¹¹⁸,
 A.G. Garcia Caffaro [id](#)¹⁷⁹, J.E. García Navarro [id](#)¹⁷⁰, M. Garcia-Sciveres [id](#)^{18a}, G.L. Gardner [id](#)¹³²,
 R.W. Gardner [id](#)⁴¹, N. Garelli [id](#)¹⁶⁵, R.B. Garg [id](#)¹⁵⁰, J.M. Gargan [id](#)⁵³, C.A. Garner [id](#)¹⁶², C.M. Garvey [id](#)^{34a},
 V.K. Gassmann [id](#)¹⁶⁵, G. Gaudio [id](#)^{74a}, V. Gautam [id](#)¹³, P. Gauzzi [id](#)^{76a,76b}, J. Gavranovic [id](#)⁹⁶,
 I.L. Gavrilenko [id](#)^{134a}, A. Gavriluk [id](#)³⁹, C. Gay [id](#)¹⁷¹, G. Gaycken [id](#)¹²⁷, E.N. Gazis [id](#)¹⁰, A. Gekow [id](#)¹²³,
 C. Gemme [id](#)^{58b}, M.H. Genest [id](#)⁶¹, A.D. Gentry [id](#)¹¹⁶, S. George [id](#)⁹⁸, W.F. George [id](#)²¹, T. Gerialis [id](#)⁴⁷,
 A.A. Gerwin [id](#)¹²⁴, P. Gessinger-Befurt [id](#)³⁷, M.E. Geyik [id](#)¹⁷⁸, M. Ghani [id](#)¹⁷⁴, K. Ghorbanian [id](#)⁹⁷,
 A. Ghosal [id](#)¹⁴⁸, A. Ghosh [id](#)¹⁶⁶, A. Ghosh [id](#)⁷, B. Giacobbe [id](#)^{24b}, S. Giagu [id](#)^{76a,76b}, T. Giani [id](#)¹¹⁸,
 A. Giannini [id](#)⁶³, S.M. Gibson [id](#)⁹⁸, M. Gignac [id](#)¹⁴⁰, D.T. Gil [id](#)^{88b}, A.K. Gilbert [id](#)^{88a}, B.J. Gilbert [id](#)⁴³,
 D. Gillberg [id](#)³⁵, G. Gilles [id](#)¹¹⁸, L. Ginabat [id](#)¹³¹, D.M. Gingrich [id](#)^{2,aj}, M.P. Giordani [id](#)^{70a,70c},
 P.F. Giraud [id](#)¹³⁹, G. Giugliarelli [id](#)^{70a,70c}, D. Giugni [id](#)^{72a}, F. Giuli [id](#)^{77a,77b}, I. Gkialas [id](#)^{9,j},
 L.K. Gladilin [id](#)³⁹, C. Glasman [id](#)¹⁰², G. Glemža [id](#)⁴⁹, M. Glisic [id](#)¹²⁷, I. Gnesi [id](#)^{45b}, Y. Go [id](#)³⁰,
 M. Goblirsch-Kolb [id](#)³⁷, B. Gocke [id](#)⁵⁰, D. Godin [id](#)¹¹¹, B. Gokturk [id](#)^{22a}, S. Goldfarb [id](#)¹⁰⁸, T. Golling [id](#)⁵⁷,
 M.G.D. Gololo [id](#)^{34c}, D. Golubkov [id](#)³⁹, J.P. Gombas [id](#)¹¹⁰, A. Gomes [id](#)^{134a,134b}, G. Gomes Da Silva [id](#)¹⁴⁸,
 A.J. Gomez Delegido [id](#)¹⁷⁰, R. Gonçalves [id](#)^{134a}, L. Gonella [id](#)²¹, A. Gongadze [id](#)^{156c}, F. Gonnella [id](#)²¹,
 J.L. Gonski [id](#)¹⁵⁰, R.Y. González Andana [id](#)⁵³, S. González de la Hoz [id](#)¹⁷⁰, C. Gonzalez Renteria [id](#)^{18a},
 M.V. Gonzalez Rodrigues [id](#)⁴⁹, R. Gonzalez Suarez [id](#)¹⁶⁸, S. Gonzalez-Sevilla [id](#)⁵⁷, L. Goossens [id](#)³⁷,
 B. Gorini [id](#)³⁷, E. Gorini [id](#)^{71a,71b}, A. Gorišek [id](#)⁹⁶, T.C. Gosart [id](#)¹³², A.T. Goshaw [id](#)⁵², M.I. Gostkin [id](#)⁴⁰,
 S. Goswami [id](#)¹²⁵, C.A. Gottardo [id](#)³⁷, S.A. Gotz [id](#)¹¹², M. Gouighri [id](#)^{36b}, A.G. Goussiou [id](#)¹⁴³,
 N. Govender [id](#)^{34c}, R.P. Grabarczyk [id](#)¹³⁰, I. Grabowska-Bold [id](#)^{88a}, K. Graham [id](#)³⁵, E. Gramstad [id](#)¹²⁹,
 S. Grancagnolo [id](#)^{71a,71b}, C.M. Grant [id](#)^{1,139}, P.M. Gravila [id](#)^{28f}, F.G. Gravili [id](#)^{71a,71b}, H.M. Gray [id](#)^{18a},
 M. Greco [id](#)¹¹³, M.J. Green [id](#)¹, C. Grefe [id](#)²⁵, A.S. Grefsrud [id](#)¹⁷, I.M. Gregor [id](#)⁴⁹, K.T. Greif [id](#)¹⁶⁶,
 P. Grenier [id](#)¹⁵⁰, S.G. Grewe [id](#)¹¹³, A.A. Grillo [id](#)¹⁴⁰, K. Grimm [id](#)³², S. Grinstein [id](#)^{13,y}, J.-F. Grivaz [id](#)⁶⁷,
 E. Gross [id](#)¹⁷⁶, J. Grosse-Knetter [id](#)⁵⁶, L. Guan [id](#)¹⁰⁹, G. Guerrieri [id](#)³⁷, R. Guevara [id](#)¹²⁹, R. Gugel [id](#)¹⁰³,
 J.A.M. Guhit [id](#)¹⁰⁹, A. Guida [id](#)¹⁹, E. Guilloton [id](#)¹⁷⁴, S. Guindon [id](#)³⁷, F. Guo [id](#)^{14,115c}, J. Guo [id](#)^{145a},

L. Guo ⁴⁹, L. Guo ^{115b,w}, Y. Guo ¹⁰⁹, A. Gupta ⁵⁰, R. Gupta ¹³³, S. Gurbuz ²⁵,
 S.S. Gurdasani ⁴⁹, G. Gustavino ^{76a,76b}, P. Gutierrez ¹²⁴, L.F. Gutierrez Zagazeta ¹³²,
 M. Gutsche ⁵¹, C. Gutschow ⁹⁹, C. Gwenlan ¹³⁰, C.B. Gwilliam ⁹⁵, E.S. Haaland ¹²⁹,
 A. Haas ¹²¹, M. Habedank ⁶⁰, C. Haber ^{18a}, H.K. Hadavand ⁸, A. Haddad ⁴², A. Hadeef ⁵¹,
 A.I. Hagan ⁹⁴, J.J. Hahn ¹⁴⁸, E.H. Haines ⁹⁹, M. Haleem ¹⁷³, J. Haley ¹²⁵, G.D. Hallowell ¹⁰⁵,
 L. Halser ²⁰, K. Hamano ¹⁷², M. Hamer ²⁵, S.E.D. Hammoud ⁶⁷, E.J. Hampshire ⁹⁸,
 J. Han ^{144a}, L. Han ^{115a}, L. Han ⁶³, S. Han ^{18a}, K. Hanagaki ⁸⁵, M. Hance ¹⁴⁰, D.A. Hangal ⁴³,
 H. Hanif ¹⁴⁹, M.D. Hank ¹³², J.B. Hansen ⁴⁴, P.H. Hansen ⁴⁴, D. Harada ⁵⁷, T. Harenberg ¹⁷⁸,
 S. Harkusha ¹⁸⁰, M.L. Harris ¹⁰⁶, Y.T. Harris ²⁵, J. Harrison ¹³, N.M. Harrison ¹²³,
 P.F. Harrison ¹⁷⁴, M.L.E. Hart ⁹⁹, N.M. Hartman ¹¹³, N.M. Hartmann ¹¹², R.Z. Hasan ^{98,138},
 Y. Hasegawa ¹⁴⁷, F. Haslbeck ¹³⁰, S. Hassan ¹⁷, R. Hauser ¹¹⁰, M. Haviernik ¹³⁷,
 C.M. Hawkes ²¹, R.J. Hawkings ³⁷, Y. Hayashi ¹⁶⁰, D. Hayden ¹¹⁰, C. Hayes ¹⁰⁹,
 R.L. Hayes ¹¹⁸, C.P. Hays ¹³⁰, J.M. Hays ⁹⁷, H.S. Hayward ⁹⁵, F. He ⁶³, M. He ^{14,115c},
 Y. He ⁴⁹, Y. He ⁹⁹, N.B. Heatley ⁹⁷, V. Hedberg ¹⁰¹, A.L. Heggelund ¹²⁹, C. Heidegger ⁵⁵,
 K.K. Heidegger ⁵⁵, J. Heilman ³⁵, S. Heim ⁴⁹, T. Heim ^{18a}, J.G. Heinlein ¹³², J.J. Heinrich ¹²⁷,
 L. Heinrich ^{113,ah}, J. Hejbal ¹³⁵, A. Held ¹⁷⁷, S. Hellesund ¹⁷, C.M. Helling ¹⁷¹,
 S. Hellman ^{48a,48b}, L. Henkelmann ³³, A.M. Henriques Correia ³⁷, H. Herde ¹⁰¹,
 Y. Hernández Jiménez ¹⁵², L.M. Herrmann ²⁵, T. Herrmann ⁵¹, G. Herten ⁵⁵, R. Hertenberger ¹¹²,
 L. Hervas ³⁷, M.E. Hesping ¹⁰³, N.P. Hessey ^{163a}, J. Hessler ¹¹³, M. Hidaoui ^{36b}, N. Hidic ¹³⁷,
 E. Hill ¹⁶², S.J. Hillier ²¹, J.R. Hinds ¹¹⁰, F. Hinterkeuser ²⁵, M. Hirose ¹²⁸, S. Hirose ¹⁶⁴,
 D. Hirschbuehl ¹⁷⁸, T.G. Hitchings ¹⁰⁴, B. Hiti ⁹⁶, J. Hobbs ¹⁵², R. Hobincu ^{28e}, N. Hod ¹⁷⁶,
 M.C. Hodgkinson ¹⁴⁶, B.H. Hodgkinson ¹³⁰, A. Hoecker ³⁷, D.D. Hofer ¹⁰⁹, J. Hofer ¹⁷⁰,
 M. Holzbock ³⁷, L.B.A.H. Hommels ³³, V. Homsak ¹³⁰, B.P. Honan ¹⁰⁴, J.J. Hong ⁶⁹,
 J. Hong ^{145a}, T.M. Hong ¹³³, B.H. Hooberman ¹⁶⁹, W.H. Hopkins ⁶, M.C. Hoppesch ¹⁶⁹,
 Y. Horii ¹¹⁴, M.E. Horstmann ¹¹³, S. Hou ¹⁵⁵, M.R. Housenga ¹⁶⁹, A.S. Howard ⁹⁶,
 J. Howarth ⁶⁰, J. Hoya ⁶, M. Hrabovsky ¹²⁶, T. Hryn'ova ⁴, P.J. Hsu ⁶⁶, S.-C. Hsu ¹⁴³,
 T. Hsu ⁶⁷, M. Hu ^{18a}, Q. Hu ⁶³, S. Huang ³³, X. Huang ^{14,115c}, Y. Huang ¹³⁷, Y. Huang ^{115b},
 Y. Huang ¹⁰³, Y. Huang ¹⁴, Z. Huang ¹⁰⁴, Z. Hubacek ¹³⁶, M. Huebner ²⁵, F. Huegging ²⁵,
 T.B. Huffman ¹³⁰, M. Hufnagel Maranha De Faria ^{84a}, C.A. Hugli ⁴⁹, M. Huhtinen ³⁷,
 S.K. Huiberts ¹⁷, R. Hulskens ¹⁰⁷, C.E. Hultquist ^{18a}, N. Huseynov ^{12,g}, J. Huston ¹¹⁰, J. Huth ⁶²,
 R. Hyneman ⁷, G. Iacobucci ⁵⁷, G. Iakovidis ³⁰, L. Iconomidou-Fayard ⁶⁷, J.P. Iddon ³⁷,
 P. Iengo ^{73a,73b}, R. Iguchi ¹⁶⁰, Y. Iiyama ¹⁶⁰, T. Iizawa ¹³⁰, Y. Ikegami ⁸⁵, D. Iliadis ¹⁵⁹,
 N. Ilic ¹⁶², H. Imam ^{84c}, G. Inacio Goncalves ^{84d}, S.A. Infante Cabanas ^{141c},
 T. Ingebretsen Carlson ^{48a,48b}, J.M. Inglis ⁹⁷, G. Introzzi ^{74a,74b}, M. Iodice ^{78a}, V. Ippolito ^{76a,76b},
 R.K. Irwin ⁹⁵, M. Ishino ¹⁶⁰, W. Islam ¹⁷⁷, C. Issever ¹⁹, S. Istin ^{22a,ap}, K. Itabashi ⁸⁵,
 H. Ito ¹⁷⁵, R. Iuppa ^{79a,79b}, A. Ivina ¹⁷⁶, V. Izzo ^{73a}, P. Jacka ¹³⁵, P. Jackson ¹, P. Jain ⁴⁹,
 K. Jakobs ⁵⁵, T. Jakoubek ¹⁷⁶, J. Jamieson ⁶⁰, W. Jang ¹⁶⁰, S. Jankovych ¹³⁷, M. Javurkova ¹⁰⁶,
 P. Jawahar ¹⁰⁴, L. Jeanty ¹²⁷, J. Jejelava ^{156a,af}, P. Jenni ^{55,f}, C.E. Jessiman ³⁵, C. Jia ^{144a},
 H. Jia ¹⁷¹, J. Jia ¹⁵², X. Jia ^{14,115c}, Z. Jia ^{115a}, C. Jiang ⁵³, Q. Jiang ^{65b}, S. Jiggins ⁴⁹,
 M. Jimenez Ortega ¹⁷⁰, J. Jimenez Pena ¹³, S. Jin ^{115a}, A. Jinaru ^{28b}, O. Jinnouchi ¹⁴²,
 P. Johansson ¹⁴⁶, K.A. Johns ⁷, J.W. Johnson ¹⁴⁰, F.A. Jolly ⁴⁹, D.M. Jones ¹⁵³, E. Jones ⁴⁹,
 K.S. Jones ⁸, P. Jones ³³, R.W.L. Jones ⁹⁴, T.J. Jones ⁹⁵, H.L. Joos ^{56,37}, R. Joshi ¹²³,
 J. Jovicevic ¹⁶, X. Ju ^{18a}, J.J. Junggeburth ³⁷, T. Junkermann ^{64a}, A. Juste Rozas ^{13,y},
 M.K. Juzek ⁸⁹, S. Kabana ^{141e}, A. Kaczmarek ⁸⁹, M. Kado ¹¹³, H. Kagan ¹²³, M. Kagan ¹⁵⁰,
 A. Kahn ¹³², C. Kahra ¹⁰³, T. Kaji ¹⁶⁰, E. Kajomovitz ¹⁵⁷, N. Kakati ¹⁷⁶, N. Kakoty ¹³,
 I. Kalaitzidou ⁵⁵, S. Kandel ⁸, N.J. Kang ¹⁴⁰, D. Kar ^{34g}, K. Karava ¹³⁰, E. Karentzos ²⁵,
 O. Karkout ¹¹⁸, S.N. Karpov ⁴⁰, Z.M. Karpova ⁴⁰, V. Kartvelishvili ⁹⁴, A.N. Karyukhin ³⁹,

E. Kasimi ¹⁵⁹, J. Katzy ⁴⁹, S. Kaur ³⁵, K. Kawade ¹⁴⁷, M.P. Kawale ¹²⁴, C. Kawamoto ⁹⁰,
 T. Kawamoto ⁶³, E.F. Kay ³⁷, F.I. Kaya ¹⁶⁵, S. Kazakos ¹¹⁰, V.F. Kazanin ³⁹, Y. Ke ¹⁵²,
 J.M. Keaveney ^{34a}, R. Keeler ¹⁷², G.V. Kehris ⁶², J.S. Keller ³⁵, J.J. Kempster ¹⁵³, O. Kepka ¹³⁵,
 J. Kerr ^{163b}, B.P. Kerridge ¹³⁸, B.P. Kerševan ⁹⁶, L. Keszeghova ^{29a}, R.A. Khan ¹³³,
 A. Khanov ¹²⁵, A.G. Kharlamov ³⁹, T. Kharlamova ³⁹, E.E. Khoda ¹⁴³, M. Kholodenko ^{134a},
 T.J. Khoo ¹⁹, G. Khorialuli ¹⁷³, J. Khubua ^{156b,*}, Y.A.R. Khwaira ¹³¹, B. Kibirige ^{34g}, D. Kim ⁶,
 D.W. Kim ^{48a,48b}, Y.K. Kim ⁴¹, N. Kimura ⁹⁹, M.K. Kingston ⁵⁶, A. Kirchhoff ⁵⁶, C. Kirfel ²⁵,
 F. Kirfel ²⁵, J. Kirk ¹³⁸, A.E. Kiryunin ¹¹³, S. Kita ¹⁶⁴, C. Kitsaki ¹⁰, O. Kivernyk ²⁵,
 M. Klassen ¹⁶⁵, C. Klein ³⁵, L. Klein ¹⁷³, M.H. Klein ⁴⁶, S.B. Klein ⁵⁷, U. Klein ⁹⁵,
 A. Klimentov ³⁰, T. Klioutchnikova ³⁷, P. Kluit ¹¹⁸, S. Kluth ¹¹³, E. Kneringer ⁸⁰,
 T.M. Knight ¹⁶², A. Knue ⁵⁰, M. Kobel ⁵¹, D. Kobylanskii ¹⁷⁶, S.F. Koch ¹³⁰, M. Kocian ¹⁵⁰,
 P. Kodyš ¹³⁷, D.M. Koeck ¹²⁷, P.T. Koenig ²⁵, T. Koffas ³⁵, O. Kolay ⁵¹, I. Koletsou ⁴,
 T. Komarek ⁸⁹, K. Köneke ⁵⁶, A.X.Y. Kong ¹, T. Kono ¹²², N. Konstantinidis ⁹⁹,
 P. Kontaxakis ⁵⁷, B. Konya ¹⁰¹, R. Kopeliansky ⁴³, S. Koperny ^{88a}, K. Korcyl ⁸⁹,
 K. Kordas ^{159,e}, A. Korn ⁹⁹, S. Korn ⁵⁶, I. Korolkov ¹³, N. Korotkova ³⁹, B. Kortman ¹¹⁸,
 O. Kortner ¹¹³, S. Kortner ¹¹³, W.H. Kostecka ¹¹⁹, M. Kostov ^{29a}, V.V. Kostyukhin ¹⁴⁸,
 A. Kotsokechagia ³⁷, A. Kotwal ⁵², A. Koulouris ³⁷, A. Kourkoumeli-Charalampidi ^{74a,74b},
 C. Kourkoumelis ⁹, E. Kourlitis ¹¹³, O. Kovanda ¹²⁷, R. Kowalewski ¹⁷², W. Kozanecki ¹²⁷,
 A.S. Kozhin ³⁹, V.A. Kramarenko ³⁹, G. Kramberger ⁹⁶, P. Kramer ²⁵, M.W. Krasny ¹³¹,
 A. Krasznahorkay ¹⁰⁶, A.C. Kraus ¹¹⁹, J.W. Kraus ¹⁷⁸, J.A. Kremer ⁴⁹, N.B. Krenkel ¹⁴⁸,
 T. Kresse ⁵¹, L. Kretschmann ¹⁷⁸, J. Kretzschmar ⁹⁵, K. Kreul ¹⁹, P. Krieger ¹⁶², K. Krizka ²¹,
 K. Kroeninger ⁵⁰, H. Kroha ¹¹³, J. Kroll ¹³⁵, J. Kroll ¹³², K.S. Krowpman ¹¹⁰, U. Kruchonak ⁴⁰,
 H. Krüger ²⁵, N. Krumnack ⁸², M.C. Kruse ⁵², O. Kuchinskaia ⁴⁰, S. Kuday ^{3a}, S. Kuehn ³⁷,
 R. Kuesters ⁵⁵, T. Kuhl ⁴⁹, V. Kukhtin ⁴⁰, Y. Kulchitsky ⁴⁰, S. Kuleshov ^{141d,141b}, M. Kumar ^{34g},
 N. Kumari ⁴⁹, P. Kumari ^{163b}, A. Kupco ¹³⁵, T. Kupfer ⁵⁰, A. Kupich ³⁹, O. Kuprash ⁵⁵,
 H. Kurashige ⁸⁷, L.L. Kurchaninov ^{163a}, O. Kurdysh ⁴, Y.A. Kurochkin ³⁸, A. Kurova ³⁹,
 M. Kuze ¹⁴², A.K. Kvam ¹⁰⁶, J. Kvita ¹²⁶, N.G. Kyriacou ¹⁰⁹, L.A.O. Laatu ¹⁰⁵, C. Lacasta ¹⁷⁰,
 F. Lacava ^{76a,76b}, H. Lacker ¹⁹, D. Lacour ¹³¹, N.N. Lad ⁹⁹, E. Ladygin ⁴⁰, A. Lafarge ⁴²,
 B. Laforge ¹³¹, T. Lagouri ¹⁷⁹, F.Z. Lahbabi ^{36a}, S. Lai ⁵⁶, J.E. Lambert ¹⁷², S. Lammers ⁶⁹,
 W. Lampl ⁷, C. Lampoudis ^{159,e}, G. Lamprinoudis ¹⁰³, A.N. Lancaster ¹¹⁹, E. Lançon ³⁰,
 U. Landgraf ⁵⁵, M.P.J. Landon ⁹⁷, V.S. Lang ⁵⁵, O.K.B. Langrekken ¹²⁹, A.J. Lankford ¹⁶⁶,
 F. Lanni ³⁷, K. Lantzsch ²⁵, A. Lanza ^{74a}, M. Lanzac Berrocal ¹⁷⁰, J.F. Laporte ¹³⁹, T. Lari ^{72a},
 D. Larsen ¹⁷, F. Lasagni Manghi ^{24b}, M. Lassnig ³⁷, V. Latonova ¹³⁵, S.D. Lawlor ¹⁴⁶,
 Z. Lawrence ¹⁰⁴, R. Lazaridou ¹⁷⁴, M. Lazzaroni ^{72a,72b}, H.D.M. Le ¹¹⁰, E.M. Le Boulicaut ¹⁷⁹,
 L.T. Le Pottier ^{18a}, B. Leban ^{24b,24a}, M. LeBlanc ¹⁰⁴, F. Ledroit-Guillon ⁶¹, S.C. Lee ¹⁵⁵,
 T.F. Lee ⁹⁵, L.L. Leeuw ^{34c,an}, M. Lefebvre ¹⁷², C. Leggett ^{18a}, G. Lehmann Miotto ³⁷,
 M. Leigh ⁵⁷, W.A. Leight ¹⁰⁶, W. Leinonen ¹¹⁷, A. Leisos ^{159,v}, M.A.L. Leite ^{84c},
 C.E. Leitgeb ¹⁹, R. Leitner ¹³⁷, K.J.C. Leney ⁴⁶, T. Lenz ²⁵, S. Leone ^{75a}, C. Leonidopoulos ⁵³,
 A. Leopold ¹⁵¹, J.H. Lepage Bourbonnais ³⁵, R. Les ¹¹⁰, C.G. Lester ³³, M. Levchenko ³⁹,
 J. Levêque ⁴, L.J. Levinson ¹⁷⁶, G. Levrini ^{24b,24a}, M.P. Lewicki ⁸⁹, C. Lewis ¹⁴³, D.J. Lewis ⁴,
 L. Lewitt ¹⁴⁶, A. Li ³⁰, B. Li ^{144a}, C. Li ¹⁰⁹, C-Q. Li ¹¹³, H. Li ⁶³, H. Li ^{144a}, H. Li ¹⁰⁴,
 H. Li ¹⁵, H. Li ⁶³, H. Li ^{144a}, J. Li ^{145a}, K. Li ¹⁴, L. Li ^{145a}, R. Li ¹⁷⁹, S. Li ^{14,115c},
 S. Li ^{145b,145a,d}, T. Li ⁵, X. Li ¹⁰⁷, Z. Li ¹⁶⁰, Z. Li ^{14,115c}, Z. Li ⁶³, S. Liang ^{14,115c},
 Z. Liang ¹⁴, M. Liberatore ¹³⁹, B. Liberti ^{77a}, K. Lie ^{65c}, J. Lieber Marin ^{84e}, H. Lien ⁶⁹,
 H. Lin ¹⁰⁹, S.F. Lin ¹⁵², L. Linden ¹¹², R.E. Lindley ⁷, J.H. Lindon ², J. Ling ⁶², E. Lipeles ¹³²,
 A. Lipniacka ¹⁷, A. Lister ¹⁷¹, J.D. Little ⁶⁹, B. Liu ¹⁴, B.X. Liu ^{115b}, D. Liu ^{145b,145a},
 E.H.L. Liu ²¹, J.K.K. Liu ³³, K. Liu ^{145b}, K. Liu ^{145b,145a}, M. Liu ⁶³, M.Y. Liu ⁶³, P. Liu ¹⁴,

Q. Liu ^{145b,143,145a}, X. Liu ⁶³, X. Liu ^{144a}, Y. Liu ^{115b,115c}, Y.L. Liu ^{144a}, Y.W. Liu ⁶³,
 Z. Liu ^{67,1}, S.L. Lloyd ⁹⁷, E.M. Lobodzinska ⁴⁹, P. Loch ⁷, E. Lodhi ¹⁶², T. Lohse ¹⁹,
 K. Lohwasser ¹⁴⁶, E. Loiacono ⁴⁹, J.D. Lomas ²¹, J.D. Long ⁴³, I. Longarini ¹⁶⁶, R. Longo ¹⁶⁹,
 A. Lopez Solis ⁴⁹, N.A. Lopez-canelas ⁷, N. Lorenzo Martinez ⁴, A.M. Lory ¹¹², M. Losada ^{120a},
 G. Löschke Centeno ¹⁵³, O. Loseva ³⁹, X. Lou ^{48a,48b}, X. Lou ^{14,115c}, A. Lounis ⁶⁷,
 P.A. Love ⁹⁴, G. Lu ^{14,115c}, M. Lu ⁶⁷, S. Lu ¹³², Y.J. Lu ¹⁵⁵, H.J. Lubatti ¹⁴³, C. Luci ^{76a,76b},
 F.L. Lucio Alves ^{115a}, F. Luehring ⁶⁹, B.S. Lunday ¹³², O. Lundberg ¹⁵¹, B. Lund-Jensen ^{151,*},
 N.A. Luongo ⁶, M.S. Lutz ³⁷, A.B. Lux ²⁶, D. Lynn ³⁰, R. Lysak ¹³⁵, V. Lysenko ¹³⁶,
 E. Lytken ¹⁰¹, V. Lyubushkin ⁴⁰, T. Lyubushkina ⁴⁰, M.M. Lyukova ¹⁵², M.Firdaus M. Soberi ⁵³,
 H. Ma ³⁰, K. Ma ⁶³, L.L. Ma ^{144a}, W. Ma ⁶³, Y. Ma ¹²⁵, J.C. MacDonald ¹⁰³,
 P.C. Machado De Abreu Farias ^{84e}, R. Madar ⁴², T. Madula ⁹⁹, J. Maeda ⁸⁷, T. Maeno ³⁰,
 P.T. Mafa ^{34c,k}, H. Maguire ¹⁴⁶, V. Maiboroda ⁶⁷, A. Maio ^{134a,134b,134d}, K. Maj ^{88a},
 O. Majersky ⁴⁹, S. Majewski ¹²⁷, R. Makhmanazarov ³⁹, N. Makovec ⁶⁷, V. Maksimovic ¹⁶,
 B. Malaescu ¹³¹, J. Malamant ¹²⁹, Pa. Malecki ⁸⁹, V.P. Maleev ³⁹, F. Malek ^{61,q}, M. Mali ⁹⁶,
 D. Malito ⁹⁸, U. Mallik ^{81,*}, S. Maltezos ¹⁰, A. Malvezzi Lopes ^{84d}, S. Malyukov ⁴⁰, J. Mamuzic ¹³,
 G. Mancini ⁵⁴, M.N. Mancini ²⁷, G. Manco ^{74a,74b}, J.P. Mandalia ⁹⁷, S.S. Mandarray ¹⁵³,
 I. Mandić ⁹⁶, L. Manhaes de Andrade Filho ^{84a}, I.M. Maniatis ¹⁷⁶, J. Manjarres Ramos ⁹²,
 D.C. Mankad ¹⁷⁶, A. Mann ¹¹², T. Manoussos ³⁷, M.N. Mantinan ⁴¹, S. Manzoni ³⁷,
 L. Mao ^{145a}, X. Mapekula ^{34c}, A. Marantis ^{159,v}, R.R. Marcelo Gregorio ⁹⁷, G. Marchiori ⁵,
 M. Marcisovsky ¹³⁵, C. Marcon ^{72a}, M. Marinescu ²¹, S. Marium ⁴⁹, M. Marjanovic ¹²⁴,
 A. Markhoos ⁵⁵, M. Markovitch ⁶⁷, M.K. Maroun ¹⁰⁶, G.T. Marsden ¹⁰⁴, E.J. Marshall ⁹⁴,
 Z. Marshall ^{18a}, S. Marti-Garcia ¹⁷⁰, J. Martin ⁹⁹, T.A. Martin ¹³⁸, V.J. Martin ⁵³,
 B. Martin dit Latour ¹⁷, L. Martinelli ^{76a,76b}, M. Martinez ^{13,y}, P. Martinez Agullo ¹⁷⁰,
 V.I. Martinez Outschoorn ¹⁰⁶, P. Martinez Suarez ¹³, S. Martin-Haugh ¹³⁸, G. Martinovicova ¹³⁷,
 V.S. Martoiu ^{28b}, A.C. Martyniuk ⁹⁹, A. Marzin ³⁷, D. Mascione ^{79a,79b}, L. Masetti ¹⁰³,
 J. Masik ¹⁰⁴, A.L. Maslennikov ⁴⁰, S.L. Mason ⁴³, P. Massarotti ^{73a,73b}, P. Mastrandrea ^{75a,75b},
 A. Mastroberardino ^{45b,45a}, T. Masubuchi ¹²⁸, T.T. Mathew ¹²⁷, J. Matousek ¹³⁷, D.M. Mattern ⁵⁰,
 J. Maurer ^{28b}, T. Maurin ⁶⁰, A.J. Maury ⁶⁷, B. Maček ⁹⁶, D.A. Maximov ³⁹, A.E. May ¹⁰⁴,
 E. Mayer ⁴², R. Mazini ^{34g}, I. Maznas ¹¹⁹, M. Mazza ¹¹⁰, S.M. Mazza ¹⁴⁰, E. Mazzeo ^{72a,72b},
 J.P. Mc Gowan ¹⁷², S.P. Mc Kee ¹⁰⁹, C.A. Mc Lean ⁶, C.C. McCracken ¹⁷¹, E.F. McDonald ¹⁰⁸,
 A.E. McDougall ¹¹⁸, L.F. Mcelhinney ⁹⁴, J.A. Mcfayden ¹⁵³, R.P. McGovern ¹³²,
 R.P. Mckenzie ^{34g}, T.C. Mclachlan ⁴⁹, D.J. Mclaughlin ⁹⁹, S.J. McMahon ¹³⁸,
 C.M. Mcpartland ⁹⁵, R.A. McPherson ^{172,ac}, S. Mehlhase ¹¹², A. Mehta ⁹⁵, D. Melini ¹⁷⁰,
 B.R. Mellado Garcia ^{34g}, A.H. Melo ⁵⁶, F. Meloni ⁴⁹, A.M. Mendes Jacques Da Costa ¹⁰⁴,
 H.Y. Meng ¹⁶², L. Meng ⁹⁴, S. Menke ¹¹³, M. Mentink ³⁷, E. Meoni ^{45b,45a}, G. Mercado ¹¹⁹,
 S. Merianos ¹⁵⁹, C. Merlassino ^{70a,70c}, C. Meroni ^{72a,72b}, J. Metcalfe ⁶, A.S. Mete ⁶,
 E. Meuser ¹⁰³, C. Meyer ⁶⁹, J-P. Meyer ¹³⁹, R.P. Middleton ¹³⁸, M. Mihovilovic ⁶⁷,
 L. Mijović ⁵³, G. Mikenberg ¹⁷⁶, M. Mikestikova ¹³⁵, M. Mikuž ⁹⁶, H. Mildner ¹⁰³, A. Milic ³⁷,
 D.W. Miller ⁴¹, E.H. Miller ¹⁵⁰, L.S. Miller ³⁵, A. Milov ¹⁷⁶, D.A. Milstead ^{48a,48b}, T. Min ^{115a},
 A.A. Minaenko ³⁹, I.A. Minashvili ^{156b}, A.I. Mincer ¹²¹, B. Mindur ^{88a}, M. Mineev ⁴⁰,
 Y. Mino ⁹⁰, L.M. Mir ¹³, M. Miralles Lopez ⁶⁰, M. Mironova ^{18a}, M. Missio ¹¹⁷, A. Mitra ¹⁷⁴,
 V.A. Mitsou ¹⁷⁰, Y. Mitsumori ¹¹⁴, O. Miu ¹⁶², P.S. Miyagawa ⁹⁷, T. Mkrtchyan ^{64a},
 M. Mlinarevic ⁹⁹, T. Mlinarevic ⁹⁹, M. Mlynarikova ³⁷, S. Mobius ²⁰, P. Mogg ¹¹²,
 M.H. Mohamed Farook ¹¹⁶, A.F. Mohammed ^{14,115c}, S. Mohapatra ⁴³, S. Mohiuddin ¹²⁵,
 G. Mokgatitwane ^{34g}, L. Moleri ¹⁷⁶, U. Molinatti ¹³⁰, B. Mondal ¹⁴⁸, S. Mondal ¹³⁶,
 K. Mönig ⁴⁹, E. Monnier ¹⁰⁵, L. Monsonis Romero ¹⁷⁰, J. Montejo Berlingen ¹³, A. Montella ^{48a,48b},
 M. Montella ¹²³, F. Montekali ^{78a,78b}, F. Monticelli ⁹³, S. Monzani ^{70a,70c}, A. Morancho Tarda ⁴⁴,

N. Morange ⁶⁷, A.L. Moreira De Carvalho ⁴⁹, M. Moreno Llácer ¹⁷⁰, C. Moreno Martinez ⁵⁷,
 J.M. Moreno Perez ^{23b}, P. Morettini ^{58b}, S. Morgenstern ³⁷, M. Morii ⁶², M. Morinaga ¹⁶⁰,
 M. Moritsu ⁹¹, F. Morodei ^{76a,76b}, P. Moschovakos ³⁷, B. Moser ¹³⁰, M. Mosidze ^{156b},
 T. Moskalets ⁴⁶, P. Moskvitina ¹¹⁷, J. Moss ^{32,n}, P. Moszkowicz ^{88a}, A. Moussa ^{36d},
 Y. Moyal ¹⁷⁶, E.J.W. Moyse ¹⁰⁶, O. Mtintsilana ^{34g}, S. Muanza ¹⁰⁵, J. Mueller ¹³³, R. Müller ³⁷,
 G.A. Mullier ¹⁶⁸, A.J. Mullin ³³, J.J. Mullin ⁵², A.E. Mulski ⁶², D.P. Mungo ¹⁶², D. Munoz Perez ¹⁷⁰,
 F.J. Munoz Sanchez ¹⁰⁴, M. Murin ¹⁰⁴, W.J. Murray ^{174,138}, M. Muškinja ⁹⁶, C. Mwewa ³⁰,
 A.G. Myagkov ^{39,a}, A.J. Myers ⁸, G. Myers ¹⁰⁹, M. Myska ¹³⁶, B.P. Nachman ^{18a}, K. Nagai ¹³⁰,
 K. Nagano ⁸⁵, R. Nagasaka ¹⁶⁰, J.L. Nagle ^{30,al}, E. Nagy ¹⁰⁵, A.M. Nairz ³⁷, Y. Nakahama ⁸⁵,
 K. Nakamura ⁸⁵, K. Nakkalil ⁵, H. Nanjo ¹²⁸, E.A. Narayanan ⁴⁶, Y. Narukawa ¹⁶⁰,
 I. Naryshkin ³⁹, L. Nasella ^{72a,72b}, S. Nasri ^{120b}, C. Nass ²⁵, G. Navarro ^{23a},
 J. Navarro-Gonzalez ¹⁷⁰, A. Nayaz ¹⁹, P.Y. Nechaeva ³⁹, S. Nechaeva ^{24b,24a}, F. Nechansky ¹³⁵,
 L. Nedic ¹³⁰, T.J. Neep ²¹, A. Negri ^{74a,74b}, M. Negrini ^{24b}, C. Nellist ¹¹⁸, C. Nelson ¹⁰⁷,
 K. Nelson ¹⁰⁹, S. Nemecek ¹³⁵, M. Nessi ^{37,h}, M.S. Neubauer ¹⁶⁹, J. Newell ⁹⁵,
 P.R. Newman ²¹, Y.W.Y. Ng ¹⁶⁹, B. Ngair ^{120a}, H.D.N. Nguyen ¹¹¹, R.B. Nickerson ¹³⁰,
 R. Nicolaidou ¹³⁹, J. Nielsen ¹⁴⁰, M. Niemeyer ⁵⁶, J. Niermann ³⁷, N. Nikiforou ³⁷,
 V. Nikolaenko ^{39,a}, I. Nikolic-Audit ¹³¹, P. Nilsson ³⁰, I. Ninca ⁴⁹, G. Ninio ¹⁵⁸, A. Nisati ^{76a},
 N. Nishu ², R. Nisius ¹¹³, N. Nitika ^{70a,70c}, J-E. Nitschke ⁵¹, E.K. Nkadimeng ^{34g}, T. Nobe ¹⁶⁰,
 T. Nommensen ¹⁵⁴, M.B. Norfolk ¹⁴⁶, B.J. Norman ³⁵, M. Noury ^{36a}, J. Novak ⁹⁶, T. Novak ⁹⁶,
 R. Novotny ¹¹⁶, L. Nozka ¹²⁶, K. Ntekas ¹⁶⁶, N.M.J. Nunes De Moura Junior ^{84b}, J. Ocariz ¹³¹,
 A. Ochi ⁸⁷, I. Ochoa ^{134a}, S. Oerdek ^{49,z}, J.T. Offermann ⁴¹, A. Ogrodnik ¹³⁷, A. Oh ¹⁰⁴,
 C.C. Ohm ¹⁵¹, H. Oide ⁸⁵, R. Oishi ¹⁶⁰, M.L. Ojeda ³⁷, Y. Okumura ¹⁶⁰, L.F. Oleiro Seabra ^{134a},
 I. Oleksiyuk ⁵⁷, S.A. Olivares Pino ^{141d}, G. Oliveira Correa ¹³, D. Oliveira Damazio ³⁰,
 J.L. Oliver ¹⁶⁶, Ö.O. Öncel ⁵⁵, A.P. O'Neill ²⁰, A. Onofre ^{134a,134e}, P.U.E. Onyisi ¹¹,
 M.J. Oreglia ⁴¹, D. Orestano ^{78a,78b}, R. Orlandini ^{78a,78b}, R.S. Orr ¹⁶², L.M. Osojnak ¹³²,
 Y. Osumi ¹¹⁴, G. Otero y Garzon ³¹, H. Otono ⁹¹, G.J. Ottino ^{18a}, M. Ouchrif ^{36d},
 F. Ould-Saada ¹²⁹, T. Ovsianikova ¹⁴³, M. Owen ⁶⁰, R.E. Owen ¹³⁸, V.E. Ozcan ^{22a},
 F. Ozturk ⁸⁹, N. Ozturk ⁸, S. Ozturk ⁸³, H.A. Pacey ¹³⁰, K. Pachal ^{163a}, A. Pacheco Pages ¹³,
 C. Padilla Aranda ¹³, G. Padovano ^{76a,76b}, S. Pagan Griso ^{18a}, G. Palacino ⁶⁹, A. Palazzo ^{71a,71b},
 J. Pampel ²⁵, J. Pan ¹⁷⁹, T. Pan ^{65a}, D.K. Panchal ¹¹, C.E. Pandini ¹¹⁸,
 J.G. Panduro Vazquez ¹³⁸, H.D. Pandya ¹, H. Pang ¹³⁹, P. Pani ⁴⁹, G. Panizzo ^{70a,70c},
 L. Panwar ¹³¹, L. Paolozzi ⁵⁷, S. Parajuli ¹⁶⁹, A. Paramonov ⁶, C. Paraskevopoulos ⁵⁴,
 D. Paredes Hernandez ^{65b}, A. Pareti ^{74a,74b}, K.R. Park ⁴³, T.H. Park ¹¹³, F. Parodi ^{58b,58a},
 J.A. Parsons ⁴³, U. Parzefall ⁵⁵, B. Pascual Dias ⁴², L. Pascual Dominguez ¹⁰², E. Pasqualucci ^{76a},
 S. Passaggio ^{58b}, F. Pastore ⁹⁸, P. Patel ⁸⁹, U.M. Patel ⁵², J.R. Pater ¹⁰⁴, T. Pauly ³⁷,
 F. Pauwels ¹³⁷, C.I. Pazos ¹⁶⁵, M. Pedersen ¹²⁹, R. Pedro ^{134a}, S.V. Peleganchuk ³⁹, O. Penc ³⁷,
 E.A. Pender ⁵³, S. Peng ¹⁵, G.D. Penn ¹⁷⁹, K.E. Pensi ¹¹², M. Penzin ³⁹, B.S. Peralva ^{84d},
 A.P. Pereira Peixoto ¹⁴³, L. Pereira Sanchez ¹⁵⁰, D.V. Perepelitsa ^{30,al}, G. Perera ¹⁰⁶,
 E. Perez Codina ^{163a}, M. Perganti ¹⁰, H. Pernegger ³⁷, S. Perrella ^{76a,76b}, O. Perrin ⁴²,
 K. Peters ⁴⁹, R.F.Y. Peters ¹⁰⁴, B.A. Petersen ³⁷, T.C. Petersen ⁴⁴, E. Petit ¹⁰⁵, V. Petousis ¹³⁶,
 A.R. Petri ^{72a,72b}, C. Petridou ^{159,e}, T. Petru ¹³⁷, A. Petrukhin ¹⁴⁸, M. Pettee ^{18a}, A. Petukhov ⁸³,
 K. Petukhova ³⁷, R. Pezoa ^{141f}, L. Pezzotti ^{24b,24a}, G. Pezzullo ¹⁷⁹, L. Pfaffenbichler ³⁷,
 A.J. Pflieger ³⁷, T.M. Pham ¹⁷⁷, T. Pham ¹⁰⁸, P.W. Phillips ¹³⁸, G. Piacquadio ¹⁵², E. Pianori ^{18a},
 F. Piazza ¹²⁷, R. Piegaia ³¹, D. Pietreanu ^{28b}, A.D. Pilkington ¹⁰⁴, M. Pinamonti ^{70a,70c},
 J.L. Pinfeld ², B.C. Pinheiro Pereira ^{134a}, J. Pinol Bel ¹³, A.E. Pinto Pinoargote ¹³¹,
 L. Pintucci ^{70a,70c}, K.M. Piper ¹⁵³, A. Pirttikoski ⁵⁷, D.A. Pizzi ³⁵, L. Pizzimento ^{65b},
 A. Plebani ³³, M.-A. Pleier ³⁰, V. Pleskot ¹³⁷, E. Plotnikova ⁴⁰, G. Poddar ⁹⁷, R. Poettgen ¹⁰¹,

L. Poggioli ¹³¹, S. Polacek ¹³⁷, G. Polesello ^{74a}, A. Poley ^{149,163a}, A. Polini ^{24b}, C.S. Pollard ¹⁷⁴,
 Z.B. Pollock ¹²³, E. Pompa Pacchi ¹²⁴, N.I. Pond ⁹⁹, D. Ponomarenko ⁶⁹, L. Pontecorvo ³⁷,
 S. Popa ^{28a}, G.A. Popeneciu ^{28d}, A. Poreba ³⁷, D.M. Portillo Quintero ^{163a}, S. Pospisil ¹³⁶,
 M.A. Postill ¹⁴⁶, P. Postolache ^{28c}, K. Potamianos ¹⁷⁴, P.A. Potepa ^{88a}, I.N. Potrap ⁴⁰,
 C.J. Potter ³³, H. Potti ¹⁵⁴, J. Poveda ¹⁷⁰, M.E. Pozo Astigarraga ³⁷, A. Prades Ibanez ^{77a,77b},
 J. Pretel ¹⁷², D. Price ¹⁰⁴, M. Primavera ^{71a}, L. Primomo ^{70a,70c}, M.A. Principe Martin ¹⁰²,
 R. Privara ¹²⁶, T. Procter ⁶⁰, M.L. Proffitt ¹⁴³, N. Proklova ¹³², K. Prokofiev ^{65c}, G. Proto ¹¹³,
 J. Proudfoot ⁶, M. Przybycien ^{88a}, W.W. Przygoda ^{88b}, A. Psallidas ⁴⁷, J.E. Puddefoot ¹⁴⁶,
 D. Pudzha ⁵⁵, D. Pyatiizbyantseva ¹¹⁷, J. Qian ¹⁰⁹, R. Qian ¹¹⁰, D. Qichen ¹⁰⁴, Y. Qin ¹³,
 T. Qiu ⁵³, A. Quadt ⁵⁶, M. Queitsch-Maitland ¹⁰⁴, G. Quetant ⁵⁷, R.P. Quinn ¹⁷¹,
 G. Rabanal Bolanos ⁶², D. Rafanoharana ⁵⁵, F. Raffaelli ^{77a,77b}, F. Ragusa ^{72a,72b}, J.L. Rainbolt ⁴¹,
 J.A. Raine ⁵⁷, S. Rajagopalan ³⁰, E. Ramakoti ⁴⁰, L. Rambelli ^{58b,58a}, I.A. Ramirez-Berend ³⁵,
 K. Ran ^{49,115c}, D.S. Rankin ¹³², N.P. Rapheeha ^{34g}, H. Rasheed ^{28b}, V. Raskina ¹³¹,
 D.F. Rassloff ^{64a}, A. Rastogi ^{18a}, S. Rave ¹⁰³, S. Ravera ^{58b,58a}, B. Ravina ³⁷, I. Ravinovich ¹⁷⁶,
 M. Raymond ³⁷, A.L. Read ¹²⁹, N.P. Readioff ¹⁴⁶, D.M. Rebuzzi ^{74a,74b}, A.S. Reed ¹¹³,
 K. Reeves ²⁷, J.A. Reidelsturz ¹⁷⁸, D. Reikher ¹²⁷, A. Rej ⁵⁰, C. Rembser ³⁷, H. Ren ⁶³,
 M. Renda ^{28b}, F. Renner ⁴⁹, A.G. Rennie ¹⁶⁶, A.L. Rescia ⁴⁹, S. Resconi ^{72a},
 M. Ressegotti ^{58b,58a}, S. Rettie ³⁷, W.F. Rettie ³⁵, J.G. Reyes Rivera ¹¹⁰, E. Reynolds ^{18a},
 O.L. Rezanova ⁴⁰, P. Reznicek ¹³⁷, H. Riani ^{36d}, N. Ribaric ⁵², E. Ricci ^{79a,79b}, R. Richter ¹¹³,
 S. Richter ^{48a,48b}, E. Richter-Was ^{88b}, M. Ridel ¹³¹, S. Ridouani ^{36d}, P. Rieck ¹²¹, P. Riedler ³⁷,
 E.M. Riefel ^{48a,48b}, J.O. Rieger ¹¹⁸, M. Rijssenbeek ¹⁵², M. Rimoldi ³⁷, L. Rinaldi ^{24b,24a},
 P. Rincke ⁵⁶, G. Ripellino ¹⁶⁸, I. Riu ¹³, J.C. Rivera Vergara ¹⁷², F. Rizatdinova ¹²⁵, E. Rizvi ⁹⁷,
 B.R. Roberts ^{18a}, S.S. Roberts ¹⁴⁰, D. Robinson ³³, M. Robles Manzano ¹⁰³, A. Robson ⁶⁰,
 A. Rocchi ^{77a,77b}, C. Roda ^{75a,75b}, S. Rodriguez Bosca ³⁷, Y. Rodriguez Garcia ^{23a},
 A.M. Rodríguez Vera ¹¹⁹, S. Roe ³⁷, J.T. Roemer ³⁷, O. Røhne ¹²⁹, R.A. Rojas ³⁷,
 C.P.A. Roland ¹³¹, J. Roloff ³⁰, A. Romaniouk ⁸⁰, E. Romano ^{74a,74b}, M. Romano ^{24b},
 A.C. Romero Hernandez ¹⁶⁹, N. Rompotis ⁹⁵, L. Roos ¹³¹, S. Rosati ^{76a}, B.J. Rosser ⁴¹,
 E. Rossi ¹³⁰, E. Rossi ^{73a,73b}, L.P. Rossi ⁶², L. Rossini ⁵⁵, R. Rosten ¹²³, M. Rotaru ^{28b},
 B. Rottler ⁵⁵, D. Rousseau ⁶⁷, D. Rousso ⁴⁹, S. Roy-Garand ¹⁶², A. Rozanov ¹⁰⁵,
 Z.M.A. Rozario ⁶⁰, Y. Rozen ¹⁵⁷, A. Rubio Jimenez ¹⁷⁰, V.H. Ruelas Rivera ¹⁹, T.A. Ruggeri ¹,
 A. Ruggiero ¹³⁰, A. Ruiz-Martinez ¹⁷⁰, A. Rummler ³⁷, Z. Rurikova ⁵⁵, N.A. Rusakovich ⁴⁰,
 H.L. Russell ¹⁷², G. Russo ^{76a,76b}, J.P. Rutherford ⁷, S. Rutherford Colmenares ³³, M. Rybar ¹³⁷,
 P. Rybczynski ^{88a}, E.B. Rye ¹²⁹, A. Ryzhov ⁴⁶, J.A. Sabater Iglesias ⁵⁷, H.F-W. Sadrozinski ¹⁴⁰,
 F. Safai Tehrani ^{76a}, S. Saha ¹, M. Sahinsoy ⁸³, B. Sahoo ¹⁷⁶, A. Saibel ¹⁷⁰, B.T. Saifuddin ¹²⁴,
 M. Saimpert ¹³⁹, M. Saito ¹⁶⁰, T. Saito ¹⁶⁰, A. Sala ^{72a,72b}, D. Salamani ³⁷, A. Salnikov ¹⁵⁰,
 J. Salt ¹⁷⁰, A. Salvador Salas ¹⁵⁸, D. Salvatore ^{45b,45a}, F. Salvatore ¹⁵³, A. Salzburger ³⁷,
 D. Sammel ⁵⁵, E. Sampson ⁹⁴, D. Sampsonidis ^{159,e}, D. Sampsonidou ¹²⁷, J. Sánchez ¹⁷⁰,
 V. Sanchez Sebastian ¹⁷⁰, H. Sandaker ¹²⁹, C.O. Sander ⁴⁹, J.A. Sandesara ¹⁰⁶, M. Sandhoff ¹⁷⁸,
 C. Sandoval ^{23b}, L. Sanfilippo ^{64a}, D.P.C. Sankey ¹³⁸, T. Sano ⁹⁰, A. Sansoni ⁵⁴, L. Santi ³⁷,
 C. Santoni ⁴², H. Santos ^{134a,134b}, A. Santra ¹⁷⁶, E. Sanzani ^{24b,24a}, K.A. Saoucha ^{86b},
 J.G. Saraiva ^{134a,134d}, J. Sardain ⁷, O. Sasaki ⁸⁵, K. Sato ¹⁶⁴, C. Sauer ³⁷, E. Sauvan ⁴,
 P. Savard ^{162,aj}, R. Sawada ¹⁶⁰, C. Sawyer ¹³⁸, L. Sawyer ¹⁰⁰, C. Sbarra ^{24b}, A. Sbrizzi ^{24b,24a},
 T. Scanlon ⁹⁹, J. Schaarschmidt ¹⁴³, U. Schäfer ¹⁰³, A.C. Schaffer ^{67,46}, D. Schaile ¹¹²,
 R.D. Schamberger ¹⁵², C. Scharf ¹⁹, M.M. Schefer ²⁰, V.A. Schegelsky ³⁹, D. Scheirich ¹³⁷,
 M. Schernau ^{141e}, C. Scheulen ⁵⁷, C. Schiavi ^{58b,58a}, M. Schioppa ^{45b,45a}, B. Schlag ¹⁵⁰,
 S. Schlenker ³⁷, J. Schmeing ¹⁷⁸, M.A. Schmidt ¹⁷⁸, K. Schmieden ¹⁰³, C. Schmitt ¹⁰³,
 N. Schmitt ¹⁰³, S. Schmitt ⁴⁹, L. Schoeffel ¹³⁹, A. Schoening ^{64b}, P.G. Scholer ³⁵, E. Schopf ¹⁴⁸,

M. Schott ²⁵, S. Schramm ⁵⁷, T. Schroer ⁵⁷, H-C. Schultz-Coulon ^{64a}, M. Schumacher ⁵⁵,
B.A. Schumm ¹⁴⁰, Ph. Schune ¹³⁹, H.R. Schwartz ¹⁴⁰, A. Schwartzman ¹⁵⁰, T.A. Schwarz ¹⁰⁹,
Ph. Schwemling ¹³⁹, R. Schwienhorst ¹¹⁰, F.G. Sciacca ²⁰, A. Sciandra ³⁰, G. Sciolla ²⁷,
F. Scuri ^{75a}, C.D. Sebastiani ³⁷, K. Sedlaczek ¹¹⁹, S.C. Seidel ¹¹⁶, A. Seiden ¹⁴⁰,
B.D. Seidlitz ⁴³, C. Seitz ⁴⁹, J.M. Seixas ^{84b}, G. Sekhniaidze ^{73a}, L. Selem ⁶¹,
N. Semprini-Cesari ^{24b,24a}, A. Semushin ^{180,39}, D. Sengupta ⁵⁷, V. Senthilkumar ¹⁷⁰, L. Serin ⁶⁷,
M. Sessa ^{77a,77b}, H. Severini ¹²⁴, F. Sforza ^{58b,58a}, A. Sfyrla ⁵⁷, Q. Sha ¹⁴, E. Shabalina ⁵⁶,
H. Shaddix ¹¹⁹, A.H. Shah ³³, R. Shaheen ¹⁵¹, J.D. Shahinian ¹³², D. Shaked Renous ¹⁷⁶,
M. Shamim ³⁷, L.Y. Shan ¹⁴, M. Shapiro ^{18a}, A. Sharma ³⁷, A.S. Sharma ¹⁷¹, P. Sharma ³⁰,
P.B. Shatalov ³⁹, K. Shaw ¹⁵³, S.M. Shaw ¹⁰⁴, Q. Shen ^{145a}, D.J. Sheppard ¹⁴⁹, P. Sherwood ⁹⁹,
L. Shi ⁹⁹, X. Shi ¹⁴, S. Shimizu ⁸⁵, C.O. Shimmin ¹⁷⁹, I.P.J. Shipsey ^{130,*}, S. Shirabe ⁹¹,
M. Shiyakova ^{40,aa}, M.J. Shochet ⁴¹, D.R. Shope ¹²⁹, B. Shrestha ¹²⁴, S. Shrestha ^{123,ao},
I. Shreyber ⁴⁰, M.J. Shroff ¹⁷², P. Sicho ¹³⁵, A.M. Sickles ¹⁶⁹, E. Sideras Haddad ^{34g,167},
A.C. Sidley ¹¹⁸, A. Sidoti ^{24b}, F. Siegert ⁵¹, Dj. Sijacki ¹⁶, F. Sili ⁹³, J.M. Silva ⁵³,
I. Silva Ferreira ^{84b}, M.V. Silva Oliveira ³⁰, S.B. Silverstein ^{48a}, S. Simion ⁶⁷, R. Simoniello ³⁷,
E.L. Simpson ¹⁰⁴, H. Simpson ¹⁵³, L.R. Simpson ¹⁰⁹, S. Simsek ⁸³, S. Sindhu ⁵⁶, P. Sinervo ¹⁶²,
S.N. Singh ²⁷, S. Singh ³⁰, S. Sinha ⁴⁹, S. Sinha ¹⁰⁴, M. Sioli ^{24b,24a}, K. Sioulas ⁹, I. Siral ³⁷,
E. Sitnikova ⁴⁹, J. Sjölin ^{48a,48b}, A. Skaf ⁵⁶, E. Skorda ²¹, P. Skubic ¹²⁴, M. Slawinska ⁸⁹,
I. Slazyk ¹⁷, V. Smakhtin ¹⁷⁶, B.H. Smart ¹³⁸, S.Yu. Smirnov ^{141b}, Y. Smirnov ⁸³,
L.N. Smirnova ^{39,a}, O. Smirnova ¹⁰¹, A.C. Smith ⁴³, D.R. Smith ¹⁶⁶, E.A. Smith ⁴¹, J.L. Smith ¹⁰⁴,
M.B. Smith ³⁵, R. Smith ¹⁵⁰, H. Smitmanns ¹⁰³, M. Smizanska ⁹⁴, K. Smolek ¹³⁶,
P. Smolyanskiy ¹³⁶, A.A. Snesarev ⁴⁰, H.L. Snoek ¹¹⁸, S. Snyder ³⁰, R. Sobie ^{172,ac},
A. Soffer ¹⁵⁸, C.A. Solans Sanchez ³⁷, E.Yu. Soldatov ⁴⁰, U. Soldevila ¹⁷⁰, A.A. Solodkov ^{34g},
S. Solomon ²⁷, A. Soloshenko ⁴⁰, K. Solovieva ⁵⁵, O.V. Solovyanov ⁴², P. Sommer ⁵¹,
A. Sonay ¹³, W.Y. Song ^{163b}, A. Sopczak ¹³⁶, A.L. Sopio ⁵³, F. Sopkova ^{29b}, J.D. Sorenson ¹¹⁶,
I.R. Sotarriva Alvarez ¹⁴², V. Sothilingam ^{64a}, O.J. Soto Sandoval ^{141c,141b}, S. Sottocornola ⁶⁹,
R. Soualah ^{86a}, Z. Soumami ^{36e}, D. South ⁴⁹, N. Soybelman ¹⁷⁶, S. Spagnolo ^{71a,71b},
M. Spalla ¹¹³, D. Sperlich ⁵⁵, B. Spisso ^{73a,73b}, D.P. Spiteri ⁶⁰, L. Splendori ¹⁰⁵, M. Spousta ¹³⁷,
E.J. Staats ³⁵, R. Stamen ^{64a}, E. Stanecka ⁸⁹, W. Stanek-Maslouska ⁴⁹, M.V. Stange ⁵¹,
B. Stanislaus ^{18a}, M.M. Stanitzki ⁴⁹, B. Stapf ⁴⁹, E.A. Starchenko ³⁹, G.H. Stark ¹⁴⁰, J. Stark ⁹²,
P. Staroba ¹³⁵, P. Starovoitov ^{86b}, R. Staszewski ⁸⁹, G. Stavropoulos ⁴⁷, A. Stefl ³⁷,
P. Steinberg ³⁰, B. Stelzer ^{149,163a}, H.J. Stelzer ¹³³, O. Stelzer ^{163a}, H. Stenzel ⁵⁹,
T.J. Stevenson ¹⁵³, G.A. Stewart ³⁷, J.R. Stewart ¹²⁵, M.C. Stockton ³⁷, G. Stoicea ^{28b},
M. Stolarski ^{134a}, S. Stonjek ¹¹³, A. Straessner ⁵¹, J. Strandberg ¹⁵¹, S. Strandberg ^{48a,48b},
M. Stratmann ¹⁷⁸, M. Strauss ¹²⁴, T. Strebler ¹⁰⁵, P. Strizenc ^{29b}, R. Ströhmer ¹⁷³,
D.M. Strom ¹²⁷, R. Stroynowski ⁴⁶, A. Strubig ^{48a,48b}, S.A. Stucci ³⁰, B. Stugu ¹⁷, J. Stupak ¹²⁴,
N.A. Styles ⁴⁹, D. Su ¹⁵⁰, S. Su ⁶³, W. Su ^{145b}, X. Su ⁶³, D. Suchy ^{29a}, K. Sugizaki ¹³²,
V.V. Sulin ³⁹, M.J. Sullivan ⁹⁵, D.M.S. Sultan ¹³⁰, L. Sultanaliyeva ³⁹, S. Sultansoy ^{3b},
S. Sun ¹⁷⁷, W. Sun ¹⁴, O. Sunneborn Gudnadottir ¹⁶⁸, N. Sur ¹⁰⁵, M.R. Sutton ¹⁵³,
H. Suzuki ¹⁶⁴, M. Svatos ¹³⁵, P.N. Swallow ³³, M. Swiatlowski ^{163a}, T. Swirski ¹⁷³,
I. Sykora ^{29a}, M. Sykora ¹³⁷, T. Sykora ¹³⁷, D. Ta ¹⁰³, K. Tackmann ^{49,z}, A. Taffard ¹⁶⁶,
R. Tafirout ^{163a}, Y. Takubo ⁸⁵, M. Talby ¹⁰⁵, A.A. Talyshev ³⁹, K.C. Tam ^{65b}, N.M. Tamir ¹⁵⁸,
A. Tanaka ¹⁶⁰, J. Tanaka ¹⁶⁰, R. Tanaka ⁶⁷, M. Tanasini ¹⁵², Z. Tao ¹⁷¹, S. Tapia Araya ^{141f},
S. Tapprogge ¹⁰³, A. Tarek Abouelfadl Mohamed ¹¹⁰, S. Tarem ¹⁵⁷, K. Tariq ¹⁴, G. Tarna ^{28b},
G.F. Tartarelli ^{72a}, M.J. Tartarin ⁹², P. Tas ¹³⁷, M. Tasevsky ¹³⁵, E. Tassi ^{45b,45a}, A.C. Tate ¹⁶⁹,
G. Tateno ¹⁶⁰, Y. Tayalati ^{36e,ab}, G.N. Taylor ¹⁰⁸, W. Taylor ^{163b}, A.S. Tegetmeier ⁹²,
P. Teixeira-Dias ⁹⁸, J.J. Teoh ¹⁶², K. Terashi ¹⁶⁰, J. Terron ¹⁰², S. Terzo ¹³, M. Testa ⁵⁴,

R.J. Teuscher ^{162,ac}, A. Thaler ⁸⁰, O. Theiner ⁵⁷, T. Thevenaux-Pelzer ¹⁰⁵, O. Thielmann ¹⁷⁸, D.W. Thomas ⁹⁸, J.P. Thomas ²¹, E.A. Thompson ^{18a}, P.D. Thompson ²¹, E. Thomson ¹³², R.E. Thornberry ⁴⁶, C. Tian ⁶³, Y. Tian ⁵⁷, V. Tikhomirov ⁸³, Yu.A. Tikhonov ³⁹, S. Timoshenko ³⁹, D. Timoshyn ¹³⁷, E.X.L. Ting ¹, P. Tipton ¹⁷⁹, A. Tishelman-Charny ³⁰, S.H. Tlou ^{34g}, K. Todome ¹⁴², S. Todorova-Nova ¹³⁷, S. Todt ⁵¹, L. Toffolin ^{70a,70c}, M. Togawa ⁸⁵, J. Tojo ⁹¹, S. Tokár ^{29a}, O. Toldaiev ⁶⁹, G. Tolkachev ¹⁰⁵, M. Tomoto ^{85,114}, L. Tompkins ^{150,p}, E. Torrence ¹²⁷, H. Torres ⁹², E. Torró Pastor ¹⁷⁰, M. Toscani ³¹, C. Tosciri ⁴¹, M. Tost ¹¹, D.R. Tovey ¹⁴⁶, T. Trefzger ¹⁷³, P.M. Tricarico ¹³, A. Tricoli ³⁰, I.M. Trigger ^{163a}, S. Trincaz-Duvoid ¹³¹, D.A. Trischuk ²⁷, A. Tropina ⁴⁰, L. Truong ^{34c}, M. Trzebinski ⁸⁹, A. Trzupke ⁸⁹, F. Tsai ¹⁵², M. Tsai ¹⁰⁹, A. Tsiamis ¹⁵⁹, P.V. Tsiareshka ⁴⁰, S. Tsigaridas ^{163a}, A. Tsirigotis ^{159,v}, V. Tsiskaridze ¹⁶², E.G. Tskhadadze ^{156a}, M. Tsooulou ¹⁵⁹, Y. Tsujikawa ⁹⁰, I.I. Tsukerman ³⁹, V. Tsulaia ^{18a}, S. Tsuno ⁸⁵, K. Tsuru ¹²², D. Tsybychev ¹⁵², Y. Tu ^{65b}, A. Tudorache ^{28b}, V. Tudorache ^{28b}, S. Turchikhin ^{58b,58a}, I. Turk Cakir ^{3a}, R. Turra ^{72a}, T. Turtuvshin ^{40,ad}, P.M. Tuts ⁴³, S. Tzamarias ^{159,e}, E. Tzovara ¹⁰³, Y. Uematsu ⁸⁵, F. Ukegawa ¹⁶⁴, P.A. Ulloa Poblete ^{141c,141b}, E.N. Umaka ³⁰, G. Unal ³⁷, A. Undrus ³⁰, G. Unel ¹⁶⁶, J. Urban ^{29b}, P. Urrejola ^{141a}, G. Usai ⁸, R. Ushioda ¹⁶¹, M. Usman ¹¹¹, F. Ustuner ⁵³, Z. Uysal ⁸³, V. Vacek ¹³⁶, B. Vachon ¹⁰⁷, T. Vafeiadis ³⁷, A. Vaitkus ⁹⁹, C. Valderanis ¹¹², E. Valdes Santurio ^{48a,48b}, M. Valente ^{163a}, S. Valentinetti ^{24b,24a}, A. Valero ¹⁷⁰, E. Valiente Moreno ¹⁷⁰, A. Vallier ⁹², J.A. Valls Ferrer ¹⁷⁰, D.R. Van Arneman ¹¹⁸, T.R. Van Daalen ¹⁴³, A. Van Der Graaf ⁵⁰, H.Z. Van Der Schyf ^{34g}, P. Van Gemmeren ⁶, M. Van Rijnbach ³⁷, S. Van Stroud ⁹⁹, I. Van Vulpen ¹¹⁸, P. Vana ¹³⁷, M. Vanadia ^{77a,77b}, U.M. Vande Voorde ¹⁵¹, W. Vandelli ³⁷, E.R. Vandewall ¹²⁵, D. Vannicola ¹⁵⁸, L. Vannoli ⁵⁴, R. Vari ^{76a}, E.W. Varnes ⁷, C. Varni ^{18b}, D. Varouchas ⁶⁷, L. Varriale ¹⁷⁰, K.E. Varvell ¹⁵⁴, M.E. Vasile ^{28b}, L. Vaslin ⁸⁵, M.D. Vassilev ¹⁵⁰, A. Vasyukov ⁴⁰, L.M. Vaughan ¹²⁵, R. Vavricka ¹³⁷, T. Vazquez Schroeder ¹³, J. Veatch ³², V. Vecchio ¹⁰⁴, M.J. Veen ¹⁰⁶, I. Veliscek ³⁰, L.M. Veloce ¹⁶², F. Veloso ^{134a,134c}, S. Veneziano ^{76a}, A. Ventura ^{71a,71b}, S. Ventura Gonzalez ¹³⁹, A. Verbytskyi ¹¹³, M. Verducci ^{75a,75b}, C. Vergis ⁹⁷, M. Verissimo De Araujo ^{84b}, W. Verkerke ¹¹⁸, J.C. Vermeulen ¹¹⁸, C. Vernieri ¹⁵⁰, M. Vessella ¹⁶⁶, M.C. Vetterli ^{149,aj}, A. Vgenopoulos ¹⁰³, N. Viaux Maira ^{141f}, T. Vickey ¹⁴⁶, O.E. Vickey Boeriu ¹⁴⁶, G.H.A. Viehhauser ¹³⁰, L. Vigani ^{64b}, M. Vigil ¹¹³, M. Villa ^{24b,24a}, M. Villaplana Perez ¹⁷⁰, E.M. Villhauer ⁵³, E. Vilucchi ⁵⁴, M.G. Vincter ³⁵, A. Visibile ¹¹⁸, C. Vittori ³⁷, I. Vivarelli ^{24b,24a}, E. Voevodina ¹¹³, F. Vogel ¹¹², J.C. Voigt ⁵¹, P. Vokac ¹³⁶, Yu. Volkotrub ^{88b}, E. Von Toerne ²⁵, B. Vormwald ³⁷, K. Vorobev ⁵², M. Vos ¹⁷⁰, K. Voss ¹⁴⁸, M. Vozak ³⁷, L. Vozdecky ¹²⁴, N. Vranjes ¹⁶, M. Vranjes Milosavljevic ¹⁶, M. Vreeswijk ¹¹⁸, N.K. Vu ^{145b,145a}, R. Vuillermet ³⁷, O. Vujinovic ¹⁰³, I. Vukotic ⁴¹, I.K. Vyas ³⁵, J.F. Wack ³³, S. Wada ¹⁶⁴, C. Wagner ¹⁵⁰, J.M. Wagner ^{18a}, W. Wagner ¹⁷⁸, S. Wahdan ¹⁷⁸, H. Wahlberg ⁹³, C.H. Waits ¹²⁴, J. Walder ¹³⁸, R. Walker ¹¹², W. Walkowiak ¹⁴⁸, A. Wall ¹³², E.J. Wallin ¹⁰¹, T. Wamorkar ^{18a}, A.Z. Wang ¹⁴⁰, C. Wang ¹⁰³, C. Wang ¹¹, H. Wang ^{18a}, J. Wang ^{65c}, P. Wang ¹⁰⁴, P. Wang ⁹⁹, R. Wang ⁶², R. Wang ⁶, S.M. Wang ¹⁵⁵, S. Wang ¹⁴, T. Wang ⁶³, T. Wang ⁶³, W.T. Wang ⁸¹, W. Wang ¹⁴, X. Wang ¹⁶⁹, X. Wang ^{145a}, X. Wang ⁴⁹, Y. Wang ^{115a}, Y. Wang ⁶³, Z. Wang ¹⁰⁹, Z. Wang ^{145b,52,145a}, Z. Wang ¹⁰⁹, C. Wanotayaroj ⁸⁵, A. Warburton ¹⁰⁷, A.L. Warnerbring ¹⁴⁸, N. Warrack ⁶⁰, S. Waterhouse ⁹⁸, A.T. Watson ²¹, H. Watson ⁵³, M.F. Watson ²¹, E. Watton ⁶⁰, G. Watts ¹⁴³, B.M. Waugh ⁹⁹, J.M. Webb ⁵⁵, C. Weber ³⁰, H.A. Weber ¹⁹, M.S. Weber ²⁰, S.M. Weber ^{64a}, C. Wei ⁶³, Y. Wei ⁵⁵, A.R. Weidberg ¹³⁰, E.J. Weik ¹²¹, J. Weingarten ⁵⁰, C. Weiser ⁵⁵, C.J. Wells ⁴⁹, T. Wenaus ³⁰, B. Wendland ⁵⁰, T. Wengler ³⁷, N.S. Wenke ¹¹³, N. Wermes ²⁵, M. Wessels ^{64a}, A.M. Wharton ⁹⁴, A.S. White ⁶², A. White ⁸, M.J. White ¹, D. Whiteson ¹⁶⁶, L. Wickremasinghe ¹²⁸, W. Wiedenmann ¹⁷⁷, M. Wielers ¹³⁸,

C. Wiglesworth , D.J. Wilbern¹²⁴, H.G. Wilkens , J.J.H. Wilkinson , D.M. Williams , H.H. Williams¹³², S. Williams , S. Willocq , B.J. Wilson , D.J. Wilson , P.J. Windischhofer , F.I. Winkel , F. Winklmeier , B.T. Winter , M. Wittgen¹⁵⁰, M. Wobisch , T. Wojtkowski⁶¹, Z. Wolffs , J. Wollrath³⁷, M.W. Wolter , H. Wolters , M.C. Wong¹⁴⁰, E.L. Woodward , S.D. Worm , B.K. Wosiek , K.W. Woźniak , S. Wozniowski , K. Wraight , C. Wu , M. Wu , S.L. Wu , S. Wu , X. Wu , X. Wu , Y. Wu , Z. Wu , J. Wuerzinger , T.R. Wyatt , B.M. Wynne , S. Xella , L. Xia , M. Xia , M. Xie , A. Xiong , J. Xiong , D. Xu , H. Xu , L. Xu , R. Xu , T. Xu , Y. Xu , Z. Xu , Z. Xu , B. Yabsley , S. Yacoob , Y. Yamaguchi , E. Yamashita , H. Yamauchi , T. Yamazaki , Y. Yamazaki , S. Yan , Z. Yan , H.J. Yang , H.T. Yang , S. Yang , T. Yang , X. Yang , X. Yang , Y. Yang , Y. Yang , W-M. Yao , C.L. Yardley , H. Ye , J. Ye , S. Ye , X. Ye , Y. Yeh , I. Yeletsikh , B. Yeo , M.R. Yexley , T.P. Yildirim , P. Yin , K. Yorita , S. Younas , C.J.S. Young , C. Young , N.D. Young¹²⁷, Y. Yu , J. Yuan , M. Yuan , R. Yuan , L. Yue , M. Zaazoua , B. Zabinski , I. Zahir , A. Zaio^{58b,58a}, Z.K. Zak , T. Zakareishvili , S. Zambito , J.A. Zamora Saa , J. Zang , D. Zanzi , R. Zanzottera , O. Zaplatilek , C. Zeitnitz , H. Zeng , J.C. Zeng , D.T. Zenger Jr , O. Zenin , T. Ženiš , S. Zenz , S. Zerradi , D. Zerwas , M. Zhai , D.F. Zhang , J. Zhang , J. Zhang , K. Zhang , L. Zhang , L. Zhang , P. Zhang , R. Zhang , S. Zhang , T. Zhang , X. Zhang , Y. Zhang , Y. Zhang , Y. Zhang , Z. Zhang , Z. Zhang , H. Zhao , T. Zhao , Y. Zhao , Z. Zhao , Z. Zhao , A. Zhemchugov , J. Zheng , K. Zheng , X. Zheng , Z. Zheng , D. Zhong , B. Zhou , H. Zhou , N. Zhou , Y. Zhou , Y. Zhou , Y. Zhou , C.G. Zhu , J. Zhu , X. Zhu , Y. Zhu , Y. Zhu , X. Zhuang , K. Zhukov , N.I. Zimine , J. Zinsser , M. Ziolkowski , L. Živković , A. Zoccoli , K. Zoch , T.G. Zorbas , O. Zormpa , W. Zou , L. Zwalinski .

¹Department of Physics, University of Adelaide, Adelaide; Australia.

²Department of Physics, University of Alberta, Edmonton AB; Canada.

^{3(a)}Department of Physics, Ankara University, Ankara; ^(b)Division of Physics, TOBB University of Economics and Technology, Ankara; Türkiye.

⁴LAPP, Université Savoie Mont Blanc, CNRS/IN2P3, Annecy; France.

⁵APC, Université Paris Cité, CNRS/IN2P3, Paris; France.

⁶High Energy Physics Division, Argonne National Laboratory, Argonne IL; United States of America.

⁷Department of Physics, University of Arizona, Tucson AZ; United States of America.

⁸Department of Physics, University of Texas at Arlington, Arlington TX; United States of America.

⁹Physics Department, National and Kapodistrian University of Athens, Athens; Greece.

¹⁰Physics Department, National Technical University of Athens, Zografou; Greece.

¹¹Department of Physics, University of Texas at Austin, Austin TX; United States of America.

¹²Institute of Physics, Azerbaijan Academy of Sciences, Baku; Azerbaijan.

¹³Institut de Física d'Altes Energies (IFAE), Barcelona Institute of Science and Technology, Barcelona; Spain.

¹⁴Institute of High Energy Physics, Chinese Academy of Sciences, Beijing; China.

¹⁵Physics Department, Tsinghua University, Beijing; China.

¹⁶Institute of Physics, University of Belgrade, Belgrade; Serbia.

¹⁷Department for Physics and Technology, University of Bergen, Bergen; Norway.

- ^{18(a)}Physics Division, Lawrence Berkeley National Laboratory, Berkeley CA; ^(b)University of California, Berkeley CA; United States of America.
- ¹⁹Institut für Physik, Humboldt Universität zu Berlin, Berlin; Germany.
- ²⁰Albert Einstein Center for Fundamental Physics and Laboratory for High Energy Physics, University of Bern, Bern; Switzerland.
- ²¹School of Physics and Astronomy, University of Birmingham, Birmingham; United Kingdom.
- ^{22(a)}Department of Physics, Bogazici University, Istanbul; ^(b)Department of Physics Engineering, Gaziantep University, Gaziantep; ^(c)Department of Physics, Istanbul University, Istanbul; Türkiye.
- ^{23(a)}Facultad de Ciencias y Centro de Investigaciones, Universidad Antonio Nariño, Bogotá; ^(b)Departamento de Física, Universidad Nacional de Colombia, Bogotá; Colombia.
- ^{24(a)}Dipartimento di Fisica e Astronomia A. Righi, Università di Bologna, Bologna; ^(b)INFN Sezione di Bologna; Italy.
- ²⁵Physikalisches Institut, Universität Bonn, Bonn; Germany.
- ²⁶Department of Physics, Boston University, Boston MA; United States of America.
- ²⁷Department of Physics, Brandeis University, Waltham MA; United States of America.
- ^{28(a)}Transilvania University of Brasov, Brasov; ^(b)Horia Hulubei National Institute of Physics and Nuclear Engineering, Bucharest; ^(c)Department of Physics, Alexandru Ioan Cuza University of Iasi, Iasi; ^(d)National Institute for Research and Development of Isotopic and Molecular Technologies, Physics Department, Cluj-Napoca; ^(e)National University of Science and Technology Politehnica, Bucharest; ^(f)West University in Timisoara, Timisoara; ^(g)Faculty of Physics, University of Bucharest, Bucharest; Romania.
- ^{29(a)}Faculty of Mathematics, Physics and Informatics, Comenius University, Bratislava; ^(b)Department of Subnuclear Physics, Institute of Experimental Physics of the Slovak Academy of Sciences, Kosice; Slovak Republic.
- ³⁰Physics Department, Brookhaven National Laboratory, Upton NY; United States of America.
- ³¹Universidad de Buenos Aires, Facultad de Ciencias Exactas y Naturales, Departamento de Física, y CONICET, Instituto de Física de Buenos Aires (IFIBA), Buenos Aires; Argentina.
- ³²California State University, CA; United States of America.
- ³³Cavendish Laboratory, University of Cambridge, Cambridge; United Kingdom.
- ^{34(a)}Department of Physics, University of Cape Town, Cape Town; ^(b)iThemba Labs, Western Cape; ^(c)Department of Mechanical Engineering Science, University of Johannesburg, Johannesburg; ^(d)National Institute of Physics, University of the Philippines Diliman (Philippines); ^(e)University of South Africa, Department of Physics, Pretoria; ^(f)University of Zululand, KwaDlangezwa; ^(g)School of Physics, University of the Witwatersrand, Johannesburg; South Africa.
- ³⁵Department of Physics, Carleton University, Ottawa ON; Canada.
- ^{36(a)}Faculté des Sciences Ain Chock, Université Hassan II de Casablanca; ^(b)Faculté des Sciences, Université Ibn-Tofail, Kénitra; ^(c)Faculté des Sciences Semlalia, Université Cadi Ayyad, LPHEA-Marrakech; ^(d)LPMR, Faculté des Sciences, Université Mohamed Premier, Oujda; ^(e)Faculté des sciences, Université Mohammed V, Rabat; ^(f)Institute of Applied Physics, Mohammed VI Polytechnic University, Ben Guerir; Morocco.
- ³⁷CERN, Geneva; Switzerland.
- ³⁸Affiliated with an institute formerly covered by a cooperation agreement with CERN.
- ³⁹Affiliated with an institute covered by a cooperation agreement with CERN.
- ⁴⁰Affiliated with an international laboratory covered by a cooperation agreement with CERN.
- ⁴¹Enrico Fermi Institute, University of Chicago, Chicago IL; United States of America.
- ⁴²LPC, Université Clermont Auvergne, CNRS/IN2P3, Clermont-Ferrand; France.
- ⁴³Nevis Laboratory, Columbia University, Irvington NY; United States of America.
- ⁴⁴Niels Bohr Institute, University of Copenhagen, Copenhagen; Denmark.

- ^{45(a)}Dipartimento di Fisica, Università della Calabria, Rende; ^(b)INFN Gruppo Collegato di Cosenza, Laboratori Nazionali di Frascati; Italy.
- ⁴⁶Physics Department, Southern Methodist University, Dallas TX; United States of America.
- ⁴⁷National Centre for Scientific Research "Demokritos", Agia Paraskevi; Greece.
- ^{48(a)}Department of Physics, Stockholm University; ^(b)Oskar Klein Centre, Stockholm; Sweden.
- ⁴⁹Deutsches Elektronen-Synchrotron DESY, Hamburg and Zeuthen; Germany.
- ⁵⁰Fakultät Physik, Technische Universität Dortmund, Dortmund; Germany.
- ⁵¹Institut für Kern- und Teilchenphysik, Technische Universität Dresden, Dresden; Germany.
- ⁵²Department of Physics, Duke University, Durham NC; United States of America.
- ⁵³SUPA - School of Physics and Astronomy, University of Edinburgh, Edinburgh; United Kingdom.
- ⁵⁴INFN e Laboratori Nazionali di Frascati, Frascati; Italy.
- ⁵⁵Physikalisches Institut, Albert-Ludwigs-Universität Freiburg, Freiburg; Germany.
- ⁵⁶II. Physikalisches Institut, Georg-August-Universität Göttingen, Göttingen; Germany.
- ⁵⁷Département de Physique Nucléaire et Corpusculaire, Université de Genève, Genève; Switzerland.
- ^{58(a)}Dipartimento di Fisica, Università di Genova, Genova; ^(b)INFN Sezione di Genova; Italy.
- ⁵⁹II. Physikalisches Institut, Justus-Liebig-Universität Giessen, Giessen; Germany.
- ⁶⁰SUPA - School of Physics and Astronomy, University of Glasgow, Glasgow; United Kingdom.
- ⁶¹LPSC, Université Grenoble Alpes, CNRS/IN2P3, Grenoble INP, Grenoble; France.
- ⁶²Laboratory for Particle Physics and Cosmology, Harvard University, Cambridge MA; United States of America.
- ⁶³Department of Modern Physics and State Key Laboratory of Particle Detection and Electronics, University of Science and Technology of China, Hefei; China.
- ^{64(a)}Kirchhoff-Institut für Physik, Ruprecht-Karls-Universität Heidelberg, Heidelberg; ^(b)Physikalisches Institut, Ruprecht-Karls-Universität Heidelberg, Heidelberg; Germany.
- ^{65(a)}Department of Physics, Chinese University of Hong Kong, Shatin, N.T., Hong Kong; ^(b)Department of Physics, University of Hong Kong, Hong Kong; ^(c)Department of Physics and Institute for Advanced Study, Hong Kong University of Science and Technology, Clear Water Bay, Kowloon, Hong Kong; China.
- ⁶⁶Department of Physics, National Tsing Hua University, Hsinchu; Taiwan.
- ⁶⁷IJCLab, Université Paris-Saclay, CNRS/IN2P3, 91405, Orsay; France.
- ⁶⁸Centro Nacional de Microelectrónica (IMB-CNM-CSIC), Barcelona; Spain.
- ⁶⁹Department of Physics, Indiana University, Bloomington IN; United States of America.
- ^{70(a)}INFN Gruppo Collegato di Udine, Sezione di Trieste, Udine; ^(b)ICTP, Trieste; ^(c)Dipartimento Politecnico di Ingegneria e Architettura, Università di Udine, Udine; Italy.
- ^{71(a)}INFN Sezione di Lecce; ^(b)Dipartimento di Matematica e Fisica, Università del Salento, Lecce; Italy.
- ^{72(a)}INFN Sezione di Milano; ^(b)Dipartimento di Fisica, Università di Milano, Milano; Italy.
- ^{73(a)}INFN Sezione di Napoli; ^(b)Dipartimento di Fisica, Università di Napoli, Napoli; Italy.
- ^{74(a)}INFN Sezione di Pavia; ^(b)Dipartimento di Fisica, Università di Pavia, Pavia; Italy.
- ^{75(a)}INFN Sezione di Pisa; ^(b)Dipartimento di Fisica E. Fermi, Università di Pisa, Pisa; Italy.
- ^{76(a)}INFN Sezione di Roma; ^(b)Dipartimento di Fisica, Sapienza Università di Roma, Roma; Italy.
- ^{77(a)}INFN Sezione di Roma Tor Vergata; ^(b)Dipartimento di Fisica, Università di Roma Tor Vergata, Roma; Italy.
- ^{78(a)}INFN Sezione di Roma Tre; ^(b)Dipartimento di Matematica e Fisica, Università Roma Tre, Roma; Italy.
- ^{79(a)}INFN-TIFPA; ^(b)Università degli Studi di Trento, Trento; Italy.
- ⁸⁰Universität Innsbruck, Department of Astro and Particle Physics, Innsbruck; Austria.
- ⁸¹University of Iowa, Iowa City IA; United States of America.
- ⁸²Department of Physics and Astronomy, Iowa State University, Ames IA; United States of America.

- ⁸³Istinye University, Sariyer, Istanbul; Türkiye.
- ⁸⁴(^a) Departamento de Engenharia Elétrica, Universidade Federal de Juiz de Fora (UFJF), Juiz de Fora; (^b) Universidade Federal do Rio De Janeiro COPPE/EE/IF, Rio de Janeiro; (^c) Instituto de Física, Universidade de São Paulo, São Paulo; (^d) Rio de Janeiro State University, Rio de Janeiro; (^e) Federal University of Bahia, Bahia; Brazil.
- ⁸⁵KEK, High Energy Accelerator Research Organization, Tsukuba; Japan.
- ⁸⁶(^a) Khalifa University of Science and Technology, Abu Dhabi; (^b) University of Sharjah, Sharjah; United Arab Emirates.
- ⁸⁷Graduate School of Science, Kobe University, Kobe; Japan.
- ⁸⁸(^a) AGH University of Krakow, Faculty of Physics and Applied Computer Science, Krakow; (^b) Marian Smoluchowski Institute of Physics, Jagiellonian University, Krakow; Poland.
- ⁸⁹Institute of Nuclear Physics Polish Academy of Sciences, Krakow; Poland.
- ⁹⁰Faculty of Science, Kyoto University, Kyoto; Japan.
- ⁹¹Research Center for Advanced Particle Physics and Department of Physics, Kyushu University, Fukuoka ; Japan.
- ⁹²L2IT, Université de Toulouse, CNRS/IN2P3, UPS, Toulouse; France.
- ⁹³Instituto de Física La Plata, Universidad Nacional de La Plata and CONICET, La Plata; Argentina.
- ⁹⁴Physics Department, Lancaster University, Lancaster; United Kingdom.
- ⁹⁵Oliver Lodge Laboratory, University of Liverpool, Liverpool; United Kingdom.
- ⁹⁶Department of Experimental Particle Physics, Jožef Stefan Institute and Department of Physics, University of Ljubljana, Ljubljana; Slovenia.
- ⁹⁷Department of Physics and Astronomy, Queen Mary University of London, London; United Kingdom.
- ⁹⁸Department of Physics, Royal Holloway University of London, Egham; United Kingdom.
- ⁹⁹Department of Physics and Astronomy, University College London, London; United Kingdom.
- ¹⁰⁰Louisiana Tech University, Ruston LA; United States of America.
- ¹⁰¹Fysiska institutionen, Lunds universitet, Lund; Sweden.
- ¹⁰²Departamento de Física Teórica C-15 and CIAFF, Universidad Autónoma de Madrid, Madrid; Spain.
- ¹⁰³Institut für Physik, Universität Mainz, Mainz; Germany.
- ¹⁰⁴School of Physics and Astronomy, University of Manchester, Manchester; United Kingdom.
- ¹⁰⁵CPPM, Aix-Marseille Université, CNRS/IN2P3, Marseille; France.
- ¹⁰⁶Department of Physics, University of Massachusetts, Amherst MA; United States of America.
- ¹⁰⁷Department of Physics, McGill University, Montreal QC; Canada.
- ¹⁰⁸School of Physics, University of Melbourne, Victoria; Australia.
- ¹⁰⁹Department of Physics, University of Michigan, Ann Arbor MI; United States of America.
- ¹¹⁰Department of Physics and Astronomy, Michigan State University, East Lansing MI; United States of America.
- ¹¹¹Group of Particle Physics, University of Montreal, Montreal QC; Canada.
- ¹¹²Fakultät für Physik, Ludwig-Maximilians-Universität München, München; Germany.
- ¹¹³Max-Planck-Institut für Physik (Werner-Heisenberg-Institut), München; Germany.
- ¹¹⁴Graduate School of Science and Kobayashi-Maskawa Institute, Nagoya University, Nagoya; Japan.
- ¹¹⁵(^a) Department of Physics, Nanjing University, Nanjing; (^b) School of Science, Shenzhen Campus of Sun Yat-sen University; (^c) University of Chinese Academy of Science (UCAS), Beijing; China.
- ¹¹⁶Department of Physics and Astronomy, University of New Mexico, Albuquerque NM; United States of America.
- ¹¹⁷Institute for Mathematics, Astrophysics and Particle Physics, Radboud University/Nikhef, Nijmegen; Netherlands.
- ¹¹⁸Nikhef National Institute for Subatomic Physics and University of Amsterdam, Amsterdam;

Netherlands.

¹¹⁹Department of Physics, Northern Illinois University, DeKalb IL; United States of America.

¹²⁰^(a)New York University Abu Dhabi, Abu Dhabi;^(b)United Arab Emirates University, Al Ain; United Arab Emirates.

¹²¹Department of Physics, New York University, New York NY; United States of America.

¹²²Ochanomizu University, Otsuka, Bunkyo-ku, Tokyo; Japan.

¹²³Ohio State University, Columbus OH; United States of America.

¹²⁴Homer L. Dodge Department of Physics and Astronomy, University of Oklahoma, Norman OK; United States of America.

¹²⁵Department of Physics, Oklahoma State University, Stillwater OK; United States of America.

¹²⁶Palacký University, Joint Laboratory of Optics, Olomouc; Czech Republic.

¹²⁷Institute for Fundamental Science, University of Oregon, Eugene, OR; United States of America.

¹²⁸Graduate School of Science, University of Osaka, Osaka; Japan.

¹²⁹Department of Physics, University of Oslo, Oslo; Norway.

¹³⁰Department of Physics, Oxford University, Oxford; United Kingdom.

¹³¹LPNHE, Sorbonne Université, Université Paris Cité, CNRS/IN2P3, Paris; France.

¹³²Department of Physics, University of Pennsylvania, Philadelphia PA; United States of America.

¹³³Department of Physics and Astronomy, University of Pittsburgh, Pittsburgh PA; United States of America.

¹³⁴^(a)Laboratório de Instrumentação e Física Experimental de Partículas - LIP, Lisboa;^(b)Departamento de Física, Faculdade de Ciências, Universidade de Lisboa, Lisboa;^(c)Departamento de Física, Universidade de Coimbra, Coimbra;^(d)Centro de Física Nuclear da Universidade de Lisboa, Lisboa;^(e)Departamento de Física, Escola de Ciências, Universidade do Minho, Braga;^(f)Departamento de Física Teórica y del Cosmos, Universidad de Granada, Granada (Spain);^(g)Departamento de Física, Instituto Superior Técnico, Universidade de Lisboa, Lisboa; Portugal.

¹³⁵Institute of Physics of the Czech Academy of Sciences, Prague; Czech Republic.

¹³⁶Czech Technical University in Prague, Prague; Czech Republic.

¹³⁷Charles University, Faculty of Mathematics and Physics, Prague; Czech Republic.

¹³⁸Particle Physics Department, Rutherford Appleton Laboratory, Didcot; United Kingdom.

¹³⁹IRFU, CEA, Université Paris-Saclay, Gif-sur-Yvette; France.

¹⁴⁰Santa Cruz Institute for Particle Physics, University of California Santa Cruz, Santa Cruz CA; United States of America.

¹⁴¹^(a)Departamento de Física, Pontificia Universidad Católica de Chile, Santiago;^(b)Millennium Institute for Subatomic physics at high energy frontier (SAPHIR), Santiago;^(c)Instituto de Investigación Multidisciplinario en Ciencia y Tecnología, y Departamento de Física, Universidad de La Serena;^(d)Universidad Andres Bello, Department of Physics, Santiago;^(e)Instituto de Alta Investigación, Universidad de Tarapacá, Arica;^(f)Departamento de Física, Universidad Técnica Federico Santa María, Valparaíso; Chile.

¹⁴²Department of Physics, Institute of Science, Tokyo; Japan.

¹⁴³Department of Physics, University of Washington, Seattle WA; United States of America.

¹⁴⁴^(a)Institute of Frontier and Interdisciplinary Science and Key Laboratory of Particle Physics and Particle Irradiation (MOE), Shandong University, Qingdao;^(b)School of Physics, Zhengzhou University; China.

¹⁴⁵^(a)State Key Laboratory of Dark Matter Physics, School of Physics and Astronomy, Shanghai Jiao Tong University, Key Laboratory for Particle Astrophysics and Cosmology (MOE), SKLPPC, Shanghai;^(b)State Key Laboratory of Dark Matter Physics, Tsung-Dao Lee Institute, Shanghai Jiao Tong University, Shanghai; China.

¹⁴⁶Department of Physics and Astronomy, University of Sheffield, Sheffield; United Kingdom.

- ¹⁴⁷Department of Physics, Shinshu University, Nagano; Japan.
- ¹⁴⁸Department Physik, Universität Siegen, Siegen; Germany.
- ¹⁴⁹Department of Physics, Simon Fraser University, Burnaby BC; Canada.
- ¹⁵⁰SLAC National Accelerator Laboratory, Stanford CA; United States of America.
- ¹⁵¹Department of Physics, Royal Institute of Technology, Stockholm; Sweden.
- ¹⁵²Departments of Physics and Astronomy, Stony Brook University, Stony Brook NY; United States of America.
- ¹⁵³Department of Physics and Astronomy, University of Sussex, Brighton; United Kingdom.
- ¹⁵⁴School of Physics, University of Sydney, Sydney; Australia.
- ¹⁵⁵Institute of Physics, Academia Sinica, Taipei; Taiwan.
- ¹⁵⁶(^a) E. Andronikashvili Institute of Physics, Iv. Javakhishvili Tbilisi State University, Tbilisi; (^b) High Energy Physics Institute, Tbilisi State University, Tbilisi; (^c) University of Georgia, Tbilisi; Georgia.
- ¹⁵⁷Department of Physics, Technion, Israel Institute of Technology, Haifa; Israel.
- ¹⁵⁸Raymond and Beverly Sackler School of Physics and Astronomy, Tel Aviv University, Tel Aviv; Israel.
- ¹⁵⁹Department of Physics, Aristotle University of Thessaloniki, Thessaloniki; Greece.
- ¹⁶⁰International Center for Elementary Particle Physics and Department of Physics, University of Tokyo, Tokyo; Japan.
- ¹⁶¹Graduate School of Science and Technology, Tokyo Metropolitan University, Tokyo; Japan.
- ¹⁶²Department of Physics, University of Toronto, Toronto ON; Canada.
- ¹⁶³(^a) TRIUMF, Vancouver BC; (^b) Department of Physics and Astronomy, York University, Toronto ON; Canada.
- ¹⁶⁴Division of Physics and Tomonaga Center for the History of the Universe, Faculty of Pure and Applied Sciences, University of Tsukuba, Tsukuba; Japan.
- ¹⁶⁵Department of Physics and Astronomy, Tufts University, Medford MA; United States of America.
- ¹⁶⁶Department of Physics and Astronomy, University of California Irvine, Irvine CA; United States of America.
- ¹⁶⁷University of West Attica, Athens; Greece.
- ¹⁶⁸Department of Physics and Astronomy, University of Uppsala, Uppsala; Sweden.
- ¹⁶⁹Department of Physics, University of Illinois, Urbana IL; United States of America.
- ¹⁷⁰Instituto de Física Corpuscular (IFIC), Centro Mixto Universidad de Valencia - CSIC, Valencia; Spain.
- ¹⁷¹Department of Physics, University of British Columbia, Vancouver BC; Canada.
- ¹⁷²Department of Physics and Astronomy, University of Victoria, Victoria BC; Canada.
- ¹⁷³Fakultät für Physik und Astronomie, Julius-Maximilians-Universität Würzburg, Würzburg; Germany.
- ¹⁷⁴Department of Physics, University of Warwick, Coventry; United Kingdom.
- ¹⁷⁵Waseda University, Tokyo; Japan.
- ¹⁷⁶Department of Particle Physics and Astrophysics, Weizmann Institute of Science, Rehovot; Israel.
- ¹⁷⁷Department of Physics, University of Wisconsin, Madison WI; United States of America.
- ¹⁷⁸Fakultät für Mathematik und Naturwissenschaften, Fachgruppe Physik, Bergische Universität Wuppertal, Wuppertal; Germany.
- ¹⁷⁹Department of Physics, Yale University, New Haven CT; United States of America.
- ¹⁸⁰Yerevan Physics Institute, Yerevan; Armenia.
- ^a Also Affiliated with an institute covered by a cooperation agreement with CERN.
- ^b Also at An-Najah National University, Nablus; Palestine.
- ^c Also at Borough of Manhattan Community College, City University of New York, New York NY; United States of America.
- ^d Also at Center for High Energy Physics, Peking University; China.
- ^e Also at Center for Interdisciplinary Research and Innovation (CIRI-AUTH), Thessaloniki; Greece.

- f* Also at CERN, Geneva; Switzerland.
- g* Also at CMD-AC UNEC Research Center, Azerbaijan State University of Economics (UNEC); Azerbaijan.
- h* Also at Département de Physique Nucléaire et Corpusculaire, Université de Genève, Genève; Switzerland.
- i* Also at Departament de Física de la Universitat Autònoma de Barcelona, Barcelona; Spain.
- j* Also at Department of Financial and Management Engineering, University of the Aegean, Chios; Greece.
- k* Also at Department of Mathematical Sciences, University of South Africa, Johannesburg; South Africa.
- l* Also at Department of Modern Physics and State Key Laboratory of Particle Detection and Electronics, University of Science and Technology of China, Hefei; China.
- m* Also at Department of Physics, Bolu Abant İzzet Baysal University, Bolu; Türkiye.
- n* Also at Department of Physics, California State University, Sacramento; United States of America.
- o* Also at Department of Physics, King's College London, London; United Kingdom.
- p* Also at Department of Physics, Stanford University, Stanford CA; United States of America.
- q* Also at Department of Physics, Stellenbosch University; South Africa.
- r* Also at Department of Physics, University of Fribourg, Fribourg; Switzerland.
- s* Also at Department of Physics, University of Thessaly; Greece.
- t* Also at Department of Physics, Westmont College, Santa Barbara; United States of America.
- u* Also at Faculty of Physics, Sofia University, 'St. Kliment Ohridski', Sofia; Bulgaria.
- v* Also at Hellenic Open University, Patras; Greece.
- w* Also at Henan University; China.
- x* Also at Imam Mohammad Ibn Saud Islamic University; Saudi Arabia.
- y* Also at Institutio Catalana de Recerca i Estudis Avancats, ICREA, Barcelona; Spain.
- z* Also at Institut für Experimentalphysik, Universität Hamburg, Hamburg; Germany.
- aa* Also at Institute for Nuclear Research and Nuclear Energy (INRNE) of the Bulgarian Academy of Sciences, Sofia; Bulgaria.
- ab* Also at Institute of Applied Physics, Mohammed VI Polytechnic University, Ben Guerir; Morocco.
- ac* Also at Institute of Particle Physics (IPP); Canada.
- ad* Also at Institute of Physics and Technology, Mongolian Academy of Sciences, Ulaanbaatar; Mongolia.
- ae* Also at Institute of Physics, Azerbaijan Academy of Sciences, Baku; Azerbaijan.
- af* Also at Institute of Theoretical Physics, Ilia State University, Tbilisi; Georgia.
- ag* Also at National Institute of Physics, University of the Philippines Diliman (Philippines); Philippines.
- ah* Also at Technical University of Munich, Munich; Germany.
- ai* Also at The Collaborative Innovation Center of Quantum Matter (CICQM), Beijing; China.
- aj* Also at TRIUMF, Vancouver BC; Canada.
- ak* Also at Università di Napoli Parthenope, Napoli; Italy.
- al* Also at University of Colorado Boulder, Department of Physics, Colorado; United States of America.
- am* Also at University of Sienna; Italy.
- an* Also at University of the Western Cape; South Africa.
- ao* Also at Washington College, Chestertown, MD; United States of America.
- ap* Also at Yeditepe University, Physics Department, Istanbul; Türkiye.
- * Deceased